

#616

MARINER 10

PULSE HEIGHT DATA  
73-085A-07A

RATE DATA  
73-085A-07B

---

## Table of Contents

1. Introduction
2. Errata/Change Log
3. LINKS TO RELEVANT INFORMATION IN THE ONLINE NSSDC INFORMATION SYSTEM
4. Catalog Materials
  - a. Associated Documents
  - b. Core Catalog Materials

---

## **1. INTRODUCTION:**

The documentation for this data set was originally on paper, kept in NSSDC's Data Set Catalogs (DSCs). The paper documentation in the Data Set Catalogs have been made into digital images, and then collected into a single PDF file for each Data Set Catalog. The inventory information in these DSCs is current as of July 1, 2004. This inventory information is now no longer maintained in the DSCs, but is now managed in the inventory part of the NSSDC information system. The information existing in the DSCs is now not needed for locating the data files, but we did not remove that inventory information.

The offline tape datasets have now been migrated from the original magnetic tape to Archival Information Packages (AIP's).

A prior restoration may have been done on data sets, if a requestor of this data set has questions; they should send an inquiry to the request office to see if additional information exists.

## 2. ERRATA/CHANGE LOG:

NOTE: Changes are made in a text box, and will show up that way when displayed on screen with a PDF reader.

*When printing, special settings may be required to make the text box appear on the printed output.*

Version	Date	Person	Page	Description of Change
01				
02				

3 LINKS TO RELEVANT INFORMATION IN THE ONLINE NSSDC INFORMATION SYSTEM:

<http://nssdc.gsfc.nasa.gov/nmc/>

[NOTE: This link will take you to the main page of the NSSDC Master Catalog. There you will be able to perform searches to find additional information]

4. CATALOG MATERIALS:

- a. Associated Documents      To find associated documents you will need to know the document ID number and then click here.  
<http://nssdcftp.gsfc.nasa.gov/miscellaneous/documents/>

- b. Core Catalog Materials

## MARINER 10

## PULSE HEIGHT DATA ON TAPE

73-085A-07A PSFP-00197

This data set has been restored. There were originally 45 7-track, 800 BPI tapes written in Binary. There was one bad tape, the tape was D40338. There are five restored tapes. The DR tapes are 3480 cartridges and the DS tapes are 9-track, 6250 BPI. The original tapes were created on an IBM 930 computer. The DR and DS numbers along with the corresponding D numbers and the time spans are as follows:

DR#	DS#	DD#	FILES	TIME SPAN
DR03225	DS03225	D40321	1	11/03/73 - 11/09/73
		D40322	2	11/10/73 - 11/15/73
		D40320	3	11/16/73 - 11/21/73
		D40319	4	11/21/73 - 11/22/73
		D40323	5	11/23/73 - 11/25/73
		D40341	6	11/29/73 - 12/01/73
		D40340	7	12/02/73 - 12/04/73
		D40343	8	12/05/73 - 12/08/73
		D40342	9	12/08/73 - 12/10/73
		D40331	10	12/11/73 - 12/16/73
		D40329	11	12/17/73 - 12/22/73
DR03226	DS03226	D40347	1	12/23/73 - 12/25/73
		D40314	2	12/26/73 - 12/28/73
		D40325	3	12/29/73 - 12/31/73
		D40324	4	01/01/74 - 01/11/74
		D40326	5	01/12/74 - 01/17/74
		D40327	6	01/18/74 - 01/23/74
		D40328	7	01/24/74 - 01/29/74
		D40346	8	01/30/74 - 02/05/74
		D40344	9	02/06/74 - 02/11/74
DR03290	DS03290	D40316	1	02/12/74 - 02/14/74
		D40315	2	02/15/74 - 02/20/74
		D40318	3	02/21/74 - 02/23/74
		D40317	4	02/24/74 - 02/26/74
		D40339	5	02/27/74 - 03/04/74
		D40332	6	03/05/74 - 03/07/74
		D40335	7	03/08/74 - 03/10/74
		D40336	8	03/11/74 - 03/16/74
		D40354	9	03/15/74 - 03/21/74
DR03278	DS03278	D40333	1	03/17/74 - 03/22/74
		D40337	2	03/23/74 - 03/28/74
		D40334	3	03/29/74 - 04/03/74
		D40353	4	04/03/74 - 04/11/74
		D40358	5	04/11/74 - 04/18/74
		D40345	6	04/18/74 - 05/02/74
		D40350	7	05/02/74 - 05/10/74
		D40355	8	05/10/74 - 05/24/74

DR#	DS#	DD#	FILES	TIME SPAN
DR03297	DS03297	D40357	1	06/24/74 - 07/10/74
		D40330	2	07/11/74 - 07/27/74
		D40348	3	07/27/74 - 08/15/74
		D40351	4	08/15/74 - 09/02/74
		D40356	5	09/02/74 - 09/13/74
		D40349	6	09/13/74 - 09/18/74
		D40352	7	09/18/74 - 09/23/74

MARINER 10

RATE DATA

73-085A-07B PSFP-00039

This data set has been restored. There were originally 6 magnetic tapes which the D tapes were 800 bpi, 7 track, and the C tapes were 1600 BPI 9 track and both D and C tapes are Binary data. The tapes were condensed onto 1 DS and 1 DR tape 9 track 6250 BPI.

DR02620	DS02620	D-40360	C-23523	1	11/03/73	-	12/31/73
		40359	23522	2	01/01/74	-	03/07/74
		40363	23526	3	03/07/74	-	03/28/74
		40364	23527	4	03/28/74	-	05/23/74
		40361	23524	5	06/24/74	-	09/23/74
		40362	23525	6	03/15/75	-	03/21/75

REQ. AGENT  
RSH

RAND NO.  
V0218

ACQ. AGENT  
WSC

MARINER 10

PULSE HEIGHT DATA

73-085A-07A

This data set consists of 45 magentic tapes. The D# tapes are 800 BPI, 7 track, contain BINARY data, and 1 file. The C# tapes are 1600 BPI, 9 track, contain BINARY data, and 1 file. The D#'s, C#'s and time span are as follows: THESE TAPES WERE MADE ON THE XDS-930 SYSTEM.

<u>D#</u>	<u>C#</u>	<u>TIME SPAN</u>
D-40321	C-23484	11/03/73 - 11/09/73
D-40322	C-23485	11/10/73 - 11/15/72
D-40320	C-23483	11/16/73 - 11/21/73
D-40319	C-23482	11/21/73 - 11/22/73
D-40323	C-23486	11/23/73 - 11/25/73
D-40338	C-23501	11/26/73 - 11/28/73
D-40341	C-23504	11/29/73 - 12/01/73
D-40340	C-23503	12/02/73 - 12/04/73
D-40343	C-23506	12/05/73 - 12/08/73
D-40342	C-23505	12/08/73 - 12/10/73
D-40331	C-23494	12/11/73 - 12/16/73
D-40329	C-23492	12/17/73 - 12/22/73
D-40347	C-23510	12/23/73 - 12/25/73
D-40314	C-23477	12/26/73 - 12/28/73
D-40325	C-23488	12/29/73 - 12/31/73
D-40324	C-23487	01/01/74 - 01/11/74
D-40326	C-23489	01/12/74 - 01/17/74
D-40327	C-23490	01/18/74 - 01/23/74
D-40328	C-23491	01/24/74 - 01/29/74
D-40346	C-23509	01/30/74 - 02/05/74
D-40344	C-23507	02/06/74 - 02/11/74
D-40316	C-23479	02/12/74 - 02/14/74
D-40315	C-23478	02/15/74 - 02/20/74

73-085A-07A con't

<u>D#</u>	<u>C#</u>	<u>TIME SPAN</u>
D-40318	C-23481	02/21/74 - 02/23/74
D-40317	C-23480	02/24/74 - 02/26/74
D-40339	C-23502	02/27/74 - 03/04/74
D-40332	C-23495	03/05/74 - 03/07/74
D-40335	C-23498	03/08/74 - 03/10/74
D-40336	C-23499	03/11/74 - 03/16/74
D-40333	C-23496	03/17/74 - 03/22/74
D-40337	C-23500	03/23/74 - 03/28/74
D-40334	C-23497	03/29/74 - 04/03/74
D-40353	C-23516	04/03/74 - 04/11/74
D-40358	C-23521	04/11/74 - 04/18/74
D-40345	C-23508	04/18/74 - 05/02/74
D-40350	C-23513	05/02/74 - 05/10/74
D-40355	C-23518	05/10/74 - 05/24/74
D-40357	C-23520	06/24/74 - 07/10/74
D-40330	C-23493	07/11/74 - 07/27/74
D-40348	C-23511	07/27/74 - 08/15/74
D-40351	C-23514	08/15/74 - 09/02/74
D-40356	C-23519	09/02/74 - 09/13/74
D-40349	C-23512	09/13/74 - 09/18/74
D-40352	C-23515	09/18/74 - 09/23/74
D-40354	C-23517	03/15/75 - 03/21/75

DLD-X  
HCK-D

DOCUMENTATION  
FOR THE  
UNIVERSITY OF CHICAGO  
CHARGED PARTICLE TELESCOPE DATA  
FROM THE  
MARINER 10 SPACECRAFT

as

Submitted to the  
National Aeronautics and Space Administration  
National Space Sciences Data Center  
Goddard Space Flight Center  
under Contract #NSG-7288

1980

S. P. Christon  
S. F. Daly\*  
J. H. Eraker  
J. E. Lamport  
G. A. Lentz  
J. A. Simpson (Principal Investigator)  
A. J. Tuzzolino  
P. H. Walpole†

Laboratory for Astrophysics and Space Research  
Enrico Fermi Institute  
University of Chicago

\*Now at Lamont-Doherety Geological Observatory, Palisades, N. Y. 10964

†Now at Department of Physics, University of Maryland

EFI Preprint No. 79-65

Table of Contents

	<u>Page</u>	
Section I	General Description of Spacecraft Operation and Mission Summary	1
Section II	Functional Description of the University of Chicago Charged Particle Telescope (UC/CPT)	8
Section III	UC/CPT Data Tape Descriptions	49
	A. Physical Description of Tapes	50
	B. Pulse Height Tape Format	50
	C. Rate Tape Format	54
Section IV	Acknowledgements	66
Section V	Appendix	67
	A. JPL UC/CPT Functional Requirement Document	68
	B. In-flight Calibration Summary of UC/CPT	81
	C. Investigation of Background in LET	95
	D. Publications and Abstracts Based on Mariner 10 UC/CPT Data to Date	112

## I.

Mariner 10 Spacecraft Configuration and  
Operation Related to the University of Chicago  
Charged Particle Telescope

This section briefly outlines aspects of the Mariner 10 spacecraft relevant to the understanding of the data submitted to the NSSDC. The functioning of the University of Chicago Charged Particle Telescope is related to Mariner 10 operational modes. No attempt is made at a comprehensive discussion of spacecraft design, performance, or trajectory, since each is adequately detailed in a NASA technical memorandum.<sup>1</sup> Spacecraft instrument interface and data processing procedures at the University of Chicago are detailed only to an extent which facilitates understanding of Sections II and III.

The UC/CPT design and functional requirements are outlined in the Jet Propulsion Laboratory (JPL) UC/CPT Functional Requirement Document of June 7, 1971. That document, which should be read and is attached as Appendix A. It gives a good overall description of the UC/CPT. The UC/CPT consisted of two telescopes: 1) the Main Telescope (MT) and 2) the Low Energy Telescope (LET). The "Mariner 10" (M10) [also named "Mariner Venus Mercury" (MVM)] spacecraft is shown in Figure I-1. Mariner 10 was a 3-axis stabilized spacecraft. The MT symmetry axis pointed at a cone angle of  $45^{\circ}$  as measured from the spacecraft-Sun vector and a clock angle of  $275^{\circ}$  as measured clockwise from the projection of the spacecraft Canopus vector (approximately toward the South Celestial Pole) in a plane perpendicular to the spacecraft-Sun vector. The LET has a cone angle of  $50^{\circ}$  and a clock angle of  $275^{\circ}$ . (See Figure I-2.)

The Mariner 10 spacecraft telemetry modes for the Non-Imaging Sciences (NIS) were NIS-1 at 2450 bits per second (BPS) and NIS-2 (490 BPS). When higher bit rates were used for the Mariner 10 "TV" transmissions the NIS-1 data was multiplexed into the "flyback" of the raster scan on the "TV" picture. The bit rate of the UC/CPT is 133 bits/second in NIS-1 and  $53 \frac{1}{3}$  bits/seconds in NIS-2. Engineering bit rates lower than NIS-2 resulted in no analysis data from the UC/CPT other than temperature, voltage and the D7 (anti-coincidence detector) ratemeter analog.

The Mariner 10 spacecraft was capable of receiving commands to turn off the D1, D2, or D7 detectors. (See Section II for details.) These commands were never sent due to the excellent performance of the CPT as a whole and the D1, D2 and D7 detectors in particular. The MT had a priority system for pulse height analysis which was overridden at the Venus encounter and at the Mercury encounters. Once a week for a 15-minute period both the MT and LET electronics were calibrated and the individual detector rates were monitored.

---

<sup>1</sup> NASA Technical Memorandum 33-734: Mariner Venus-Mercury 1973 Project Final Report. Volumes 1 and 2.

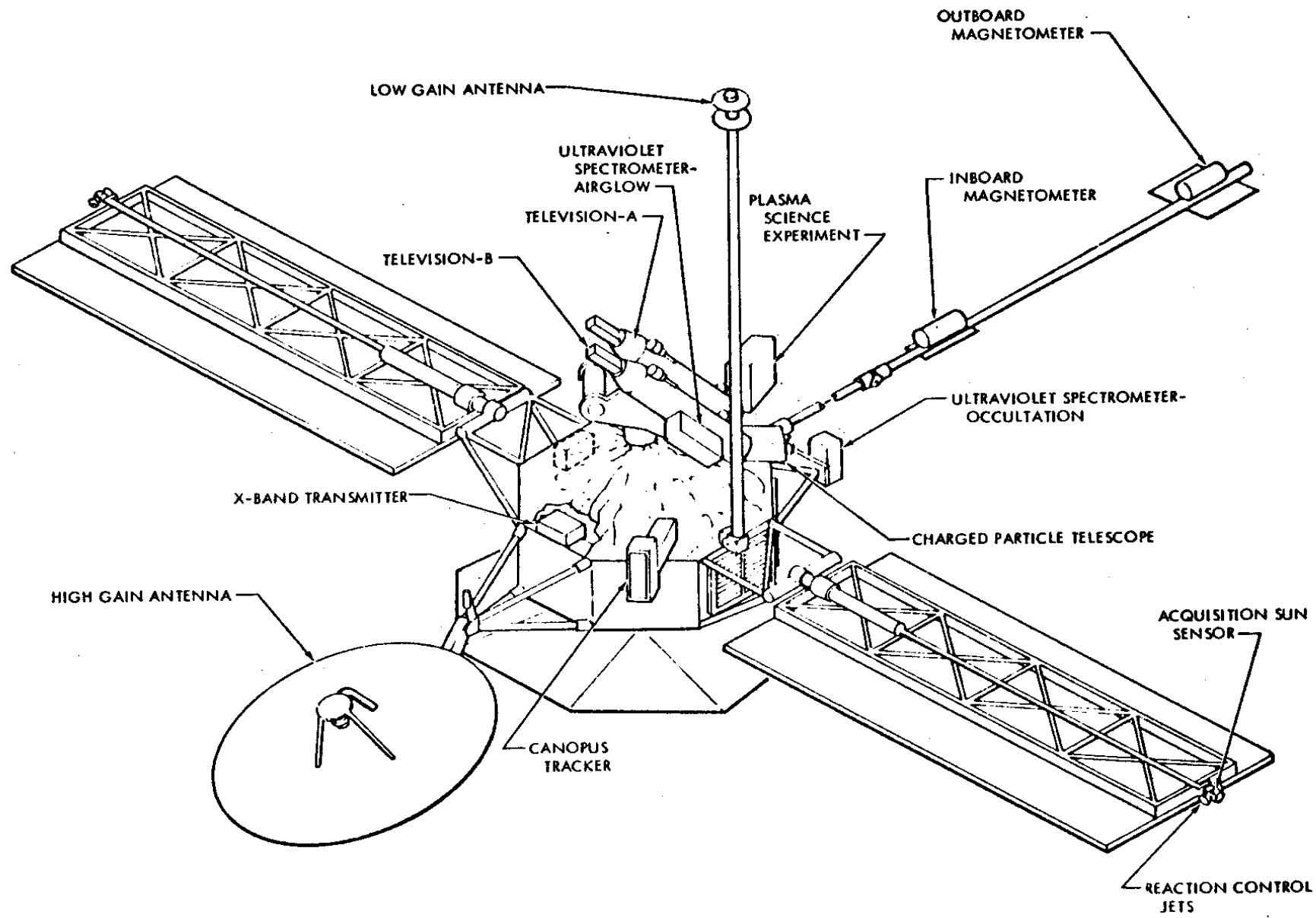
During the prime mission (launch until Day 109, 1974) the tracking of Mariner 10 was nearly complete. Following the prime mission the tracking coverage decreased. Solar occultation permitted no NIS data reception from about Day 145-175, 1974. Intermittent data was received from then until Mercury II encounter Day 265, 1974. NIS data was also obtained around Mercury III encounter from Day 74-80, 1975.

In Figure I-3 the projection of the M10 trajectory onto the Ecliptic plane is plotted with the Earth-Sun line fixed. This figure illustrates that Mariner 10 had a perhelion of 0.46 A.U. and an orbital period of 6 months.

Figure I-1. A view of the Mariner Venus/Mercury spacecraft from the Sun-shaded side. Shown are all the various scientific experiments. The solar panels provided power for the operation of the entire spacecraft. The spacecraft was tri-axially oriented with one spacecraft-fixed axis continually pointing toward the Sun and another pointing toward the star Canopus.

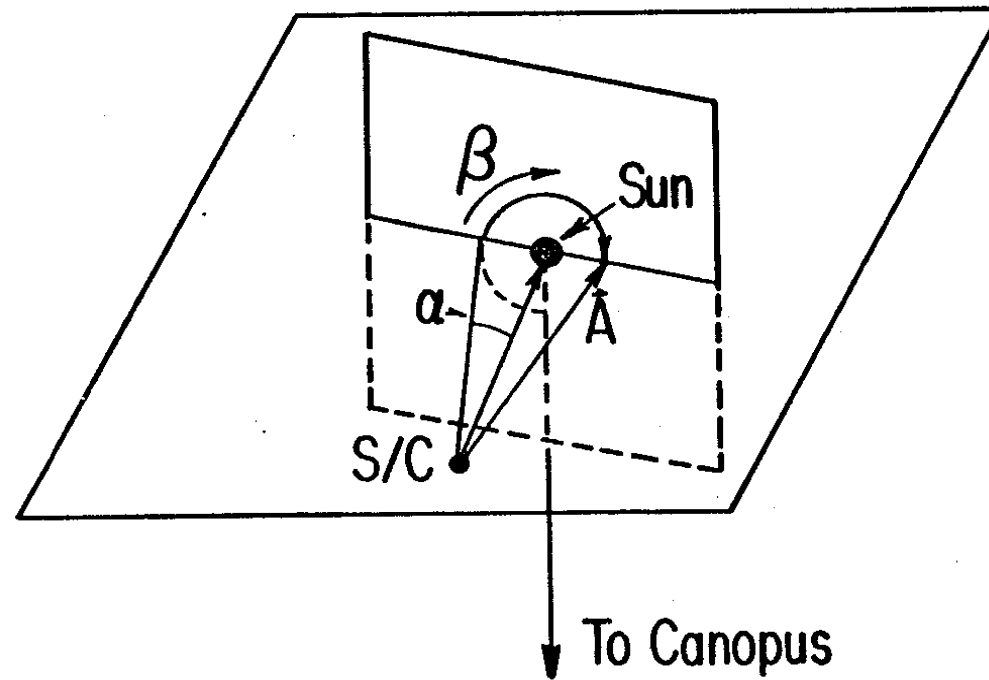
Figure I-2. The Mariner 10 spacecraft is a tri-axially oriented spacecraft with one spacecraft fixed axis directed toward the Sun. The viewing direction of the UC/CPT telescopes are consequently fixed with respect to the spacecraft-Sun line and uniquely defined by the specification of the cone and clock angles. Canopus is a large OB star near the South Celestial Pole.

Figure I-3. The trajectory of the Mariner 10 spacecraft projected onto the Ecliptic Plane. The Earth-Sun line is held fixed. Launch of the Mariner 10 spacecraft occurred on November 3, 1973. The encounters of the spacecraft with Venus and Mercury are denoted by VI, MI, etc. An idealized Interplanetary Magnetic Field (IMF) line for a solar wind speed of  $500 \text{ KM S}^{-1}$  is denoted by the dashed line. The direction of the view cone axis of the UC/CPT MT at the point of intersection of the IMP line and spacecraft trajectory is shown by the small arrow.



Mariner Venus/Mercury 1973 Spacecraft (Shaded Side)

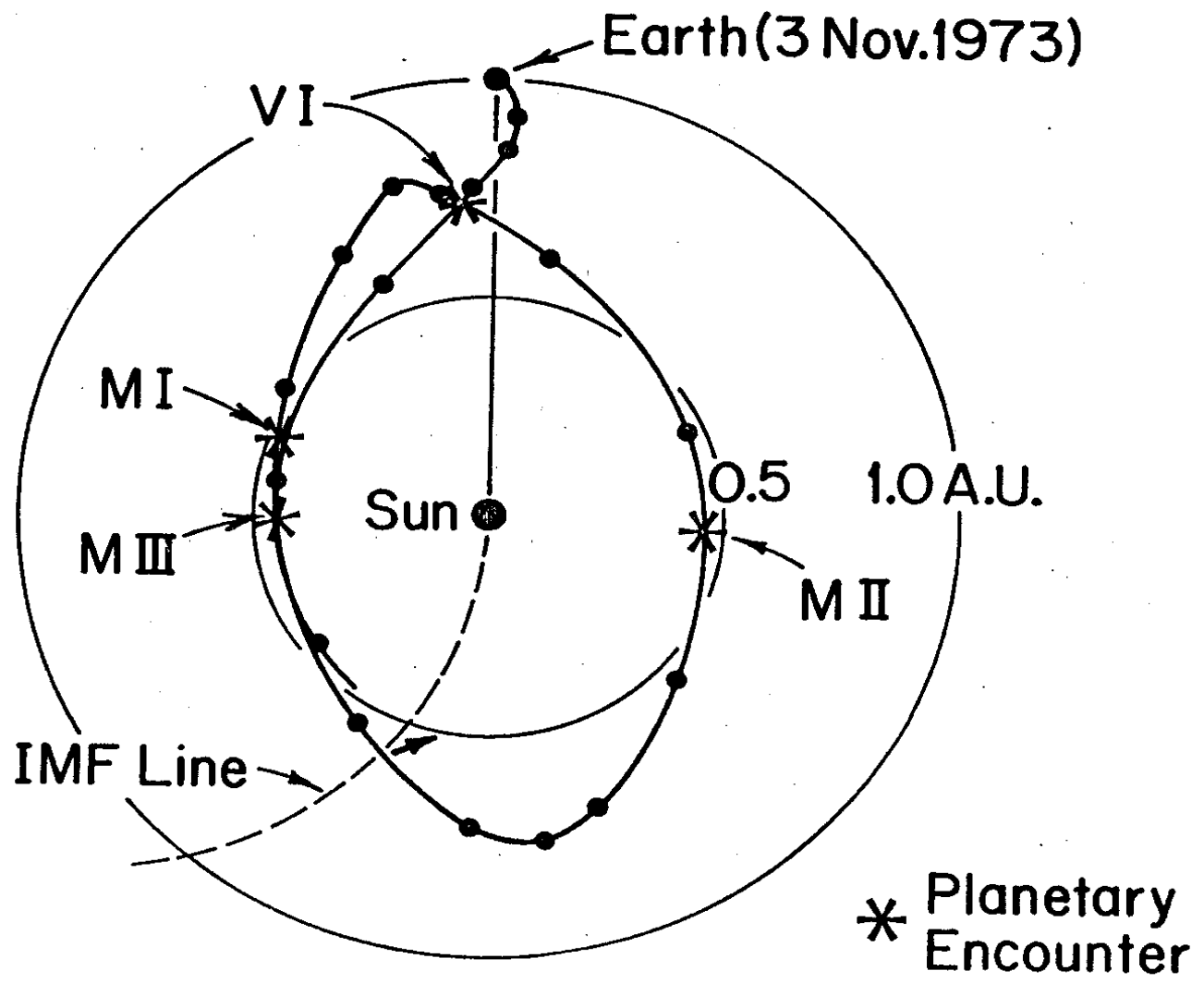
## Definition of Cone and Clock Angle



$\alpha$  = cone angle

$\beta$  = clock angle

$\vec{A}$  = axis of telescope



S 375

## II.

Functional Description of the  
University of Chicago  
Charged Particle Telescope

A summary description of both the physical and electronic characteristics of the UC/CPT is presented in this section. Knowledge of these characteristics is essential to correct interpretation of the pulse height and counting rate data described in this document.

The design of the University of Chicago Main System Telescopes (MT) and Low Energy Telescopes (LET) on the Mariner 10 (M10), Pioneer 10 and Pioneer 11 (PIO 10/11) spacecraft are nearly identical. The only structural difference between the M10 and PIO 10/11 MT's is that the M10 MT was constructed with two titanium windows ( $\sim 176 \text{ mg/cm}^2$  total) while the PIO 10/11 MTs have only one Ti window ( $88 \text{ mg/cm}^2$  total thickness). Structurally there are no differences between the M10 and PIO 10/11 LETs. A detailed description of the PIO 10/11 telescopes which is also relevant to the understanding of the M10 telescopes can be found in the Preliminary Documentation for the University of Chicago Pioneer 10 Charged Particle Instrument Data submitted to the NSSDC (NSSDC Tech. Ref. File No. B21970).

Two major differences between the M10 and PIO 10/11 spacecraft exist. These differences limit the range of particle measurements possible on each spacecraft. These differences are:

- 1) The M10 spacecraft is triaxially oriented while PIO 10/11 spacecraft are spin-stabilized.
- 2) Concerning electron measurements, the presence of a  $\gamma$ -ray background from the radioactive thermal generators (RTGs) on the PIO 10/11 spacecraft makes the measurement of interplanetary electrons with kinetic energies below  $\sim 2 \text{ MeV}$  by the PIO 10/11 instruments difficult except in the presence of extremely large electron fluxes. The M10 spacecraft has no RTGs, consequently, the M10 instrument can measure electrons down to  $\sim 200 \text{ keV}$  in kinetic energy.

The UC/CPT MT and LET are shown schematically in Figure II-1. Thickness measurements and material properties for the elements in the view cones of the telescopes are given in Tables II-1 and II-2, respectively. Pathlengths in  $\text{gm/cm}^2$  for non-scattering particles are listed in Tables II-3 and II-4. These were calculated from the properties and thicknesses in Tables II-1 and II-2. Pathlengths in the MT are given for those particle trajectories which enter the telescope: 1) along the telescope axis (V); 2) at a median angle for triggering the "small cone" (MSC) geometry coincidence logic "IDs" (ID4, ID5, and ID7); and 3) at a median angle for triggering the "large cone" (MLC) geometry coincidence logic "IDs" (ID2 and ID3.) The median angles for the different geometries were determined from pathlength distributions generated during Monte Carlo simulations of the penetration of an isotopic flux of particles into the telescopes. Counting rate and pulse height coincidence logic identification is determined for particles by their range of penetration into the detector stack. Definitions of the counting rate and pulse height ID's are listed in Table II-5 for each telescope.

The pulse height analysis in the MT is organized by a priority system. The "high priority" IDs are IDs 2, 3, 4 and 5. All other IDs are classed as "low priority" (see Table II-5.) The high priority IDs all provide 2 (or 3 in the particular case of ID5) dimensional pulse height information on particles

stopping within the telescope. The instrument's pulse height transmission scheme is such that it accepts the first pulse height event regardless of priority. If any high priority event occurs within the analysis period, the first high priority event is accepted and the instrument "locks out" pulse height analysis for the remainder of that analysis period. When this pulse height priority scheme was overridden, as it was during every planetary encounter, all pulse height events had equal priority.

Detector separations, as determined from blueprints, and measurements of the radii of the flight detectors were used to calculate geometrical factors for the major analysis IDs of the telescopes. These geometrical factors were determined by Monte-Carlo numerical analysis assuming the presence of an isotropic flux of particles incident on the first Ti window. They are listed with the half-cone opening angles of the telescopes in Table II-6. The 0%, 50% and 100% electronic thresholds of each detector in the MT and LET are listed in Table II-7. The three thresholds values for each detector are in millivolts (mV) and correspond to input voltages at which the discriminator fires 0%, 50% and 100% of the time. All mV/channel calibrations were converted to MeV/channel for each detector using the MeV/mV factors listed in this table.

The range of incident energies in each of six major MT IDs for nucleon species from Hydrogen through Oxygen were calculated using the MT detector thicknesses. These results are listed in Table II-8 and shown graphically in Figure II-2.

The M10 MT and LET pulse height analysis electronics response was carefully measured prior to launch using a calibrated pulser. Approximately 1000 readouts were taken at each mV setting in order to measure the mean response channel to an accuracy of  $\approx 3\%$ . The mV readings may be converted into MeV deposited in the detector using individual detector MeV/mV conversion factors given in Table II-8. This represents the final calibration for the instrument since the pulseheight analyzer electronics proved stable within  $\sim 1\%$  during the mission (see Appendix B.) These calibration results are plotted in the set of drawings included as Figure II-3. One should notice that the channel vs. mV calibration for each detector of the MT includes 3 linear ramps connected by 2 "knees". This type of ramp arrangement allows for an expanded dynamic range around the track positions of electrons - Hydrogen - Helium and Carbon - Nitrogen - Oxygen. The calibrations of the pulse height electronics (Table II-9) and the path-lengths through the MT detector elements (Table II-3) were used to generate the "ELOSS" graphs which are included as Figure II-5. In general, these are plots of energy deposited in one detector displayed versus energy deposited in another detector. These graphs accurately predict the position of the elemental and isotopic "tracks" of the flight data within each ID matrix. The calibration of the M10 and P10 10/11 MT electron response will be discussed in a separate publication (J. H. Eraker, PhD thesis, 1980.) The active anti-coincidence shield, D7, was calibrated so that the data numbers, DN, returned by the spacecraft can be accurately converted into a counting rate. The calibration is summarized in Table II-10.

The LET is shown schematically in Figure II-1. It is a relatively simple system which consists of a very thin flat fully depleted surface barrier detector, L1, and a second composite detector, L2. The L2 detector consists of an annular lithium-drifted-silicon ring, L2a, electrically connected to a flat lithium-

drifted-silicon detector, L2f. The LET detectors are enclosed by a passive shield which stops nucleons with energy  $< 50$  MeV/nucleon. This telescope is designed to measure low energy protons and alphas with energy from 0.5 - 1.8 MeV/nucleon and has a very high degree of immunity of contamination by low energy electron fluxes (Christon et al, 1979.) A background due to cosmic ray leakage exists in this telescope. This background contribution is described in the memos attached as Appendix C.)

Thickness measurements of the LET elements in the telescope view cone are listed in Table II-1. The logic for pulse height and counting rate coincidence for the two LET IDs is given in Table II-5. The geometrical factor of the LET for particles entering through the opening cone is  $0.485 \text{ cm}^2 \text{ ster}$ . The principal characteristics of the L1 and L2 electronic thresholds are given in Table II-7 along with the MeV/mV factors.

Only the L1 detector is pulse height analyzed, the L1 mV/channel calibrator is given in Table II-11 and plotted in Figure II-3. All LET pulse height events are of equal priority. The L1 amplifier is linear throughout its dynamic range. The calibration in Table II-11 along with the L1 MeV/mV conversion factors (Table II-7) form the basis of the M10 LET calibration. The L1 electronics proved stable to within 1% during the mission (see Appendix B).

M10 roll calibrate maneuvers were discontinued after only two due to a difficulty in reacquiring the correct 3-axis orientation.

Table II-1  
THICKNESS MEASUREMENTS 9/4/73

UC/MT ELEMENT	DETECTOR* MATERIAL		MEASURED THICKNESS (x 10 <sup>-4</sup> cm)
1	Ti Window	Ti	1.85
2	Ti Window	Ti	1.85
3	D1 Sensitive	Si	704.
4	D1 Li Window	Si	59.
5	D2 Sensitive	Si	1416.
6	D2 Li Window	Si	105.
7	Mylar	MY	9.1
8	Aluminum	AL	5.1
9	D3 Sensitive	Si	880.
10	D3 Li Window	Si	70.
11	Mylar	MY	9.1
12	Aluminum	AL	5.1
13	D4 Sensitive	Si	978.
14	D4 Li Window	Si	96.
15	Mylar	MY	51.
16	Magnesium	AL	127.
17	Cesium Iodide	CsI	11989. ± 127.0
18	D5 Sensitive	Si	507.
19	D5 Li Window	Si	44.
20	Mylar	MY	9.1
21	Aluminum	AL	5.1
22	D6 Sensitive	Si	978.
23	D6 Li Window	Si	122.

UC/LET ELEMENT	DETECTOR MATERIAL		MEASURED THICKNESS (x 10 <sup>-4</sup> cm)
1	Ti Window		1.85
2	L1 Sensitive		37.4
3	L2f Sensitive		362
4	L2f Li Window		37

\* Those elements enclosed by brackets are the electronically active detectors.

## MATERIAL PROPERTIES 9/4/73

DETECTOR MATERIAL		IONIZATION POTENTIAL (eV)	DENSITY (gm/cm <sup>3</sup> )	A/Z
Mylar	MY	72.6 (Δ)	1.392 (γ)	1.9197 (Δ)
Magnesium	MG	151.0 (Δ)	1.74 (μ)	2.0267 (Δ)
Aluminum	AL	163.0 (Δ)	2.6987 (\$)	2.0755 (Δ)
Silicon	SI	173.5 (~)	2.33 (+)	2.006 (Δ)
Titanium	TI	247.0 (Δ)	4.512 (π)	2.1772 (≠)
Cesium Iodide	CSI	552.0 (Δ)	4.510 (\$)	2.4055 (Δ)
Epoxy Glass	EP	100.0 (*)	1.839	2.00 (*)
Plastic Scintillator	PS		1.030	2.00 (*)

## KEY

- (Δ) Detector Response Driver Addendum -- code 0064 - R. C. Taft  
 (\*) Estimated  
 (+) Dow-Corning, Supplier Information  
 (≠) Physical Constants, WHJ Childs  
 (π) (0.163 lb/in<sup>3</sup>) Reactive Metals Inc., Supplier Information  
 (\$) Handbook of Physics and Chemistry, Chemical Rubber  
 (γ) Dupont Inc., Supplier Information  
 (μ) AIP Handbook, 3rd Ed.  
 (~) Nuclear Data, Section A, Vol. 3, No. 3, Oct. 1962, p. 349

Mylar is known properly as Poly (Ethylene Terephthalate)

Pathlengths are determined by multiplying the thicknesses measured (in cm.) by the densities (in gm/cm<sup>3</sup>)

Dimension of pathlength is gm/cm<sup>2</sup>.

Shields (MY, AL) :

15 x 10 <sup>-5</sup> in. -----	3.81	x 10 <sup>-4</sup> cm. -----	→	MYLAR	BIGGS 283 EPOXY
3 x 10 <sup>-5</sup> in. -----	.762	x 10 <sup>-4</sup> cm. -----	→	ALUMINUM	
20 x 10 <sup>-5</sup> in. -----	5.08	x 10 <sup>-4</sup> cm. -----	→	ALUMINUM	
3 x 10 <sup>-5</sup> in. -----	.762	x 10 <sup>-4</sup> cm. -----	→	ALUMINUM	
15 x 10 <sup>-5</sup> in. -----	3.81	x 10 <sup>-4</sup> cm. -----	→	MYLAR	

Pathlengths for shields are computed by approximating epoxy density by mylar density and adding material pathlengths.

Table II-3

M10 UC/CPT MT: Pathlengths For Elements at  
 Various Trajectory Incidence Angles  
 (Tolerance =  $\pm 0.005\%$  Due to Roundoff)  
 (All pathlengths in  $\text{g cm}^{-2}$ )

MT Element No.	V	MSC	MLC
1 & 2 combined	.00167	.00170	.00173
3	.1640	.1649	.1676
4	.01375	.01382	.01405
5	.3299	.3355	.3362
6	.02446	.02488	.02492
7	.00127	.00129	.00131
8	.00138	.00149	.00143
9	.2050	.2083	.2118
10	.01631	.01657	.01685
11	.00127	.00129	.00131
12	.00138	.00140	.00143
13	.2279	.2315	.2354
14	.02237	.02273	.02311
15	.02920	.02967	
17	5.4069	5.4934	
18	.1181	.1200	
19	.01290	.01311	
22	.2279	.2315	
23	.02843	.02890	

Table II-4

M10 UC/CPT LET: Pathlengths For Elements at  
 Various Trajectory Incidence Angles  
 (Tolerance =  $\pm 0.005\%$  Due to Roundoff)  
 (All pathlengths in  $\text{g cm}^{-2}$ )

	<u>Vertical Incidence</u>	<u>Mean Incidence</u>
1. Ti Window	0.00084	0.00088
2. L1	.00871	.00913
3. L2 anular	.2039	-
4. L2 flat-sensitive	.0855	.0896
5. L2 flat-Li window	.0075	.0078

Table II-5

MVM Logic Coding for Redundant Pulse Height Analysis (PHA) and Counting Rates

<u>MT PHA ID</u>	<u>Event Priority</u>	<u>Detector Coincidence and Alternating Counting Rate Title</u>	<u>Counting Rate Titles</u>
0	Low	No Analyzable event	
1	Low	$D1\overline{27} \overline{A} \overline{XT}$	ID1
2	High	$D1\overline{237} \overline{A} \overline{X2}$	ID2
3	High	$D1\overline{23457} \overline{A}$	-
4	High	$D1\overline{2457} \overline{A}$	-
5	High	$D1\overline{24567} \overline{A}$	ID5
6	Low	$D1\overline{24567} \overline{A}$	-
7	Low	$D1\overline{24567} \overline{A}$	ID7
8	Invalid		
9	Low	$D2\overline{4567} \overline{A} \overline{XT}$	-
10	Low	$D1\overline{24567} \overline{A}$	-
11	Low	$D1\overline{4567} \overline{A} \overline{X2^*}$	-
12	Invalid		
13	Low	$D2\overline{4567} \overline{A} \overline{XT}$	ID13
14	Low	$D1\overline{24567} \overline{A}$	ID14
15	Low	$D1\overline{4567} \overline{A} \overline{X2}$	-

---

<u>LET PHA ID</u>	<u>Detector Coincidence and Alternating Counting Rate Title</u>	<u>Counting Rate Titles</u>
0	L12	L1N2
1	L12	L1L2

Key:  $D1 = D1 + X_1$ ,  $D2 = D2 + X_2$  $\overline{A}$  = No analysis, readout or transfer in progress

\* = Cannot occur if instrument is functioning properly

 $X_i$  = Command to disable detector  $D_i$

Table II-6  
MVM 73 Geometrical Factors

This is a list of the minimum and maximum geometrical factors for a given geometry. The range of G is due to the unknown sensitive edge(s).  $\theta/2$  is the half-cone angle, that is, 1/2 of the particles triggering that ID into at angles less than or equal to  $\theta/2$ .

<u>ID</u>	<u>G (cm<sup>2</sup> sr)</u>	<u><math>\theta/2</math> (degrees)</u>
<u>MT</u>		
1	G(ID1)      6.68 - 8.11	47-58
2,3	G(Large Cone) 1.11 - 1.50	32
4,5,7	G(Small Cone) 0.347 - 0.507	24
 <u>LET</u>		
L1N2,L1L2	G(LET)      0.485	38

Table II-7  
Mariner 10 Detector Calibration

<u>Detector</u>	<u>Conversion Factor</u> (MeV/mV)	<u>Threshold*</u> (mV)
D1	.2083	.65 - .86 - 1.20
D2	.2105	.90 - 1.14 - 1.50
D3	.226	.65 - .76 - .95
D4	.227	.65 - .79 - .95
D5	.213	.65 - .83 - 1.20
D6	.223	.50 - .73 - 1.00
L1	.218	1.20 - 1.58 - 1.80
L2	.216	.60 - .85 - 1.11

\* Discriminator fires 0% - 50% - 100% of the time.

Amplifier Output at 50% Threshold

<u>Detector</u>	<u>50% Threshold</u> (mV)	<u>Output</u> (mV)	<u>Amplifier</u> <u>Noise (mV)</u>
D1	.86	130.	90.
D2	1.14	200.	120.
D3	.76	~200.	160.
D4	.79	~200.	100.
D5	.83	130	120.
D6	.73	~200.	150
D7	≈.4		
L1	1.58	350.	100.
L2	.85	~200	160.

11/21/73

Table II-8  
 MARINER 10 THRESHOLD ENERGIES\*  
 (in units of MeV/nucleon)

CHARGED PARTICLE	MT PHA ID					
	ID1	ID2	ID3	ID4	ID5	ID7
${}^1_1\text{H}^1$	.610	10.5/(10.3)**	19.7	23.9	29.2	67.0
${}^2_1\text{H}^2$	.348	7.08	13.3	16.1	19.6	44.9
${}^3_1\text{H}^3$	.244	5.60	10.5	12.8	15.5	35.5
${}^3_2\text{He}^3$	.559	12.4	23.2	28.2	33.6	79.2
${}^4_2\text{He}^4$	.432	10.5/(10.3)**	19.7	23.9	28.6	67.0
${}^6_3\text{Li}^6$	.458	13.3	24.8	30.1	35.7	85.2
${}^7_3\text{Li}^7$	.389	12.2	22.7	27.6	32.8	77.8
${}^9_4\text{Be}^9$	.399	14.6	27.2	33.1	39.5	94.1
${}^{11}_5\text{B}^{11}$	.404	16.8	31.4	38.0	45.5	107.9
${}^{12}_6\text{C}^{12}$	.462	19.7	36.6	44.5	52.6	126.6
${}^{14}_7\text{N}^{14}$	.470	21.5	39.9	48.6	57.5	138.8
${}^{16}_8\text{O}^{16}$	.463	23.3	43.1	52.5	62.1	149.9

\* 100% efficiency points from Table II-7 used as thresholds.

\*\* Computed from Northcliffe and Schilling tables.

MARINER 10 ELECTRONIC CALIBRATION DATA 6/24/73  
 ~ 1000 Readouts to Define Each Channel Number

<u>mV</u>	<u>D1</u> Channel	<u>D2</u> Channel	<u>D5</u> Channel
1.00	3.48	4.12	3.59
1.25	4.49	4.77	4.12
1.50	5.13	5.92	4.78
1.75	5.93	6.91	5.64
2.00	6.93	7.76	6.48
2.25	7.83	8.74	7.36
2.50	8.76	9.86	8.16
3.00	10.52	11.81	9.65
4.00	14.05	15.75	12.81
5.00	17.74	19.76	16.14
7.50	26.61	29.58	24.08
10.00	35.26	39.11	31.71
15.00	53.26	59.02	47.77
20.00	71.34	78.60	64.07
22.50	80.14	88.42	71.77
24.00	85.49	93.51	76.46
25.00	88.94	95.43	79.55
26.00	92.33	96.61	82.65
27.50	97.76	98.17	87.62
30.00	106.13	100.53	95.70
32.50	110.42	102.97	103.76
35.00	112.07	104.31	111.74
36.00	112.67	104.74	115.05
37.50	113.26	105.48	118.79
40.00	114.40	106.57	121.71
45.00	115.37	108.73	123.72
50.00	117.98	111.26	125.25
60.00	121.87	115.99	129.9
70.00	126.27	120.16	134.08
75.00	128.31	122.04	136.11
100.00	137.26	132.65	145.35
150.00	155.87	155.28	164.26
160.00	159.81	159.96	168.35
165.00	161.65	162.04	170.18
170.00	163.57	164.04	172.04
175.00	165.58	165.75	174.02
180.00	167.52	166.93	175.89
190.00	170.76	168.66	179.71
200.00	172.36	169.89	183.44
300.00	182.06	180.17	220.68
350.00	185.72	184.18	239.03
400.00	189.34	188.06	250.00
500.00	195.66	195.43	
600.00	201.60	202.32	
1000.00	226.40	231.74	
1200.00	238.18	245.42	

Table II-10  
MARINER 10 D7 CALIBRATION

<u>DN*</u>	<u>mV</u>	<u>HZ</u>
0	27.6	5.52
5	144.6	56.8
10	261.6	129.3
15	378.6	235.8
20	495.6	489.4
25	612.6	1101
30	729.6	2255
35	846.6	3846
40	963.6	6272
45	1081	8792
50	1198	11.94 x 10 <sup>3</sup>
55	1315	14.76 x 10 <sup>3</sup>
60	1432	18.35 x 10 <sup>3</sup>
65	1549	22.37 x 10 <sup>3</sup>
70	1666	26.11 x 10 <sup>3</sup>
75	1733	30.32 x 10 <sup>3</sup>
80	1900	35.00 x 10 <sup>3</sup>
85	2017	39.68 x 10 <sup>3</sup>
90	2134	44.80 x 10 <sup>3</sup>
95	2251	50.05 x 10 <sup>3</sup>
100	2368	55.48 x 10 <sup>3</sup>
105	2485	62.24 x 10 <sup>3</sup>
110	2602	70.14 x 10 <sup>3</sup>
115	2719	77.92 x 10 <sup>3</sup>
120	2836	86.88 x 10 <sup>3</sup>
125	2953	96.24 x 10 <sup>3</sup>

\*Analog "data number" see Section III.1.b

MARINER 10 LET ELECTRONIC CALIBRATION DATA 6/25/73  
 ~ 1000 Readouts to Define Each Channel Number

<u>mV</u>	<u>LI CHANNEL</u>	<u><math>\Delta CH / \Delta MV</math></u>
1.5	5.40	3.6
2.0	6.80	2.8
3.0	10.37	3.57
4.0	13.95	3.58
5.0	17.50	3.55
6.0	21.09	3.59
8.0	28.27	3.59
9.0	31.86	3.59
10.0	35.47	3.61
12.0	43.06	3.79
14.0	50.30	3.62
16.0	57.51	3.60
18.0	64.79	3.64
20.0	72.04	3.62
22.0	79.21	3.58
24.0	86.57	3.68
26.0	93.63	3.53
28.0	101.03	3.70
30.0	108.15	3.56
32.0	115.28	3.56
33.0	118.8	3.52
34.0	121.76	2.96
35.0	122.0	.24

Figure II-1. This figure is a schematic view of the two University of Chicago charged particle telescopes onboard the Mariner 10 spacecraft. The detectors denoted with an asterisk are pulse height analyzed. The detectors are numbered sequentially starting from the top of the opening cone of each telescope. The detectors are placed in various coincidence combinations as described in Section II. Counting rates for selected combinations are accumulated and read out along with pulse height analyses in the data format described in Appendix A.

Mariner 10  
The University of Chicago

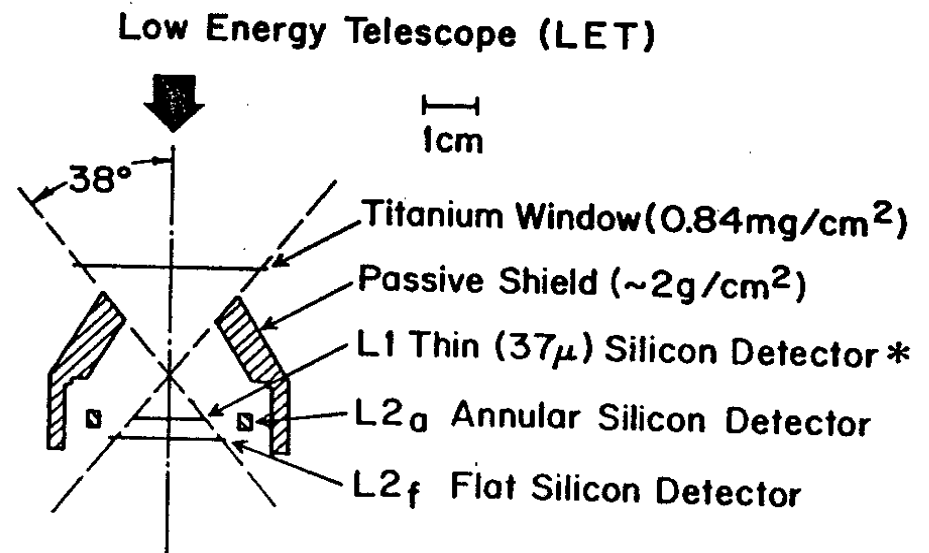
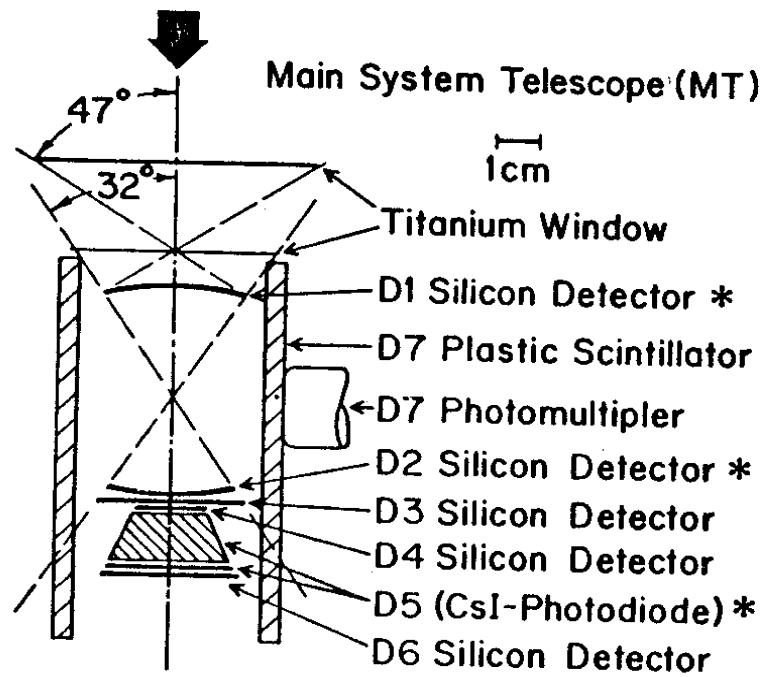


Figure II-2

University of Chicago Charged Particle Telescope Energy Intervals for MT Nucleonic.

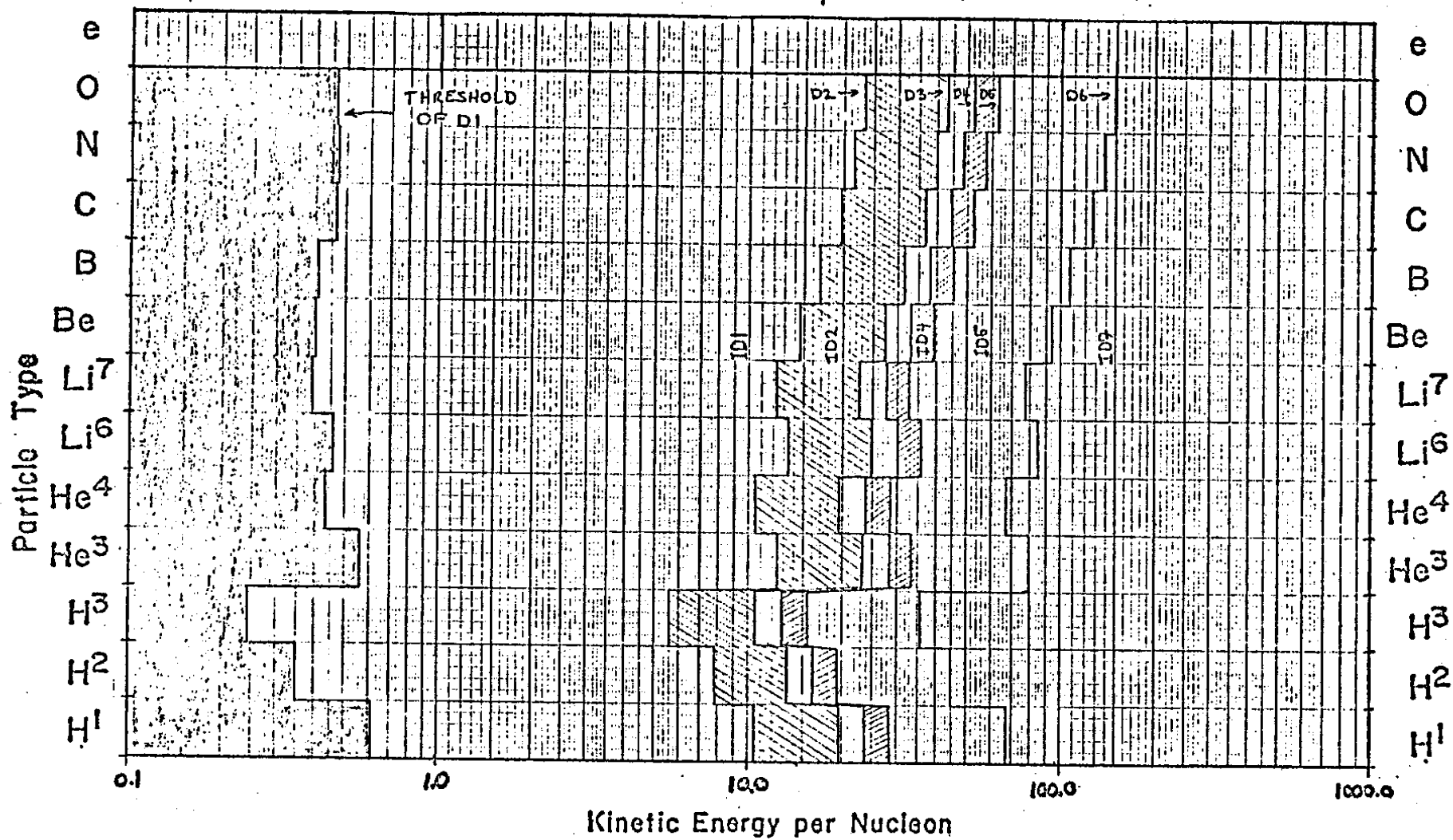


Figure II-3  
D1, D2, D5, and L1  
Pulse Height Analysis Channels vs. millivolts  
(Plots of Tables II-9 and II-11)

CHANNEL

MVM '73 LET CALIBRATION 6/25/73

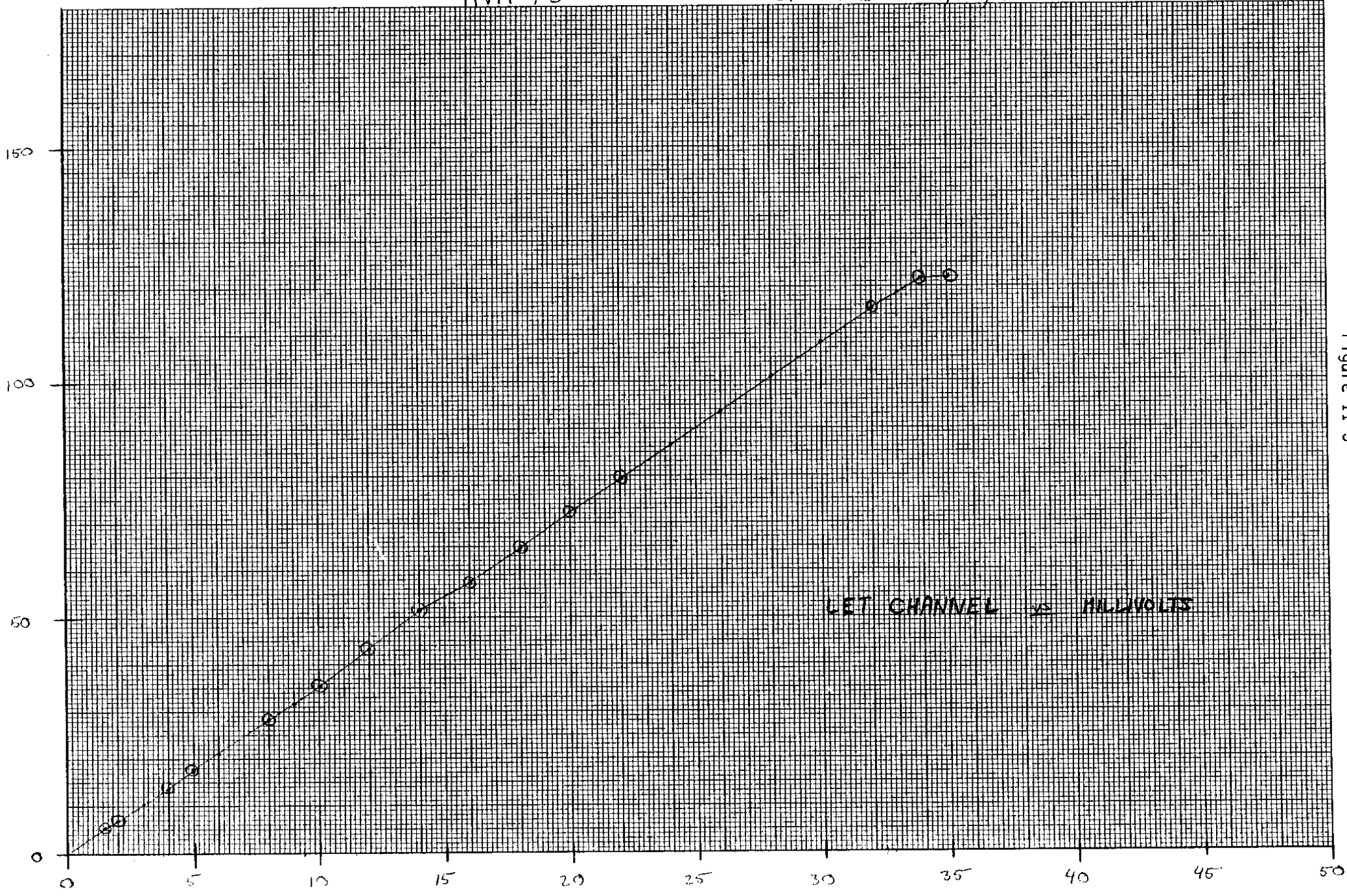


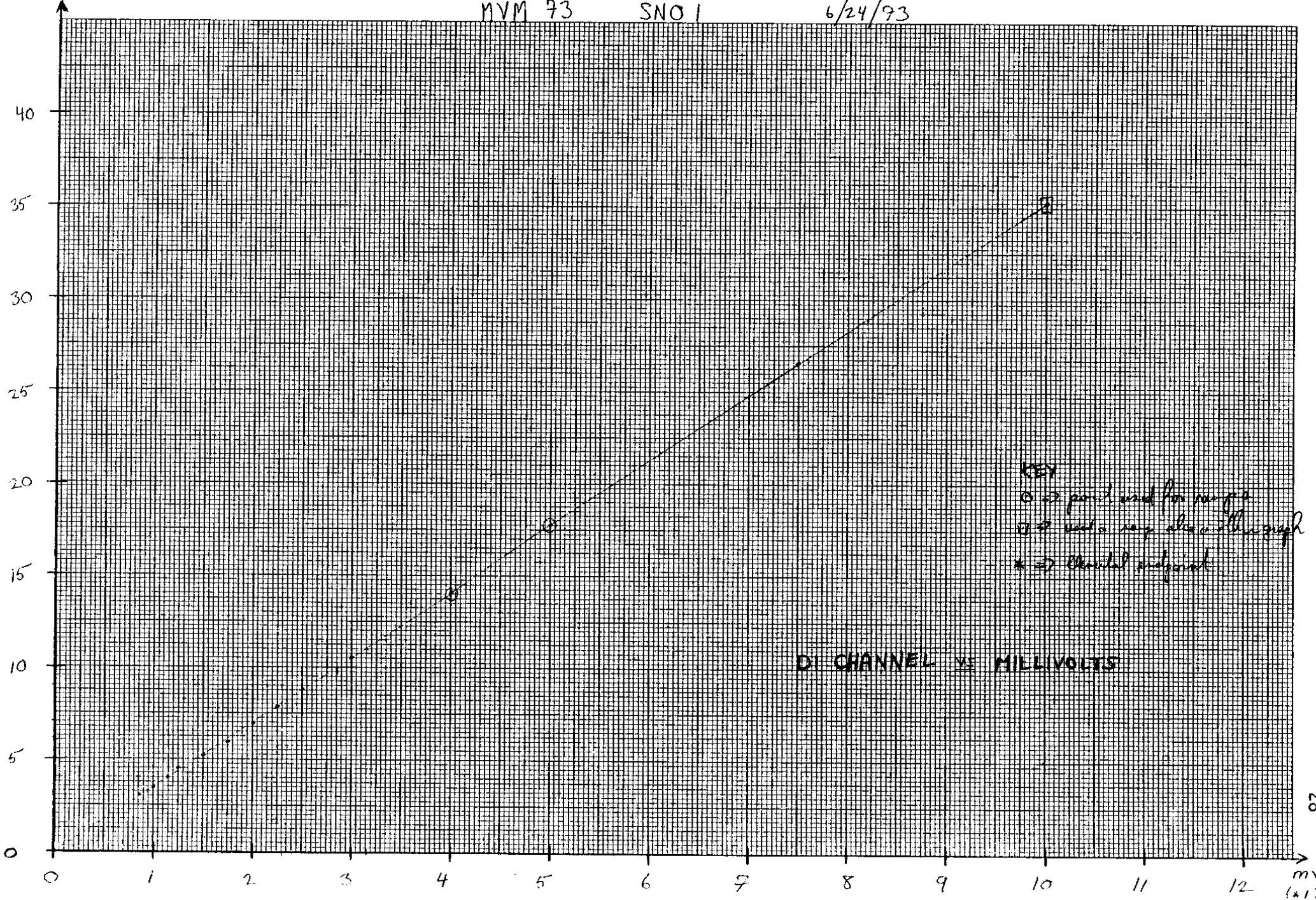
Figure II-3

MVM '93

SNO 1

6/24/93

CHANNEL



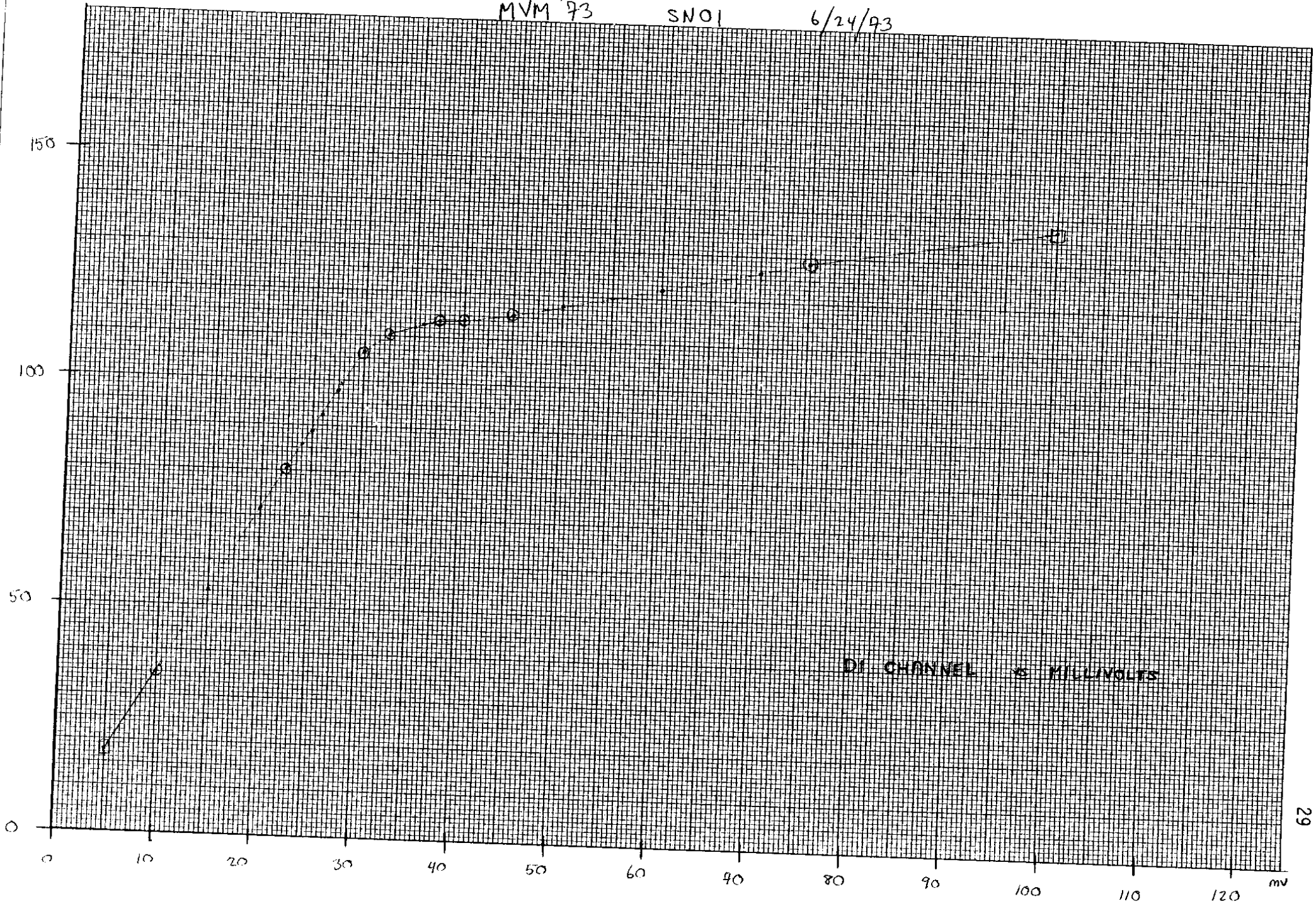
KEY  
○ → point used for range  
□ → used range also with graph  
\* → channel adjustment

CHANNEL

MVM '93

SNO1

6/24/93



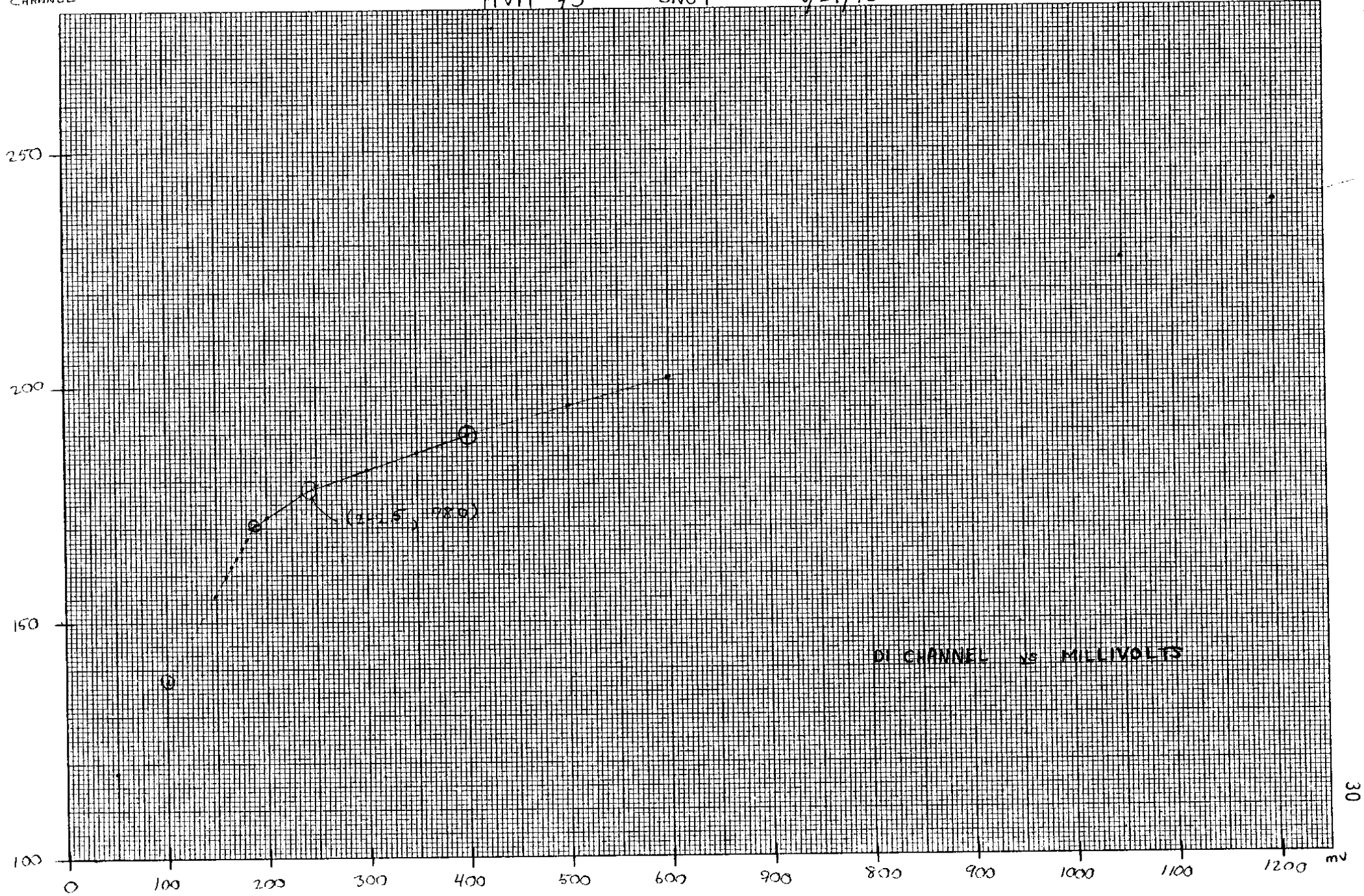
DI CHANNEL MILLIVOLTS

CHANNEL

MVM '73

SN01

6/24/73



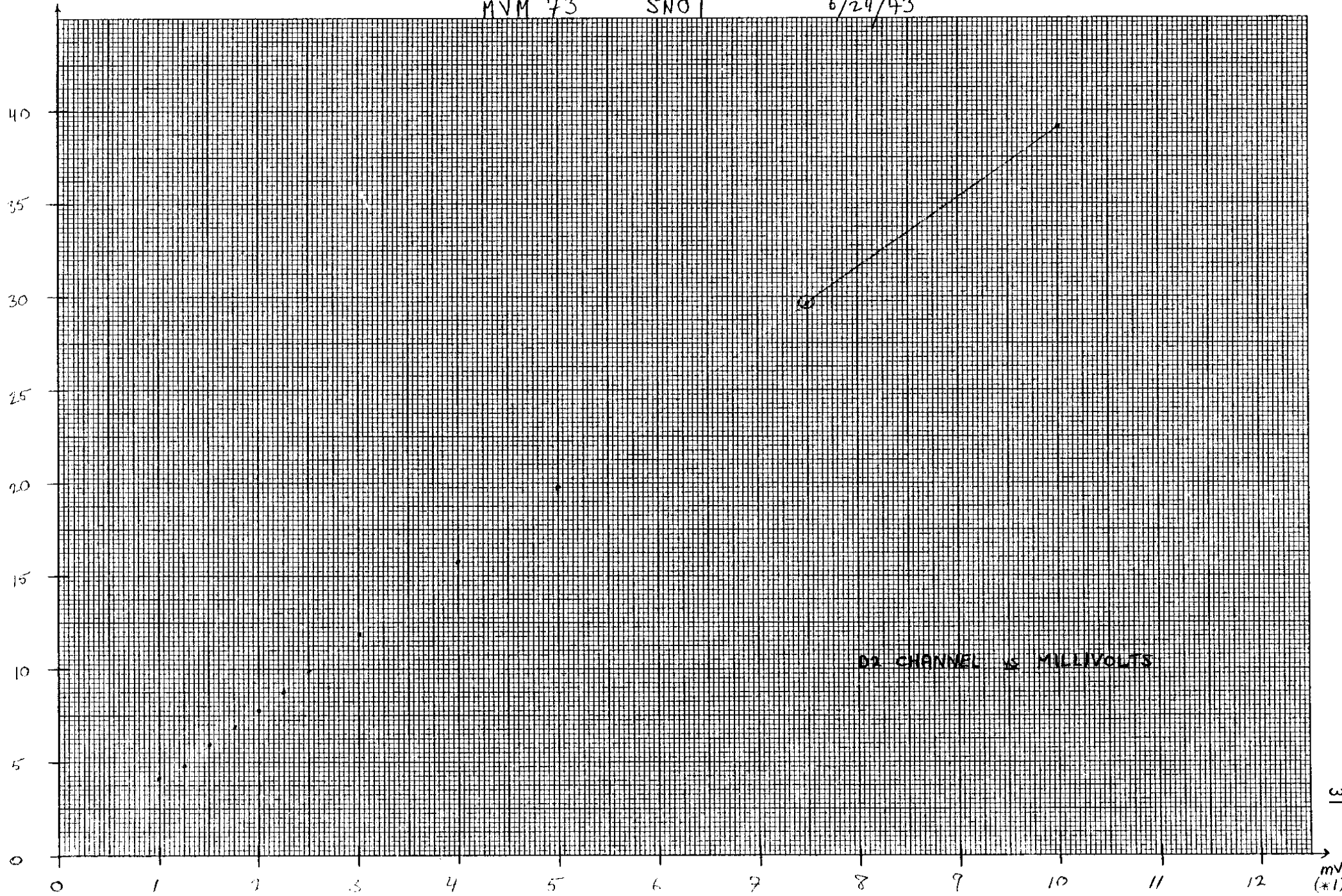
30

CHANNEL

MVM '73

SNO 1

6/24/73

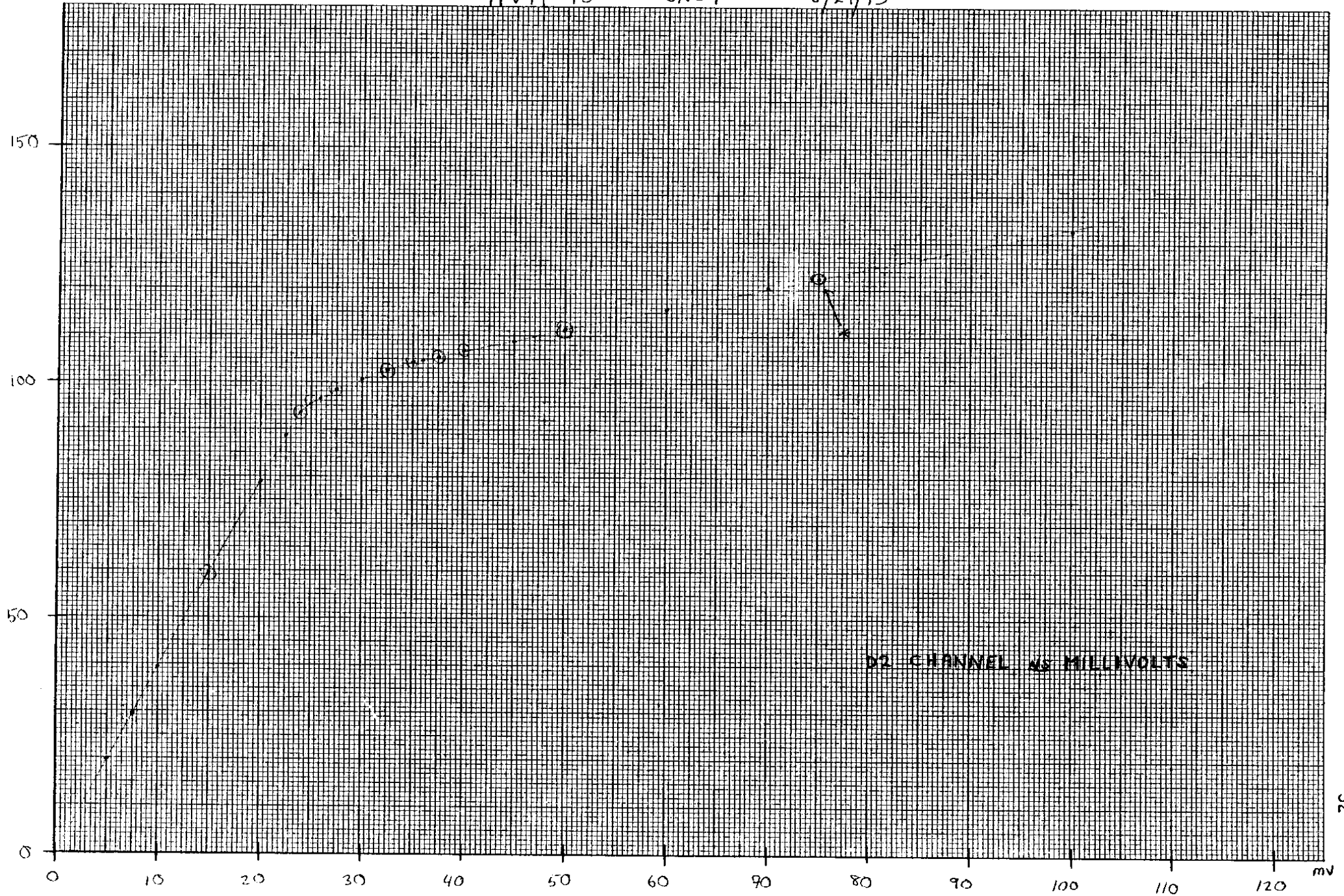


CHANNEL

MVM '93

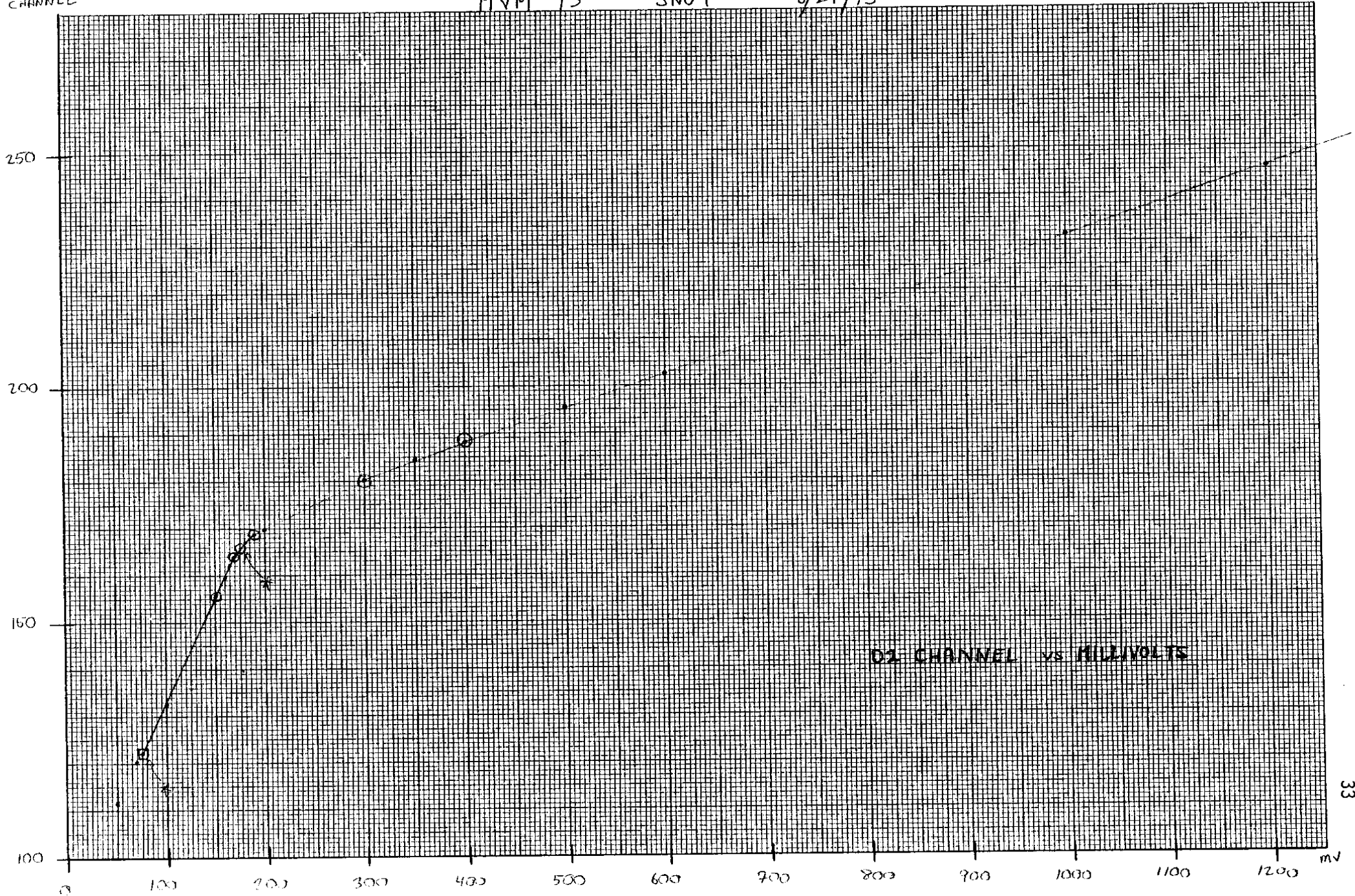
SNO1

6/24/93



CHANNEL

MVM '93 SNO1 6/24/93

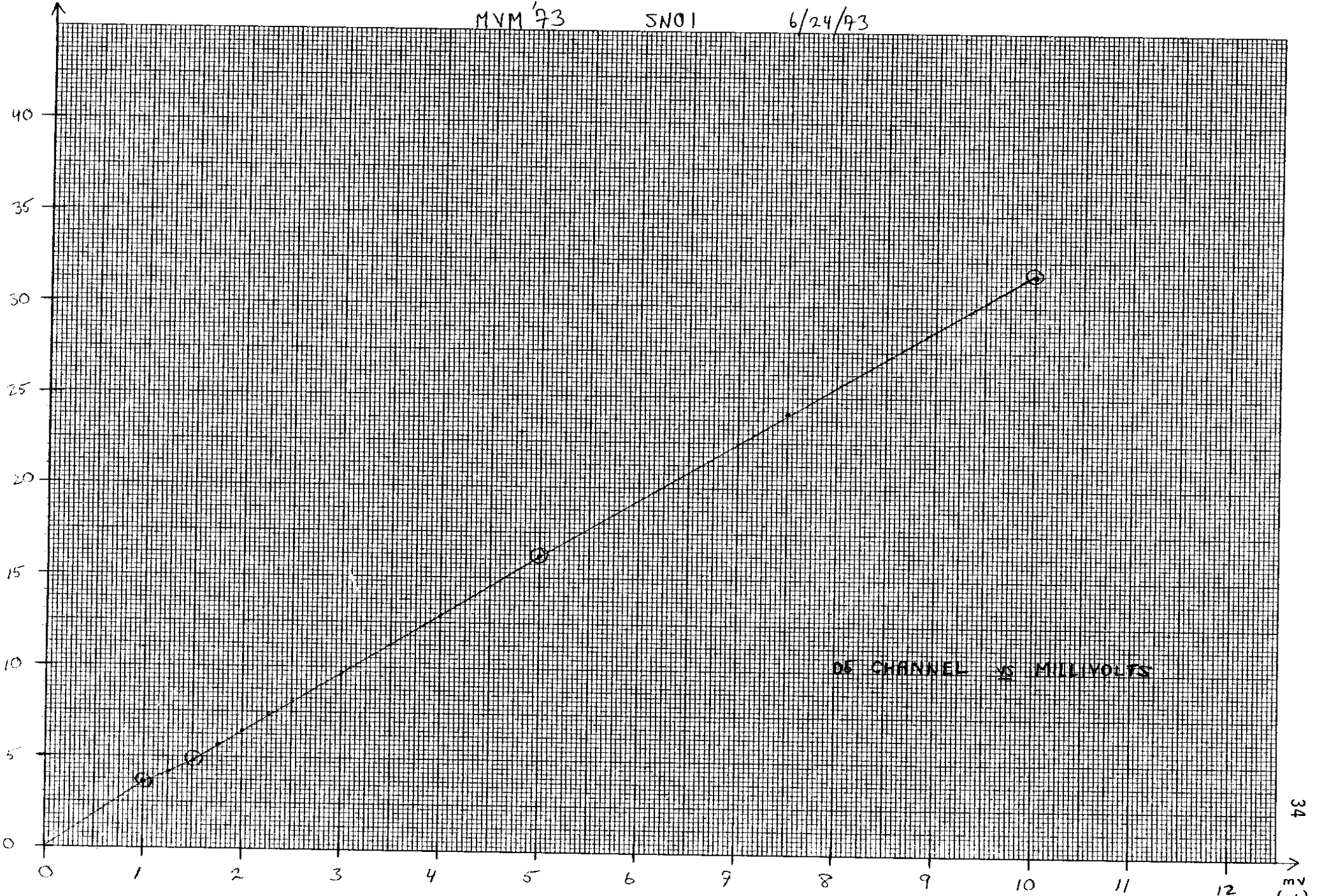


MVM '73

SN01

6/24/73

CHANNEL



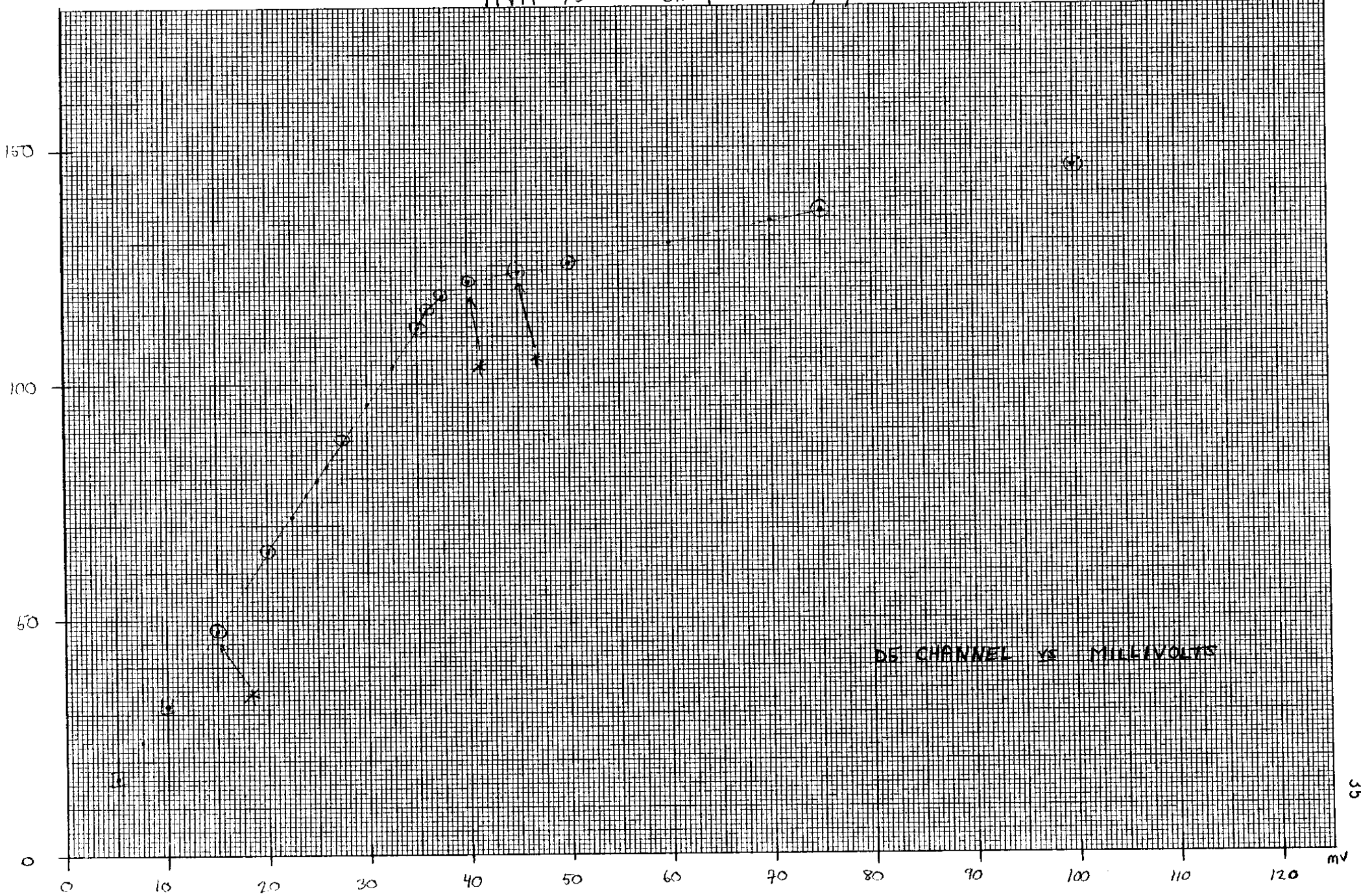
34  
23  
13

CHANNEL

MVM '73

SNO 1

6/24/73



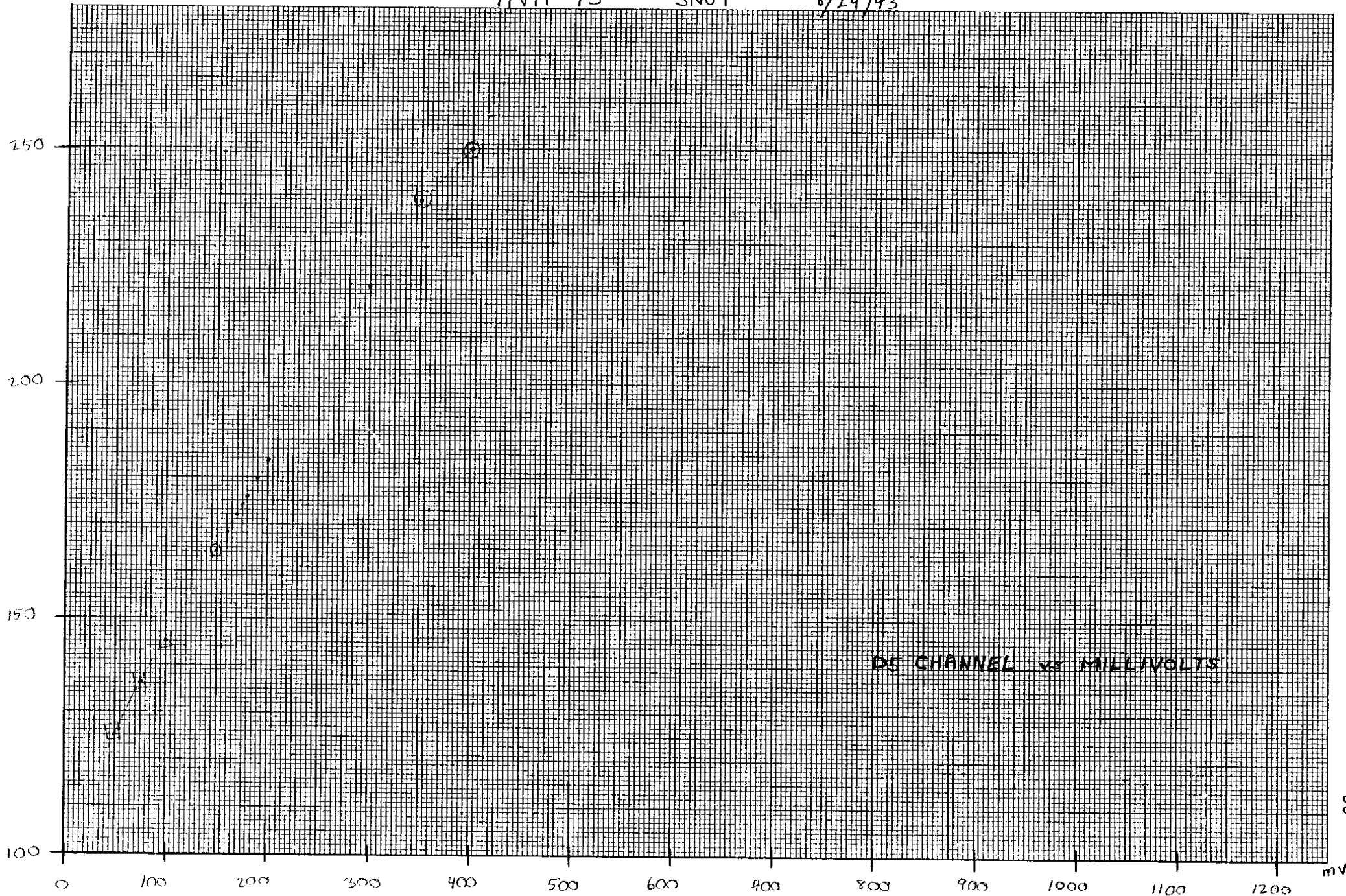
35

CHANNEL

MVM '73

SN01

6/24/93



DS CHANNEL vs MILLIVOLTS

Figures II-4  
"ELOSS" GRAPHS\*

KEY

MVM: MARINER VENUS MERCURY  
SNT: SERIAL #1 (THE FLIGHT UNIT)  
MLC: MEDIAN INCIDENCE LARGE CONE  
MSC: MEDIAN INCIDENCE SMALL CONE  
1,2,5: DETECTOR 1,2,5  
F: FORWARD INCIDENCE  
B: BACKWARD INCIDENCE

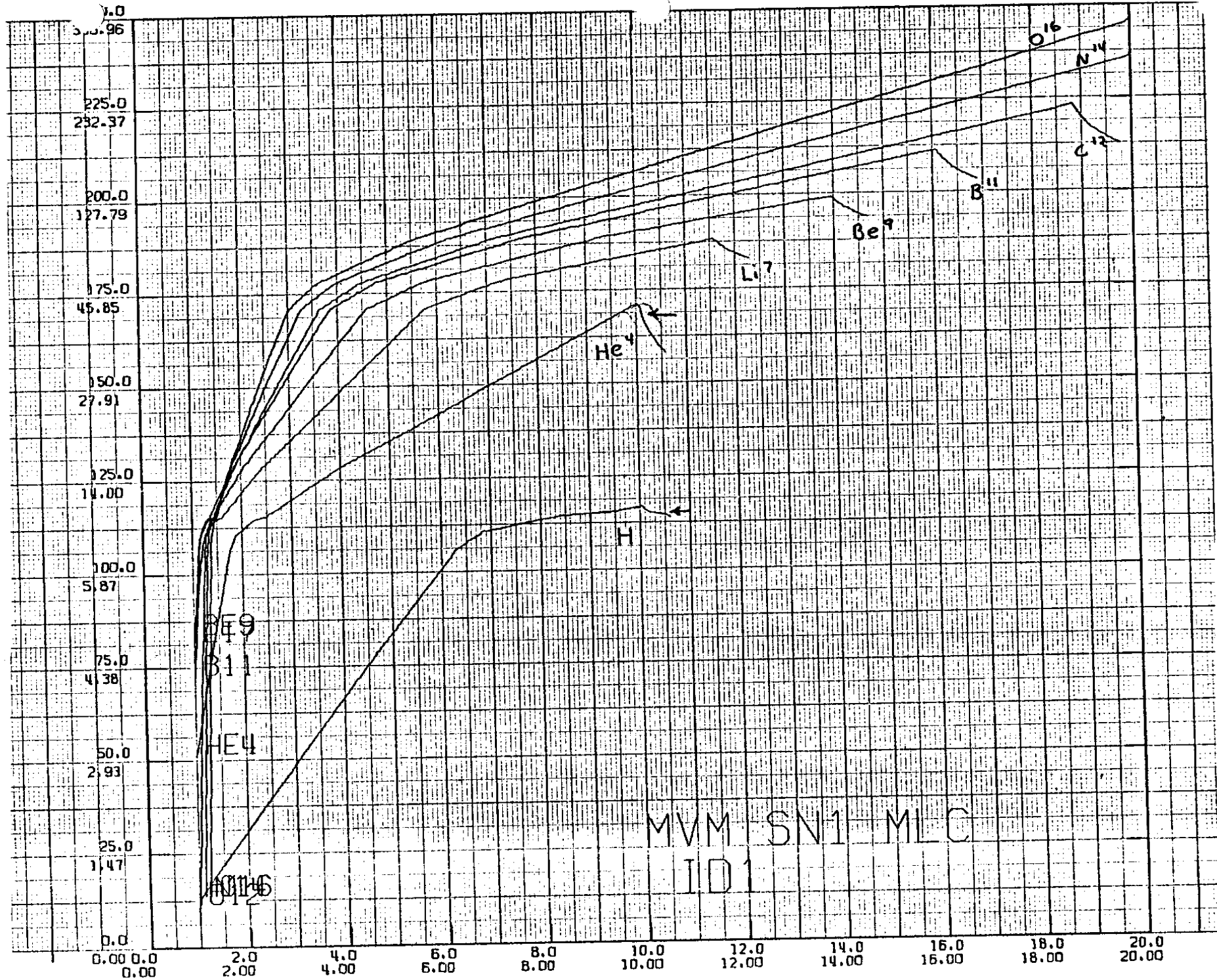
The usual label of the graph scales is:

CHANNEL  
MeV Deposited in Detector

When plotting ID1, DI, D2, or D5 vs E the abscissa is:

"Incident Energy At Top of Telescope"

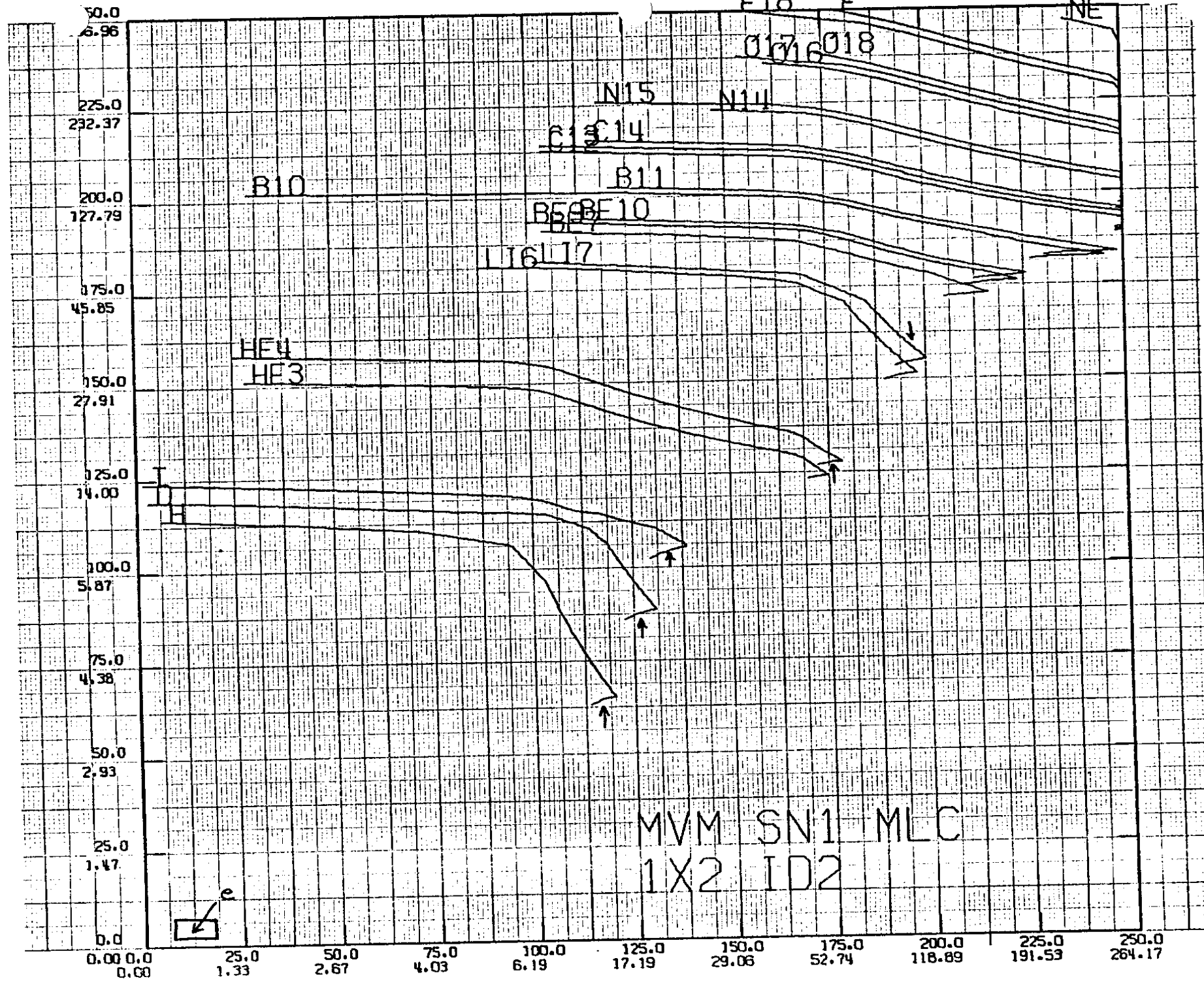
\* See Section II.

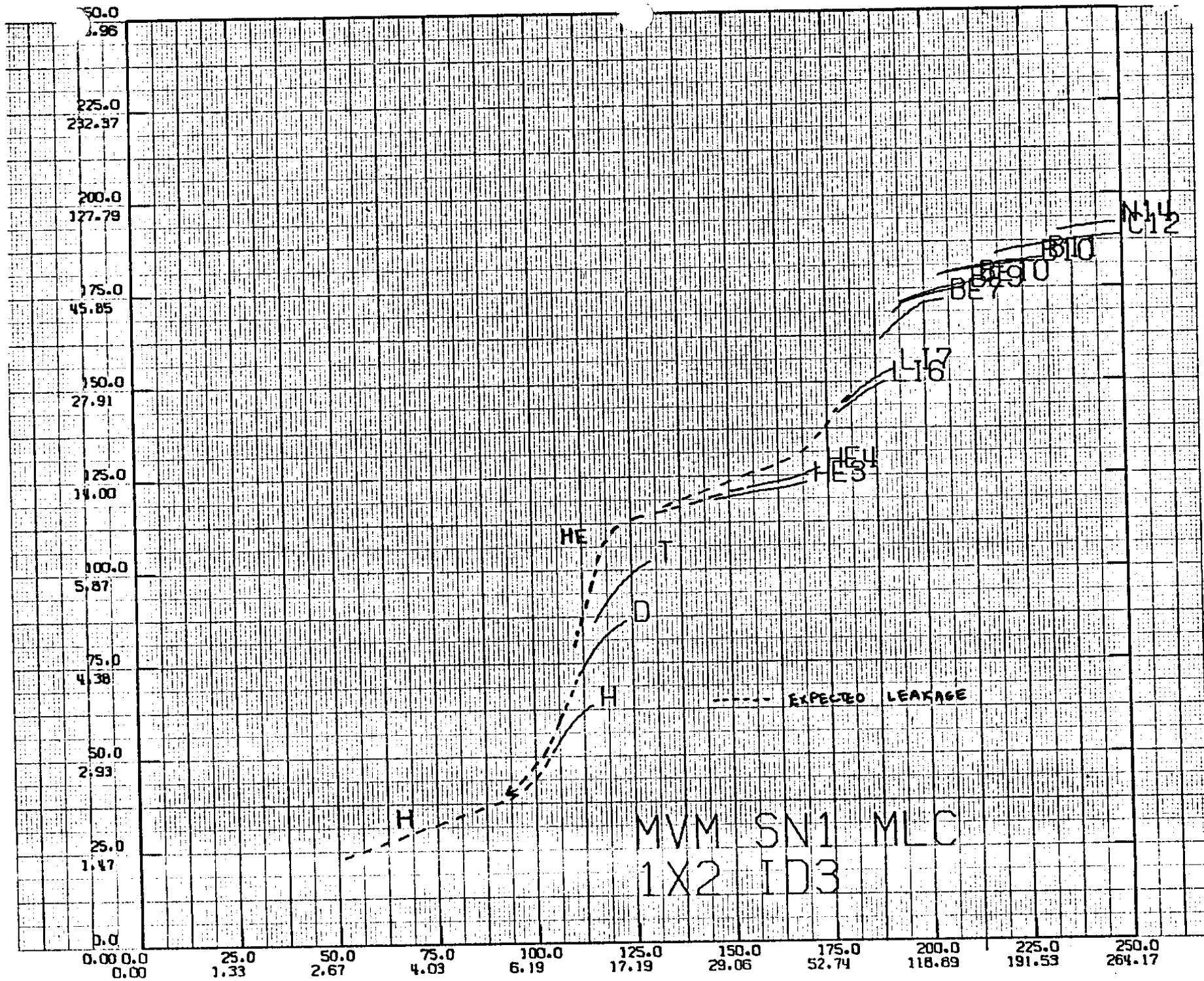


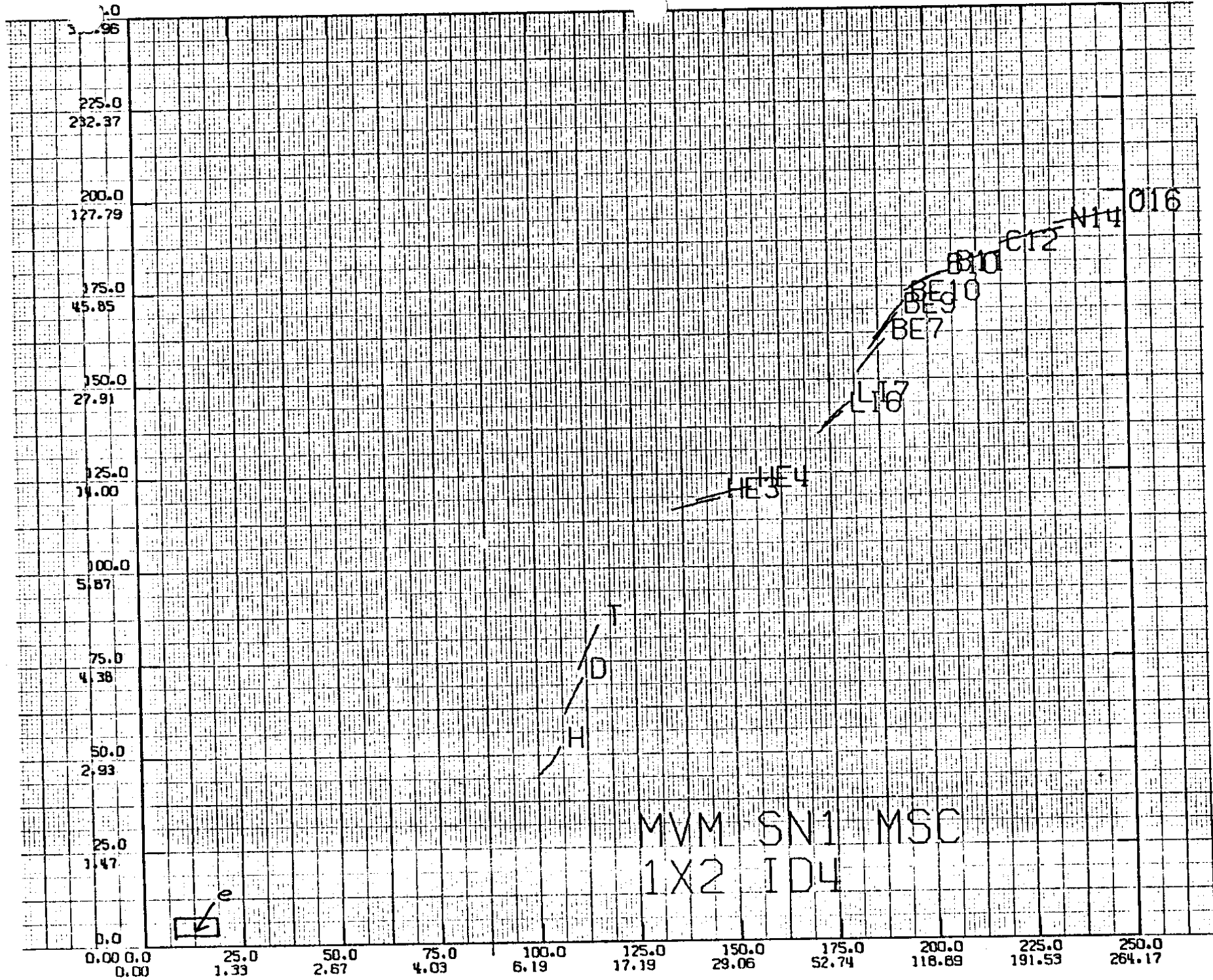
10/13/73

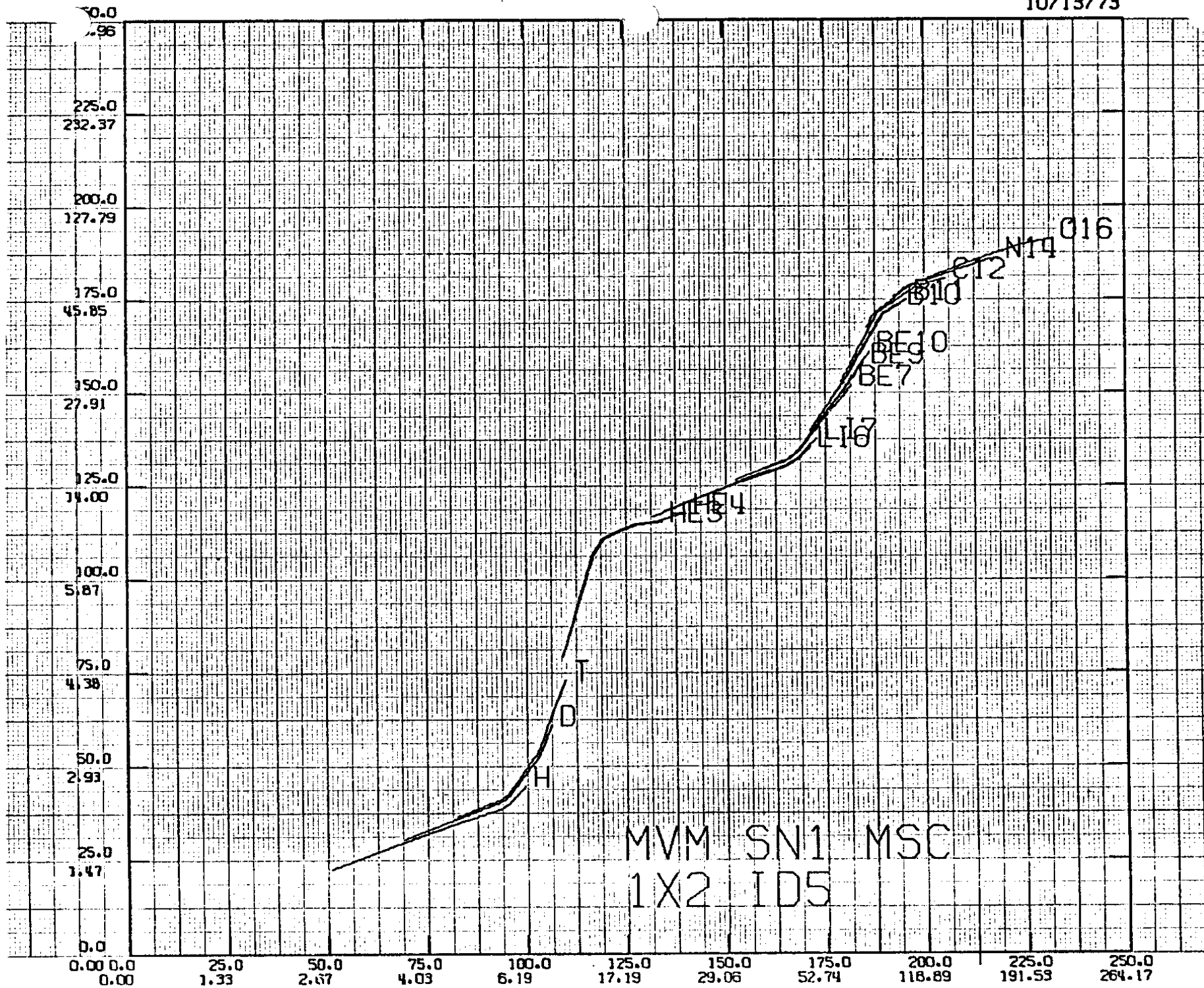
E18 E

NE

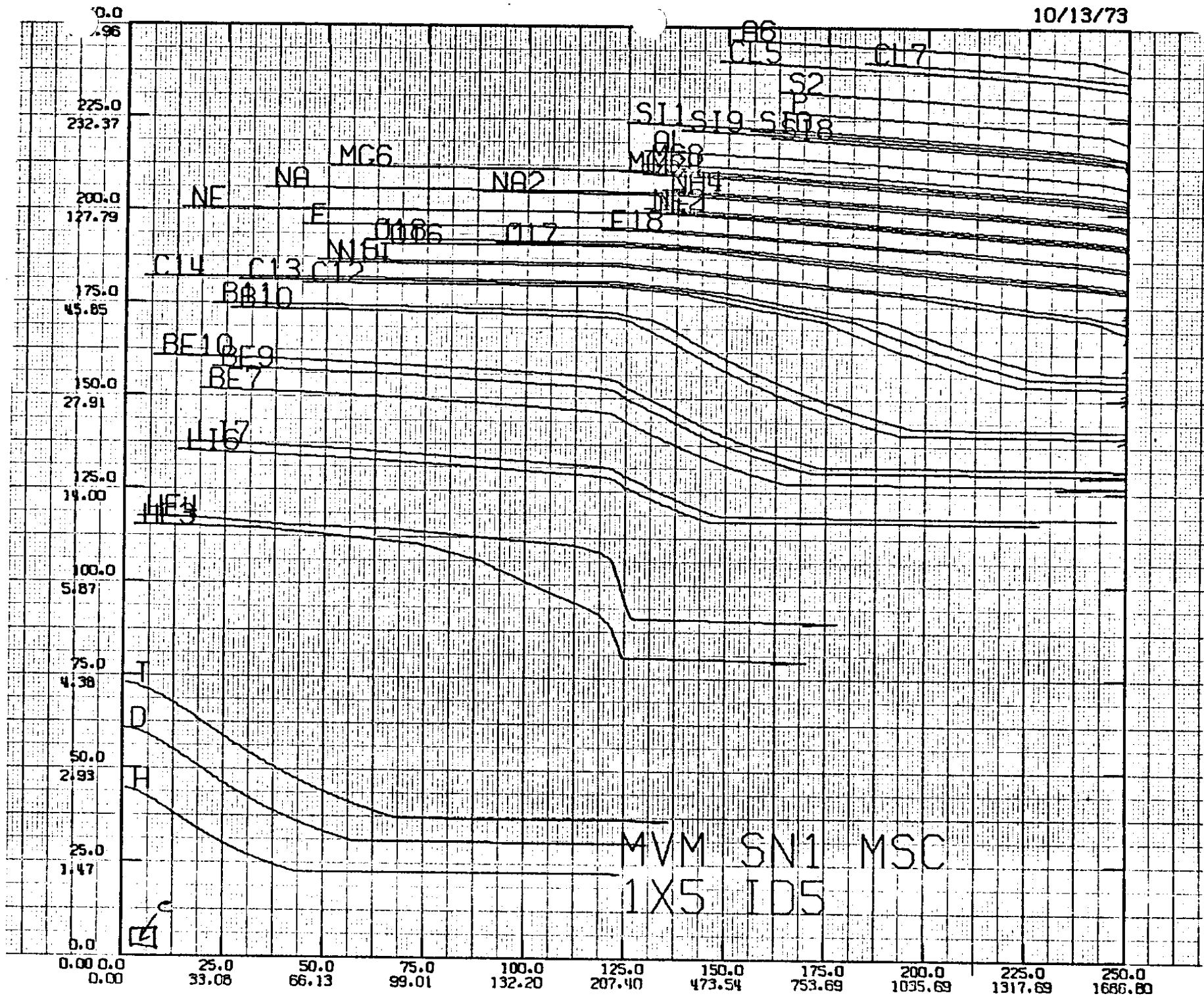


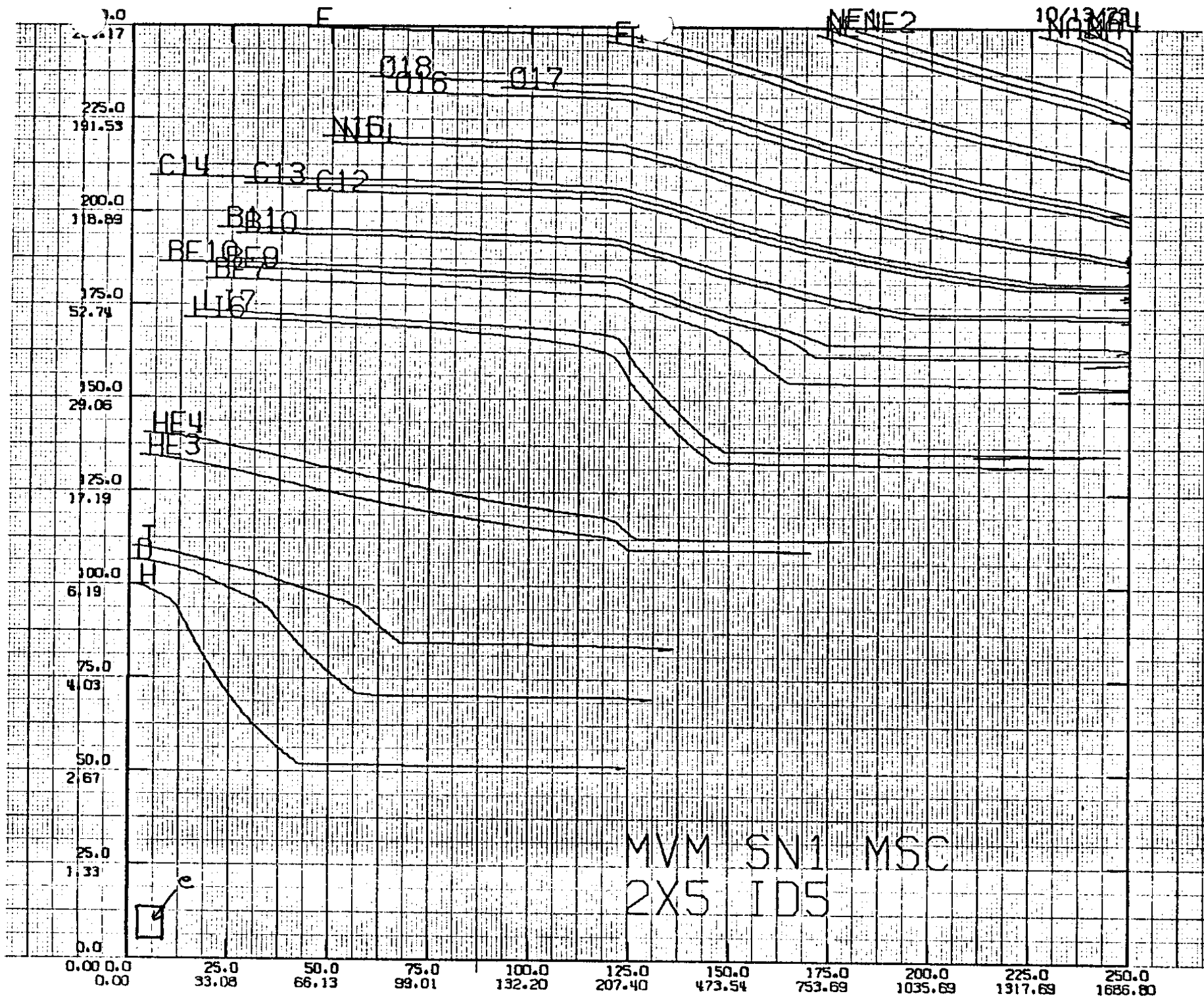


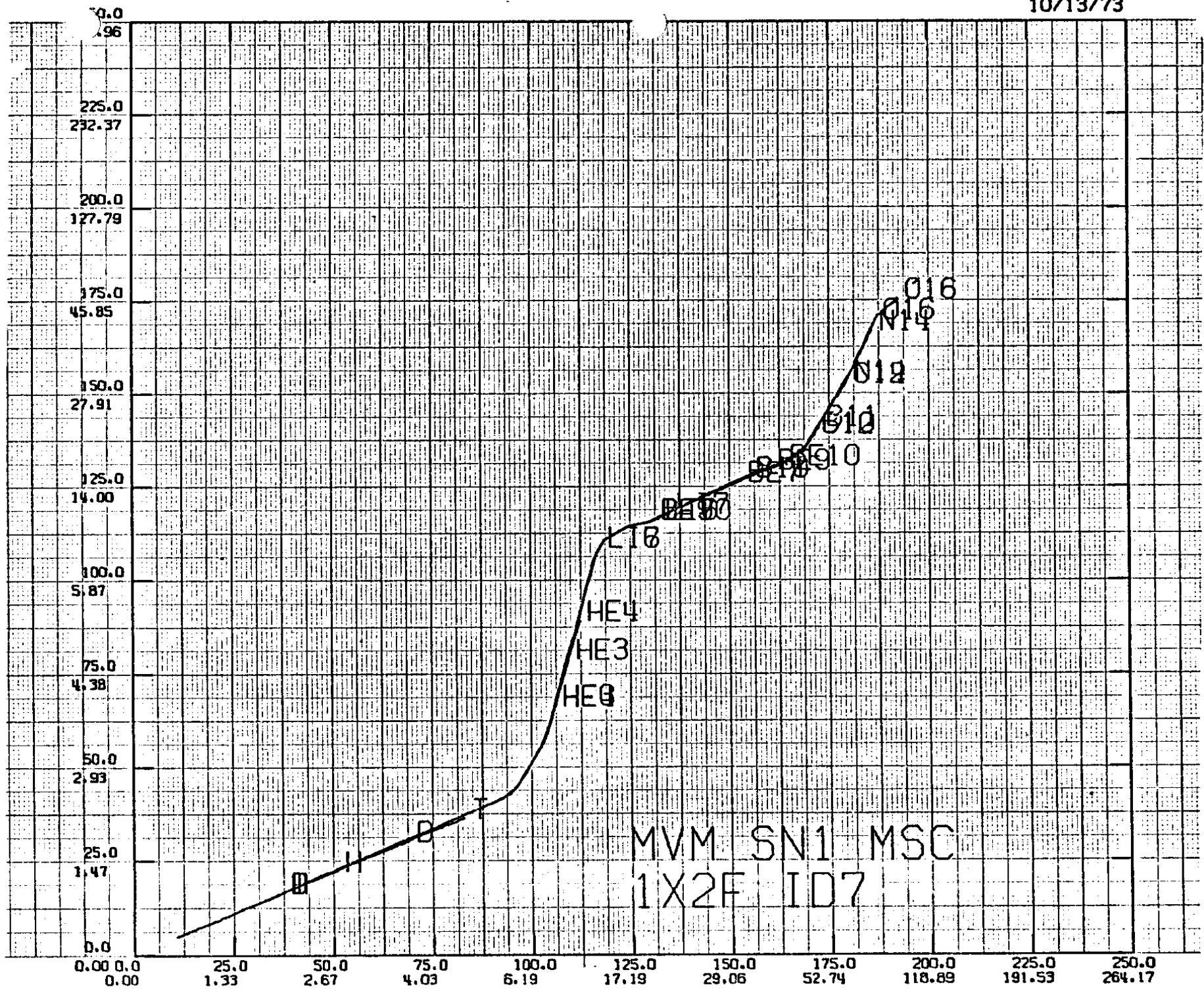




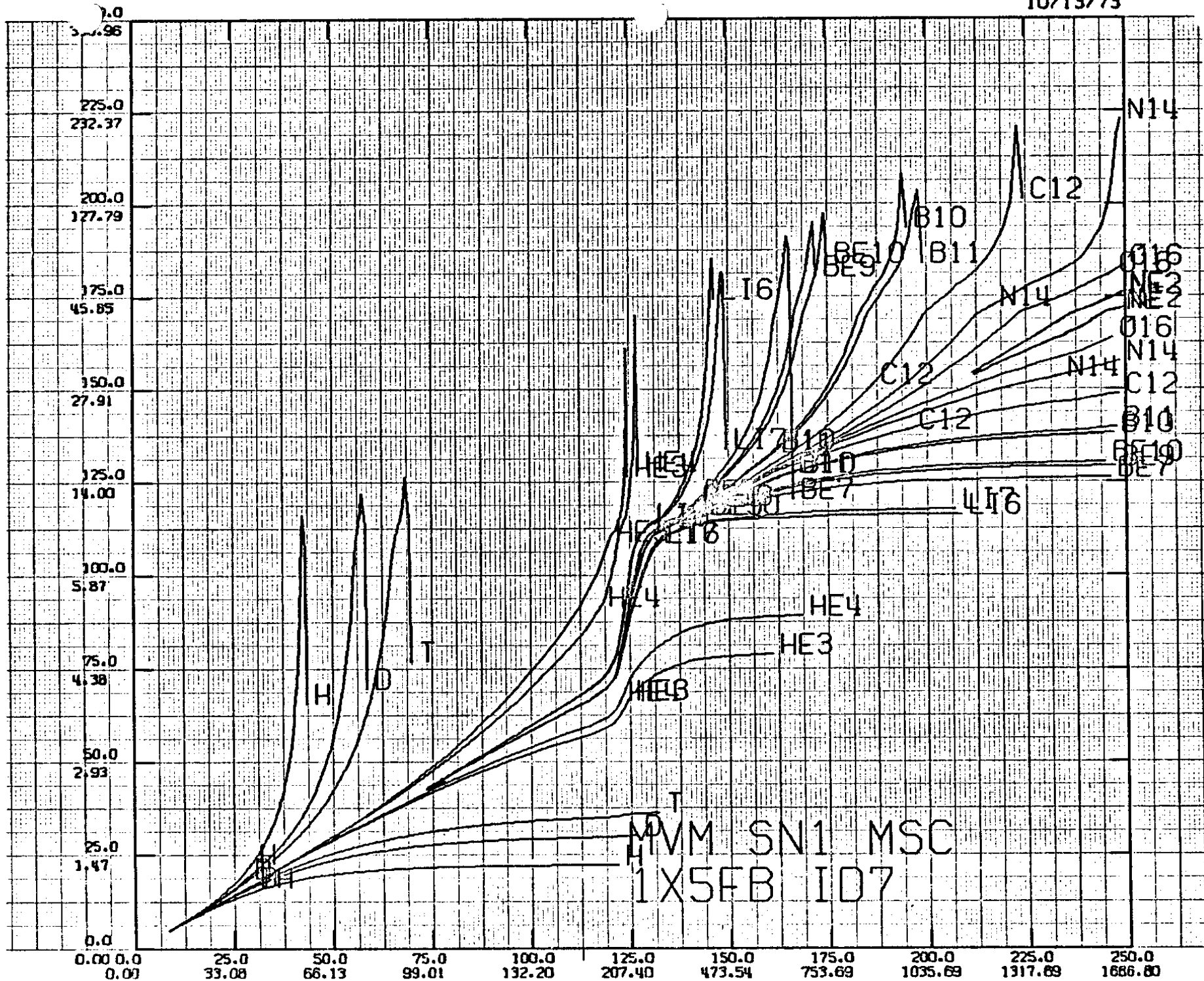
10/13/73

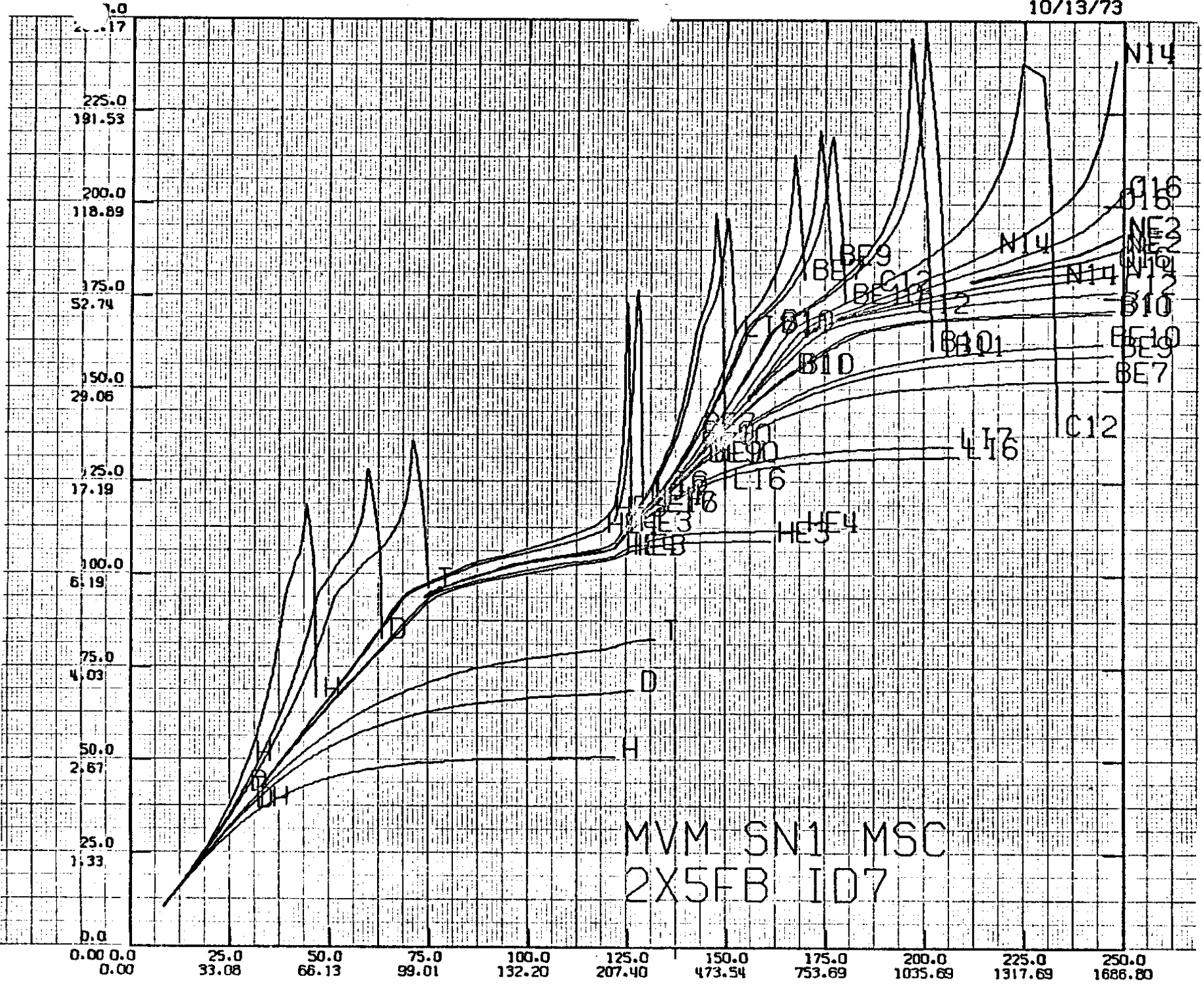












III.  
Documentation of the Mariner 10 Data Tapes  
Submitted by the  
University of Chicago

### A. Introduction

The University of Chicago submission of data from the Mariner 10 spacecraft consists of 2 sets of data tapes containing, respectively, the computed counting rates from the UC/CPT and the collected pulse height data from that instrument for the entire mission from launch through the end of the extended mission (that is, from Day 307, 1973 through Day 80, 1975). An electronic and physical description of the charged particle telescope, its calibrations, and the definitions of energy range, "IDs", and particle species for the rate and pulse height data is described in Section II. The sections below which describe the tapes will use the detector and ID specifications as defined in Section II.

The data tapes submitted to the National Space Sciences Data Center (NSSDC) are relatively independent of the Mariner 10 spacecraft data system mode. The exceptions are noted in the description of the rate tape below; however, detailed descriptions of the Mariner 10 spacecraft, its interface with the UC/CPT, the purpose for the mission, etc. are available from references in Section I and Appendix A.

The tapes submitted to the NSSDC are industry-standard 7-track 800 bpi binary magnetic tapes. The data as recorded thereon is a mixture of fixed-point (integer) data in 2's-complement 24-bit word form, 48-bit floating point (see Figure III-1 for the Computer-Word format) and 24-bit flag words. Each of these data representations is specified in the tape formats below.

### B. UC/CPT Counting Rate Average Tape

#### Rate Tape Format and Content:

The UC/CPT measured counting rates in 8 energy intervals (See Table II-5; the abbreviations for the rates specified there are used in the following). While the particle counts upon which these rates were computed were all accumulated over the same time interval, they were read out of the Mariner 10 spacecraft data system at three different times. The rates D2-6 and D12 were read out at the same time and are referred to as "R1-frame" rates. The scalers for D1-6D7, D1-5D67 and the L1L2 rate scalers produce "R2-frame" rates while the L1L2 and D1D27 produce the "R3-frame" rates. Although the R1, R2 and R3-type rates are read out of the instrument on different frames and therefore at slightly different times, the times over which all rates are accumulated is the same; thus, the "interval start time" and "interval stop time" specified below give the times between which counting rates appearing in all frame types were accumulated. Since the different frame rates are read out at different times (that is, in different spacecraft data-frames), there may be differences in the effective data coverage; therefore, separate data coverage times are provided for each rate type.

An analog rate for the D7 detector is also present. This value is converted from the "data number" (DN) which is a sample of the output of the analog rate meter readouts during the interval of time specified for the rates above.

An "observation" as it is recorded on the rate tape is defined to be the collection of all of the rates computed over a 1-minute interval of real-time together with some identifying information, data quality indicators and supporting spacecraft or instrument parameters. It is recorded as a logical record of 44 24-bit words. Twelve such logical records are collected together and recorded on tape as a physical record (that is, as 528 24-bit words plus an end-of-record gap). All records on the tape will contain 12 non-zero logical records except--possibly--the last physical record; this record may contain from 1-12 non-zero logical records, any part-filled records being filled with zeros. If the last physical record on a data tape does contain 12 non-zero logical records, then an additional physical record of all zeros will be placed on the tape; the tape is then terminated with a double end of file. No other end of file marks occur on the rate tape.

Figure III-2 gives the content of a logical record by word number and bit value within the 24-bit word. The following paragraphs describe each of the words (or word-pairs, as required) in the detail necessary to allow a user to utilize the data.

Word 1: Bits 0-11 of word 1 give the year as an unsigned 12-bit integer 1973-1975. The spacecraft number (in bits 12-23) is a 12-bit unsigned integer and is always zero.

Word 2: This is a status word of which bits 10-23 are used as flags to indicate spacecraft or instrument operating status during the time interval reported in this logical record. The bits in the status word will be set for all states of the data which occurred during this interval; in particular, if any of the instrument commands are sent from the ground and accepted by the instrument during the interval, the bit for that command will be set to 1, otherwise it will be zero. If any of these commands were to be enabled or disabled several times during any observation interval, there would be no indication of how often this occurred. The content of these flags and status bits are as follows:

Bits 10-11: Engineering rate (see Table III-1)

Bits 12-13: Spacecraft engineering format (see Table III-1)

Bits 14-16: Spacecraft operating mode (see Table III-1)

Bits 17-18: Spacecraft transmission bit rate  
 Bit 17 is set if any 2,450 bit per second data was transmitted during the observation interval, while bit 18 is set if there was any 490 bit per second transmission during the observation interval.

Bits 19: Set to one if the X1 command was sent during the observation interval (see Section I for the description of these commands.)

- Bit 20:** Set to one if the X2 command was sent during the observation interval.
- Bit 21:** Set to one if the X7 command was sent during the observation interval.
- Bit 22:** Set to one if the calibrate command was received by the UC/CPT during the observation interval.
- Bit 23:** Set to one if the priority override (see instrument description) command was received by the UC/CPT during the observation interval.

Word 3: The spacecraft Master Data Record (MDR) status is described in Figure III-1. This status word can be considered as a 24-bit, unsigned integer.

Word 4: The ground data handling stations for the Mariner spacecraft appended a data quality indicator (DQI) to the data as it was recorded on the ground. This DQI indicated whether all accumulator values contributing to a rate calculation were taken from frames of the highest quality or whether some of the values were taken from frames of lower transmission quality. In general, the rate tapes used only good data frames, but under some conditions all frames were included in a rate computation. The number of "unreliable" frames which were included in the rate computation are recorded as an unsigned integer in bits 0-11 of word 4. The number of good frames is similarly recorded in bits 12-23. A user of the rate tape may elect to ignore any periods which include any "unreliable" frames.

Words 5-6: This is the time of the beginning of the count-accumulation interval over which this observed rate was computed. This is a floating-point number. The units are in seconds of the year (1-31,622,400).

Words 7-8: This is the time of the ending of the count-accumulation which was used to compute the rate for this observation. The units are the same as Words 5-6.

Words 9-10: The floating point seconds of coverage for the R1 (see the explanation above) from rates. The total coverage for a particular frame-rate type may or may not be the same as the interval (Words 5-8) because the rate-computation algorithm may suspend count-accumulation for a given frame rate type if transmission noise caused the loss of 1 or more frames of that frame rate type. Such data gaps may decrease the total number of seconds for which valid-count data was available during the observing interval.

Words 11-12: This is the floating-point seconds of coverage for the R2-frame rate type.

Words 13-14: This is the floating-point seconds of coverage for the R3-frame rate type.

Words 15-16: A 48-bit floating-point word giving the computed rate in

counts per second of the R1 frame rate, D2-6.

Words 17-18: A 48-bit floating-point word giving the computed rate in counts per second of the R2 frame rate, D12.

Words 19-20: A 48-bit floating-point word giving the counting rate in counts per second of the R2 frame rate, D1-6D7.

Words 21-22: A 48-bit floating-point word giving the counting rate in counts per second of the R2 frame rate, D1-5D67.

Words 23-24: A 48-bit floating-point word giving the counting rate in counts per second of the R2 frame rate, L1L2.

Words 25-26: A 48-bit floating-point word giving the counting rate in counts per second for the R3 frame rate, L1L2.

Words 27-28: A 48-bit floating-point word giving the counting rate in counts per second of the R3 frame rate, D1D27.

Words 29-30: A 48-bit floating-point word giving a sample counting rate in counts per second of the analog D7 rate meter data number (DN) during the 1-minute interval.

Words 31-32: A 48-bit floating-point word giving the CPT temperature in degrees Fahrenheit during the 1-minute interval.

Words 33-34: A 48-bit floating-point word giving a sample of the temperature of the spacecraft bay nearest to the CPT (bay 7) in degrees Fahrenheit during the 1-minute interval.

Words 35-36: A 48-bit floating-point word giving a sample of the temperature in degrees Fahrenheit of the spacecraft battery during the 1-minute interval.

Words 37-38: A 48-bit floating-point word giving a sample of the spacecraft buss voltage in volts during the 1-minute interval.

Words 39-40: A 48-bit floating-point word giving a sample of the buss current in amperes during the 1-minute interval.

Words 41-42: This is an artificial end-of-interval time. It is normally the end of each 1-minute interval (expressed as seconds of year) from an initial time specified during the processing run which generated the particular rate tape. It is normally initiated at the beginning of a particular day at hour zero and minute zero.

Words 43-44: Not Used.

#### Discussion of Timing and Rate Computation Algorithms Used:

The start and stop times of each interval (in seconds of the year) are given on the output tape as described above. The start times are monotonically

increasing, but can be spaced with more than 1 minute between them if data gaps of 1 minute or longer occur. That is, if no valid data frames are received within 1 minute of the end time of a particular interval, then one (or more) succeeding intervals will not be represented with a logical record on the rate tape. On the other hand, if it is possible to compute a rate over any part of a 1-minute interval, then a logical record will be generated with the computed rate or rates and the appropriate seconds of coverage (words 9-14) for the interval. The start time of an interval will be the same as the stop time of the previous interval if the data is continuous (that is, there are no gaps at the beginning of one interval or at the end of the preceding interval.) The amount of data that must be missing before the rate-computation algorithm considers that a data gap has been seen varies with the bit rate. These times are:

<u>Bit Rate (BPS)</u>	<u>Minimum Length of Data Gap (seconds)</u>
2450	1
490	3

If a data gap occurs within a 1-minute interval, the rates are averaged over the gap since the accumulators are non-resetting. Thus, all rates are computed over a fixed time interval (variable intervals are not allowed).

The algorithm used to compute the rates from each accumulator register over 1-minute intervals is:

$$R_A(t_{i-1}) = \frac{\sum (A_i - A_{i-1})}{\sum (t_i - t_{i-1})}$$

where:  $R_A$  is the rate in counts per second for the interval starting at  $t_{i-1}$ .

$A_i$  is the value of the accumulator register at time  $t_i$

$t_i$  is the time of successive readouts (based on the current bit rate.)

The "analog" output (words 29-40) are computed by averaging the engineering-units conversion of analog readouts--which occur at a regular interval within the observation period--and presenting this average in the observation logical record. Filled frames are ignored. If observations from an entire interval are missing or filled, the analog average will be zero.

### C. UC/CPT Pulse Height Tape

This section supplies the minimum format and functional-specifications information to allow the user to read the University of Chicago Mariner 10 Pulse Height Tapes. These tapes contain all of the pulse height information from the CPT for the mission in a form accessible to a FORTRAN-language program. Individual pulse height frames are not time-tagged, but are tabulated in blocks corresponding to 15 minutes of elapsed time at the spacecraft (spacecraft time). Additional bookkeeping and supporting instrument data are supplied to allow for the general use of the pulse height information.

The tape is structured as follows: Non-zero pulse height events are extracted from the raw experimental data records beginning at a specified time and are collected over the following 15 minutes. A highly variable number of these events per 15 minutes, depending primarily upon solar activity, are stored. At the end of the 15-minute period, two or more physical records are written onto the pulse height magnetic tape. The first of these records is a "header" record which contains timing and other supporting information necessary for the analysis of the data. The next record(s) contain(s) the pulse height data which was accumulated over the 15-minute period described by the header record. Depending on the number of events which were collected during the 15-minute period, more than one physical record may be necessary to record them since the physical data records are limited to a maximum size.

The following subsections will describe the contents and the method of collection and computation which are involved in producing the header and the data pulse height records.

#### Pulse Height Tape Header Content:

The pulse height header record is made up of 120 24-bit words containing 60 floating-point words. (See Figure III-1 for the floating-point word format.) Table III-4 describes the content of each floating-point word in the header record. That table is organized in terms of floating-point words, each of which consists of two, 24-bit words in the computer which generated the tapes. An explanation of certain of the entries in that table will be given in the paragraphs below.

Two general comments about the timing of the data are necessary before a detailed discussion of the header contents. The first is that the computer program which generated these pulse height tapes was operating on a "requested start time" and "requested end time" which corresponded to even quarter-hour intervals; that is, on the hour, 15 minutes after the hour, 30 minutes after the hour, etc. However, because the spacecraft frame from which the pulse height data was extracted did not occur exactly on a quarter-hour boundary, the actual beginning and end time of an interval will not necessarily be on a quarter-hour boundary. Both the requested and actual start and end times are recorded. Secondly, the "15-minute" time blocks described above may not, in fact, include 15-minutes-worth of data due to any one of a number of circumstances. Among these are the fact that there may have been a spacecraft transmission outage during the 15-minute period, in which case the beginning and end time may correspond to a 15-minute period, but less than 15 minutes-worth data is actually included; another possibility is that there are missing 15-minute intervals because of a lack of data coverage during an extended period of time covering several intervals (15-minute intervals during which no data can be collected are not recorded on the tape); finally, a 15-minute interval may be terminated by a change in the spacecraft or instrument status (for example, entry of the CPT into calibrate mode) in which case a 15-minute interval is terminated prematurely, and another "15-minute interval" will be started which will finish out the 15-minute interval which was started in the other spacecraft/CPT mode. In all cases, during an interruption due to a status change or to a data gap, a partial "15-minute" data block is generated to finish the interval out to as near to a requested end time as is possible.

The comments in the following paragraphs are intended to expand upon the brief description of the header content given in Table III-2.

The header record for a 15-minute block of data contains 60 floating-point words. The format of these floating-point words has been described previously (Figure III-1). In all of the comments which follow "word k" refer to word number "k" of Table III-2.

The first word of the header contains the floating-point constant -1.0 which is used as an aid in distinguishing a header record from a data record (which cannot have this bit configuration in the first word.) Word 2 through 5 contain the requested (that is, the even 15-minute) start time and end time and the actual (that is, related to the time of the frame of the first and last non-zero pulse height words which are contained in the 15-minute block) begin time and end time of the 15-minute data block. Each time is expressed as 1 plus the fractional day of 1972; that is, day 1, hour 0 of 1972 is expressed as 1.00 with the decimal accurate to 1 millisecond.

Word 9 gives the command state of the CPT for the data in that "15-minute" period. The detector D1, D2 and D5 can be commanded off from the ground, the priority scheme of the instrument can be overridden or the instrument can be put into a calibrate mode. The state of the instrument with reference to these options is given in word 9 and can be determined using the algorithm given in the table.

Words 11, 12 and 13 summarize the coverage and quality of data for the main telescope during the 15-minute period. From these words can be determined the total number of seconds in the 15-minute period over which pulse height data could be collected, total number of non-filled and the total number of filled main frames that were available during the 15-minute period.

Words 14, 35-40, 49-56 report selected rates computed from the CPT over the 15-minute period (or fractional period) covered by the data records following the header. The algorithm for the calculation of the rate averages is given in Appendix III.A.

The other items in the table are self-explanatory.

#### Data Record Format:

Following the header record (as described above) there will be recorded one or more physical records which contain the non-zero pulse heights from the 15-minute period described in the header record. The physical records will have a variable length. The minimum number of 24-bit words (4, 6-bit-character words) will be 150 and the maximum number of words will be 1,020 (4,080 characters.) The number of words in any physical data record will be a multiple of three (that is,  $N=3 \times M$  where  $50 < M < 340$ .)

Two 24-bit words are required to record either a main telescope or a low energy telescope event. The format in either case is different. Figure III-3

shows the representation of an event in the word pair for each of the main telescope and low energy telescope, while Table III-3 describes each of the parameters recorded.

The first two words of a physical record do not contain pulse height data, but give some statistics describing the record. The first word of each physical record always contains the number of the physical data record within the 15-minute period. The records are numbered starting with 1 after each header. The second word contains the number of data word pairs (described above, in Figure III-3 and Table III-2) and will be an integer between 1 and 509. The pulse height event word-pairs starting with words 3 and 4 are then recorded up to a maximum number which can be contained in the physical record. If more than 509 word-pairs are required to record all non-zero pulse height events for a 15-minute interval, a new record will be started. If, at any time, the accumulation period is terminated before a physical record is filled by the end-time specification, the physical record will be terminated and will be written out as a short record. In the particular case where the record would be less than 150 words, it is "padded-out" to 150 words with word-pairs consisting of zeros, which are indistinguishable from low energy telescope word-pairs; therefore, it is important to use the word-pair count appearing in word 2 in order to index through a physical record.

There will always be an integral number of 15-minute intervals on a particular physical tape; that is, every tape begins with a header record for a 15-minute interval. Each physical tape is terminated with a double end-of-file.

Appendix III.A  
 Algorithm for Calculation of Rate Averages for  
 Pulse Height Tapes  
For the Mariner 10 CPT Experiment

The source of rate and livetime data is the rate tape. The interval on the PHT is nominally 15 minutes and that of the rate tape is 1 minute.

If a change in X1, X2, X7, Priority, or Calibrate occurs, the 1 minute (on the rate tape) rates are not broken, but a flag is set. The PHT interval is broken at the time the status change occurs. The rates on the rate tape that indicate a status change occurred will not be included on the PHT.

Normally, with coverage > 0 with no changes in X1, X2, X7 or P, the rate that goes onto the PHT is calculated from the formula:

$$R = \frac{\sum R_i t_i}{\sum t_i}$$

where

$R_i$  = rate on rate tape for  $i$ th summing interval

$t_i$  = livetime from rate tape for  $i$ th summing interval

For example, if the PHT interval is 15 minutes and the rate tape interval is 1 minute, then there are 15 summing intervals during the PHT interval.

Here, for each rate of the 7 rates, the time word >0 and the rate  $\geq 0$ .

If there is a status change during a rate interval, the rate for that summing interval is set to zero as well as the time in the above formula.

A rate word and time word can both = -1.

This means:

- 1) There was no coverage, or
- 2) There was a spike on the rate plots and the words were set to -1 for the time period of the spike.

Table III-1

A. Mariner 10 Spacecraft Rates, Modes and Format

Measurement	Bits Configuration	Use
Engineering Rates:	00	Forbidden
	01	2450 bps (Eng.-A)
	10	33-1/3 bps (Eng.-B)
	11	8-1/3 bps (Eng.-C)
Engineering Format	00	Forbidden
	01	Fixed Engineering Format
	10	Primary Engineering Format
	11	Maneuver Engineering Format
Engineering Mode	001	Filled
	010	Filled
	100	Filled

B. MDR Status Word

Bit	Use*
12	RCVR Status
13	SDA Status
14	TCP Status 0 = in lock, 1 = out-of-lock, or not in use
15	SSA Status
16	DDA Status
17	BDA Status
18	FDS Minor Frame Correction flag (1 = corrected)
19	Earth Received GMT Correction flag (1 = corrected)
20	Errors in sync word of NIS frames (1 = errors)
21	Bad leading/trailing sync of NIS (1 = bad)
22	GCF block error flag (1 = error flag set)
23	
24	Missing data in sequence (1 = some data missing)

\*Note: These flags mark generally insignificant anomalies and are usually ignored.

Table III-2  
Pulse Height Tape Header For The  
Mariner 10 CPT Data

Word	Description
1	-1.0
2	The requested start time for the nominal interval in units of (1+decimal days of 1972).
3	The requested start time of the nominal interval in the same units.
4	Actual time of the first non-zero PHA word occurring in the interval in the same units.
5	The time of the last pulse height observation recorded in the interval in the same units.
6	The data quality indicator F/T where F=the number of main telescope and LET pulse height main frames in the 15-minute interval for which the data quality bit was set to 1 (that is, suspect data.)  T=the total number of main frames of pulse height data in the interval.
7	0.0
8	The initial bit rate for data in the 15-minute interval; this will either be 490 or 2450
9	Instrument status bookkeeping bits; this word will have the value $32*D1+16*D2+8*D7+4*P+C$ where  D1=0 if detector D1 is on; =1 if D1 was commanded off D2=0 if detector D2 is on; =1 if D2 was commanded off D7=0 if detector D7 is on; =1 if it was turned off at any time during the interval.  P=0 if the priority mode was normal during all of the intervals; if the priority override command was sent P will be 1.  C will be 0 if no calibrate data appears in the 15-minute interval; it will be set to 1 if any calibrate data is presented.
10	0.0
11	The number of seconds of main telescope pulse height data, including non-zero pulse height frames and "0" frames (that is, where PH1=PH2=PH5=0.)
12	The number of main telescope pulse height frames including the count of all non-zero and zero pulse height frames but excluding filled frames. The data quality indicator in the pulse height frame may be 0 (good) or 1 (suspect).
13	The number of filled main frames.

Table III-2 (continued)  
Pulse Height Tape Header for the Mariner 10 CPT Data

Word	Description
14	D12 counting rate.
15	Same as 13.
16	The lowest value of the signal-to-noise ratio ( $[\text{Signal-Noise}]/\text{Noise}$ ) which was observed during the 15-minute interval.
17	The highest value of the signal-to-noise ratio which was observed during the interval.
18-33	The total number of pulse height events having ID's 0-15.
34	Satellite number (73 for Mariner-10).
35	The L1N2 counting rate.
36	D1N2 counting rate.
37	D26 counting rate.
38	D6N7 counting rate.
39	0.0
40	D5N6 counting rate.
41	The number of seconds of low energy telescope pulse height data including both non-zero and zero frames.
42	The number of non-zero main telescope events or the sum of words 18-33.
43	The number of non-filled frames (=the number of events x5).
44	The number of events in channels 1-27 for L1N2.
45	The number of events in channels 0-127 for L1L2.
46-48	0.0
49	L1L2 counting rate.
50	D12 counting rate livetime.
51	L1N2 counting rate livetime.
52	D1N2 counting rate livetime.
53	D26 counting rate livetime.
54	D6N7 counting rate livetime.
55	D5N6 counting rate livetime.
56	L1L2 counting rate livetime.
57	The total number of physical data records following the header.
58-60	The date the pulse height tape was generated (month,day,year).

TABLE III-3

University of Chicago Charged Particle Telescope

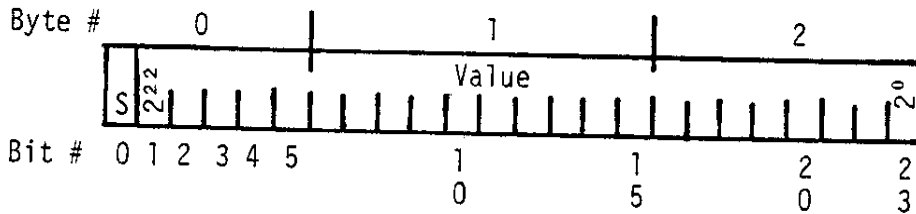
Mariner 10

Description of Data Block Word-Pair Parameters

Descriptor	Description
ID (main telescope)	Range identification for particle in main telescope; integer 0-15.
ID (LET)	Range identification for a particle in the LET; 1 for L1L2, 2 for L1L2.
DQI	Data quality indicator; set to 0 for good data, to 1 for suspect data.
D1	The telemetered pulse height analysis channel reported for the event from the detector 1. Integer, 0-255.
D2	The telemetered pulse height analysis channel reported for the event from the detector 2. Integer, 0-255.
D5	The telemetered pulse height analysis channel reported for the event from the detector 5. Integer, 0-255.
LET CH	Telemetered value of the PHA channel for the L1 detector of the low energy telescope. Integer, 0-127.

Figure III-1  
 Definition of XDS-930 Computer  
 System Internal Number Formats

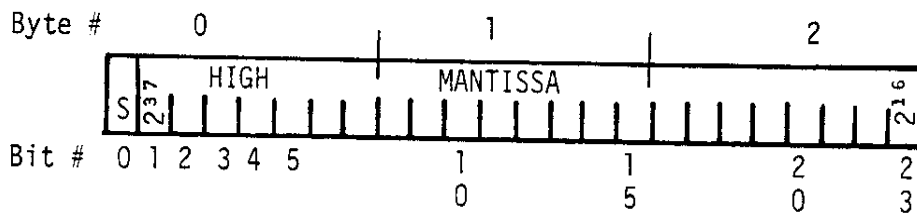
1. Integer - a 3-byte (24-bit) two's-complement number (X) having a value range of  $-8,388,608 \leq X \leq 8,388,607$ ; schematically.



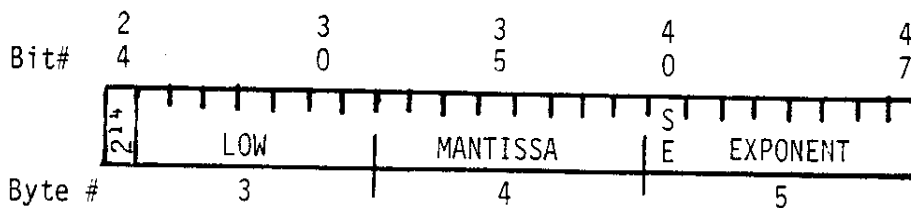
where S=0 (X positive) or 1 (X negative) is the sign-bit

2. Real: (also called Floating-Point) a 6-byte (48-bit or 2-word) number consisting of a normalized, 39-bit two's-complement mantissa (value) and an 9-bit two's-complement exponent; schematically.

Higher-Address Word\*



Lower-Address Word\*



where S is the sign of the mantissa and SE is the sign of the exponent.

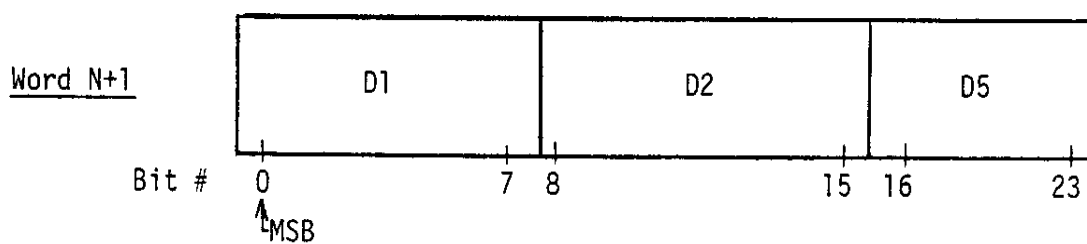
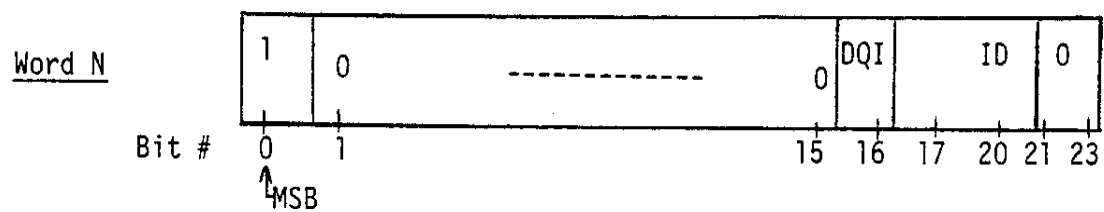
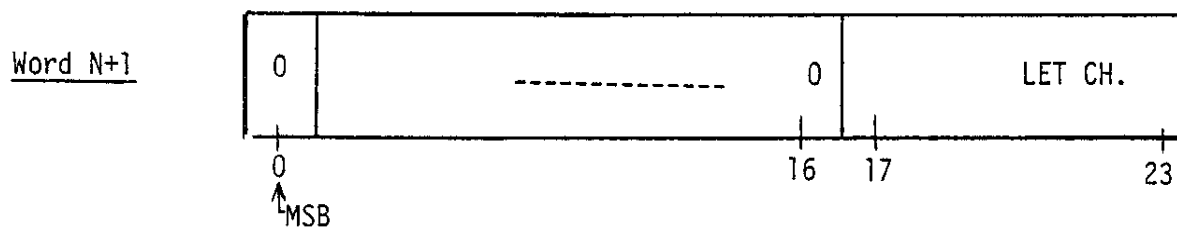
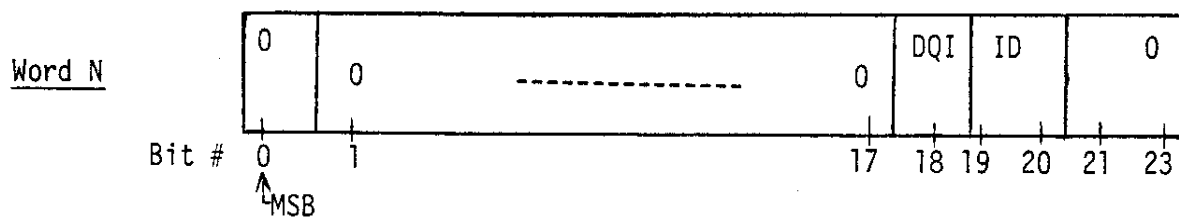
\*The "Lower-Address Word" appears first (is read first) from the tape; thus, the byte order as read will be:

3,4,5,0,1,2

Figure III-2  
 Logical Record Format  
 for the  
 UC/CPT Counting Rate Average Tape

Bit #	0	1	2	3	4	5	6	7	8	9	0	1	2	3	4	5	6	7	8	9	0	1	1	2	2	2	2	Word #
	YEAR										SPACECRAFT NUMBER										1							
	STATUS																									2		
	MDR STATUS																									3		
	NUM. BAD FRAMES (DQI=1)										NUM. GOOD FRAMES (DQI=0)										4							
	INTERVAL START TIME																									5		
	(in sec. of the year)																									6		
	INTERVAL STOP TIME																									7		
	(in sec. of the year)																									8		
	SEC. OF DATA (COVERAGE) FOR										R1											9						
	FRAME RATES																									10		
	SEC. OF DATA (COVERAGE) FOR										R2											11						
	FRAME RATES																									12		
	SEC. OF DATA (COVERAGE) FOR										R3											13						
	FRAME RATES																									14		
	MAIN R1 FRAME RATE --																									15		
	D2-6																									16		
	MAIN R1 FRAME RATE --																									17		
	D12																									18		
	MAIN R2 FRAME RATE --																									19		
	D1-6D7																									20		
	MAIN R2 FRAME RATE --																									21		
	D1-D67																									22		
	MAIN R2 FRAME RATE --																									23		
	L1L2																									24		
	MAIN R3 FRAME RATE --																									25		
	L1L2																									26		
	MAIN R3 FRAME RATE --																									27		
	D1D27																									28		
	D7 RATE																									29		
	METER																									30		
	ANALOG ---																									31		
	CPT TEMPERATURE																									32		
	ANALOG --																									33		
	BAY 7 TEMPERATURE																									34		
	ANALOG --																									35		
	BATTERY TEMPERATURE																									36		
	ANALOG --																									37		
	OUTPUT VOLTAGE																									38		
	ANALOG --																									39		
	OUTPUT CURRENT																									40		
	END OF INTERVAL TIME																									41		
	(actual 1 minute boundary time in sec. of the year)																									42		
	SPARE																									43		
	SPARE																									44		

FIGURE III-3

Mariner 10Pulse Height Data Word Format\*A. Main Telescope Word PairB. LET Word Pair

\*See Table III-3 for explanation of terms.

IV.

Acknowledgements

#### IV. Acknowledgements

A project of this scope with such outstanding results would never have been possible without the dedicated efforts of the Jet Propulsion Laboratory staff who were associated with the Mariner 10 project. We would especially like to thank Jim Dunne for his excellent work as project scientist; Jack Tupman, Project Data Manager; and Donna Shirley of the navigation section. We would also like to thank Al Matzke of the Boeing Company who "babysat" the CPT through many days of spacecraft interface, integration and performance testing. We would also like to thank Fred Sopron at the University of Chicago who did much of the work involved in the construction and testing of the CPT.

Finally, we the three principle authors, Stephen P. Christon, James H. Eraker and Gordon A. Lentz, take full responsibility for the accuracy and presentation of the information in this document. We would especially like to thank Regina Stafford and Cathy Johnson for their hard work in transforming the original manuscript into a presentable document.

#### V. Appendicies

- A. JPL UC/CPT Functional Requirement Document
  - B. In-Flight Calibration Summary of UC/CPT
  - C. Investigation of Background in LET
  - D. Publications and Abstracts Based on Mariner 10  
UC/CPT Data to Date
-

Appendix A  
JPL UC/CPT Functional  
Requirement Document

(This Appendix is a revision of the original document)

JPL FUNCTIONAL REQUIREMENT  
MARINER VENUS MERCURY 1973 FLIGHT EQUIPMENT  
CHARGED PARTICLE TELESCOPE

1.0 SCOPE

1.1 This document covers the functional requirements of the Charged Particle Telescope Subsystem of the Mariner Venus Mercury 1973 Spacecraft.

2.0 APPLICABLE DOCUMENTS

2.1 The following documents form a part of this Functional Requirement.

DOCUMENT:

Jet Propulsion Laboratory

M73-3-100 Mariner Venus Mercury 1973 Spacecraft Characteristics and Restraints

3.0 FUNCTIONAL DESCRIPTION

3.1 Scientific Objectives

The two charged particle telescopes and instrument for Mariner Venus Mercury 1973 mission are designed for the following primary scientific objectives:

- a. To study Mercury's environment and planetary characteristics derived from particle measurements:
  - i. Search for trapped radiation at Mercury (e.g., electrons above 200 keV, protons above 400 keV).
  - ii. Particles associated with a magnetotail and bow shock (as evidence for an intrinsic magnetic field, ionosphere, etc.).
  - iii. Fluxes reaching the planet from interplanetary space near the orbit of Mercury. This includes electrons, protons, He, Li, Be, B, C, N and O from the sun under quiet and flare conditions, as well as the isotopes Deuterium, Tritium and He<sup>3</sup>, and He<sup>4</sup>.
- b. To investigate the origin and propagation of energetic particles reaching the orbit of Mercury from solar flares and solar active centers in order to determine the presently unknown factors which establish the flux levels at the surface of the planet. This includes measurements of anisotropies in the charged particle fluxes obtained by rolling the spacecraft at time intervals to be selected throughout the mission.

- i. Charged particle spectra, fluxes and composition.
  - ii. Obtain differential energy spectra at low energy for protons and alpha-particles of solar origin which will define the limits for solar neutron fluxes decaying at  $\sim 0.4A.U.$
  - iii. Propagation studies simultaneously with Pioneers F and G which will be located beyond the orbit of Earth.
- c. Studies bearing on solar and galactic origin and the modulation of quasi-steady fluxes of particles in interplanetary space.
- i. Separate identification of solar and galactic components.
  - ii. Charged particle density gradients and solar modulation.

A secondary objective of the instrument on the Mariner mission is to search for charged particles associated with planet Venus in a trajectory pass through the plasma cavity.

### 3.2 Purposes of the Two Telescopes

#### a. Purposes of Main Telescope (M.T.)

Measure differential energy spectra and fluxes of:

Electrons 200 keV- 15 MeV

Protons, H<sup>2</sup>, H<sup>3</sup>, He<sup>3</sup>, He<sup>4</sup>, Li, Be, B, C, N, O in various energy ranges between 0.6 and 500 NeV/nucleon.

#### b. Purposes of Low Energy Telescope (L.E.T.)

- i. To extend downward in energy the separate measurement of proton and alpha particle energy spectra.
  - (a) by  $dE/dx$  vs. range measurement:
    - protons 0.5 to 8.5 MeV
    - alpha particles 2.0 to 25 MeV (total energy).
  - (b) Fluxes of nuclei above 0.4 MeV.
- ii. To measure the P and alpha-fluxes without interference from high flux levels of solar electrons; namely, fluxes  $\geq 10^{-3}$  electrons/second.
- iii. To survive radiation damage by solar particles by a factor  $\sim 10^2$  beyond the radiation damage limit of the main telescope D<sub>1</sub> and/or D<sub>2</sub> elements.

3.3 Illustrations

- 3.3.1 See Figure II-1 for a cross-section of the charged particle telescope assembly.

### 3.4 Major Functional Elements

#### 3.4.1 Telescopes

The instrument contains two telescope assemblies, each having an unobstructed view cone for accepting charged particles of  $70^\circ$ . These telescopes are termed:

- a. The Main Telescope
- b. The Low Energy Telescope Subsystem

The construction of each is such that the detector array and mechanical housing assembly define the effective field of view. There is a backward field of view of  $50^\circ$  for the Main Telescope which can tolerate  $\sim 1 - 2 \text{ gm/cm}^2$  material in the field of view.

#### 3.4.2 Detectors

##### 3.4.2.1 Main Telescope

The main telescope consists of seven detectors. Detectors D1, D2, D3, D4 and D6 are lithium-drifted solid state silicon detectors; D5 is a CsI crystal coupled to a solid state photodiode and D7 is a plastic scintillator used in conjunction with a photomultiplier tube. D7 is used in anti-coincidence with the other detectors to define the telescope acceptance cone and backward cone and, in addition, to provide a measure of the total flux of particles incident upon the instrument.

##### 3.4.2.2 Low Energy Telescope (LET)

The LET consists of three detectors:  $L_1$ , a very thin conventional surface barrier detector;  $L_A$ , an annular lithium-drifted n-i-p detector; and  $L_F$ , a flat lithium-drifted windowless detector.

Detectors  $L_A$  and  $L_F$  are electrically connected so as to be equivalent to a single detector, hereinafter designated  $L_2$ . The  $L_2$  detector serves to separate particles which penetrate  $L_1$  from those which are stopped in  $L_1$ .

The field of view of the LET is defined by the mechanical enclosure and by the geometrical configuration of the detectors relative to each other.

##### 3.4.3 Photomultiplier Tube (PMT)

The photomultiplier tube is optically coupled to the plastic scintillator to provide high gain response to the scintillation light pulses which occur as a result of passage of a charged particle through the plastic.

#### 3.4.4 Charged Sensitive Amplifier (CSA)

The charge outputs of the detectors are amplified by the CSA and generate the pulses which are to be analyzed and counted.

#### 3.4.5 Amplifier (AMP)

The amplifier provides necessary additional gain for pulses from the PMT and wave shaping necessary for proper operation of the discriminator and logic operation.

#### 3.4.6 Log-Linear Amplifier (MA)

The CSA outputs for  $D_1$ ,  $D_2$  and  $D_5$  are amplified by the log amplifier. These outputs are those which will be pulse height analyzed.

#### 3.4.7 Post Amplifier (PA)

The CSA outputs for  $D_3$ ,  $D_4$  and  $D_6$  are amplified by the post amplifier and routed to the discriminators for use in the counting rate mode.

#### 3.4.8 Discriminators

The discriminator is designed to provide the necessary output signals when the height of the input pulse is greater than a minimum height. The output pulses are of constant magnitude and are used for counting and logical functions.

#### 3.4.9 Delay Lines (DL)

The pulses which are to be height analyzed are delayed by a set period of time, such that the coincidence logic can be established for their analysis.

#### 3.4.10 Linear Gates (LG)

The gates allow the transmission of the pulses to the PHA if the necessary coincidence is present.

#### 3.4.11 Low Power Logic

The logic utilizes the information pulses from the discriminators, the PHA/Rate multiplexer and flight data system to generate the logic functions for the analysis and counting of pulses, and the identification of the pulses to be analyzed.

#### 3.4.12 Pulse Height Analyzer

The pulses to be analyzed are applied to the input of the height to time convertor (HTC). The magnitude of the pulse determines

the number of 500 kHz pulses which are allowed to pass to the accumulators. The 500 kHz clock is the timing for the conversion of analog (height) to digital data.

### 3.4.13 Accumulator and Shift Registers

The Accumulator and Shift Registers are used for temporary storage of the data from the analysis and rate modes for both telescopes. The information is formatted here for transfer to the spacecraft data handling system. The analysis mode, comprised of 32 bits, contains three 8-bit numbers representing the measurement of  $dE/dx$  and  $E$  values from D1, D2 and D5. This information, in turn, characterizes the particle and its energy. The remaining eight bits of the analysis mode word include indicator bits used to establish particle identification, priority mode, the normal or calibrate mode of instrument operation, and identification of the readout.

### 3.4.14 PHA/RATE Multiplexer

Spacecraft commands are provided which are used to multiplex data from the analysis and counting modes.

### 3.4.15 Count Rate Meter

The count rate meter provides an analog signal which is a function of the flux of charged particles incident on D7.

### 3.4.16 In-flight Calibrator

Upon command, known magnitude pulses in a set of sequence are applied to provide calibration for the analysis of counting modes. A command is to be available during S/C integration, test, launch preparation, etc., which will exercise the calibration mode for the purpose of systems testing and "go-no-go" tests.

### 3.4.17 Voltage Converter

The single level voltage is converted to the various levels required by the electronics.

## 3.5 Data Format and Telemetry Bit Rate

- a. The instrument data cycle is based upon a five level multiplex system, keyed to the minor frame rate. The five levels contain four basic data words, one of which repeats in the first and third position of each sequence. Words are composed of pulse height analysis and rate information as outlined below:

Level 1: (MT PHA data) DQI (1 bit), PHA ID (4 bits), read out ID status (2 bits), calibrate/normal priority (2 bits), D1 PHA channel (8 bits), D2 PHA channel (8 bits), D5 PHA channel (8 bits).

Level 2: DQI (1 bit), LET PHA (8 bits), LET ID (1 bit), D1237 scaler (12 bits), D24567 scaler (10 bits).

Level 3: Same as Level 1.

Level 4: DQI (1 bit), L12 scaler (14 bits), D124567 scaler (8 bits, D124567 scaler (8 bits).

Level 5: DQI (1 bit), L12 scaler (16 bits), D127 scaler (14 bits).

- b. Data in each level is accumulated during the interval between readouts for that level in a separate register for each line. Information is shifted out of the registers by a shift burst occurring during the CPT read interval in the minor frame.
- c. The data segments consist of 32 bits each for 5 levels which repeat each major frame or five minor frames. Thus, the average bit rate is keyed to the spacecraft non-imaging science data rate and is either 133 bits/second or 53 1/3 bits/second.
- d. Table I illustrates the CPT data format, Table II status and logic.
- e. An indication bit is to be provided in engineering format to indicate when the output of the CPT is in real-time, and when it is tape recorded.

### 3.6 Special Requirements

The following requirements are necessary if the performance parameters specified under paragraph 5.0 are to be achieved.

#### 3.6.1 Optical Pointing

The instrument is body fixed and each telescope requires an unobstructed view cone of  $70^{\circ}$ . The MT requires a field-of-view in the backward direction of  $50^{\circ}$ . The backward field-of-view can tolerate 1 - 2 gm/cm<sup>2</sup> of material in the field-of-view. The MT cone axis shall have the following S/C coordinates: cone  $45^{\circ}$ , clock  $275^{\circ}$ . The LET shall have the following coordinates: cone  $50^{\circ}$ , clock  $275^{\circ}$ .

#### 3.6.2 Restraints on Orientation

During the normal cruise mode, the telescope shall be placed such that it is not directly illuminated by the sun.

- 3.6.3 Spacecraft roll maneuvers are to be provided so that the two telescopes can measure the anisotropy of the charge particle fluxes as a function of roll angle with respect to the normal, stabilized mode. Information on the roll angle is to be provided in the

engineering format for use by the CPT experimenters. An error in angular resolution of about  $\pm 3^\circ$  is allowable.

- 3.6.4 The bit error rate at Mercury is not to drop below  $\sim 10^{-3}$  and nominally is to be better than  $10^{-4}$ .

#### 4.0 INTERFACE DEFINITION

##### 4.1 Mechanical

The CPT Instrument provides a flat mounting base and is supported by means of seven (7) through-bolts. The mounting base is rectangular, measuring 7 inches x 9 inches. If intertray connector harness is adopted, the 9 inch dimension of the housing will increase to 11 inches, maximum, however, the mounting bolt pattern will not be altered.

##### 4.2 Electrical

###### 4.2.1 Flight Data System (FDS)

###### a. From the (FDS)

- i. Calibrate command (transmitted from earth).
- ii. Spacecraft roll status.
- iii. PHA/Rate Multiplex Advance.
- iv. PHA/Rate Multiplex bit shift pulses.
- v. PHA/Rate Multiplexer Synch.
- vi. PHA/Rate Multiplexer word gate - 32 bits.
- vii. Priority override command (transmitted).
- viii. X1 command transmitted.  
X2 command transmitted.  
X7 command transmitted.
- ix. Reset command (transmitted).  
Takes i, vii, and viii to normal mode.

###### b. To the FDS

- i. PHA/Rate Digital data - 32 bits.
- ii. D7 analog count rate.
- iii. CPT Temperature.

###### 4.2.2 Umbilical Functions

The CPT requires no umbilical functions, except in the event that ground test otherwise precludes commanding instrument into calibrate mode as required.

###### 4.2.3 Power Subsystem

- a. Instrument power: 2400 Hz square wave 50 V rms during cruise and encounter.

- b. Heater power: D.C. voltage which may be set by Earth-based signals for thermal control, pending thermal analysis data.

#### 5.0 PERFORMANCE PARAMETERS

#### 6.0 PHYSICAL CHARACTERISTICS AND RESTRAINTS

##### 6.1 Weight

The weight of the instrument is 7.8 lb.

##### 6.2 Volume

The mounting base of the instrument is 7 inches by 11 inches. Maximum envelope dimensions are 13.625 inches (to the end of the telescope extension) by 7.0 inches by 6.0 inches in height (including the test connector attachment), occupying a volume of less than 575 cubic inches.

##### 6.3 Power

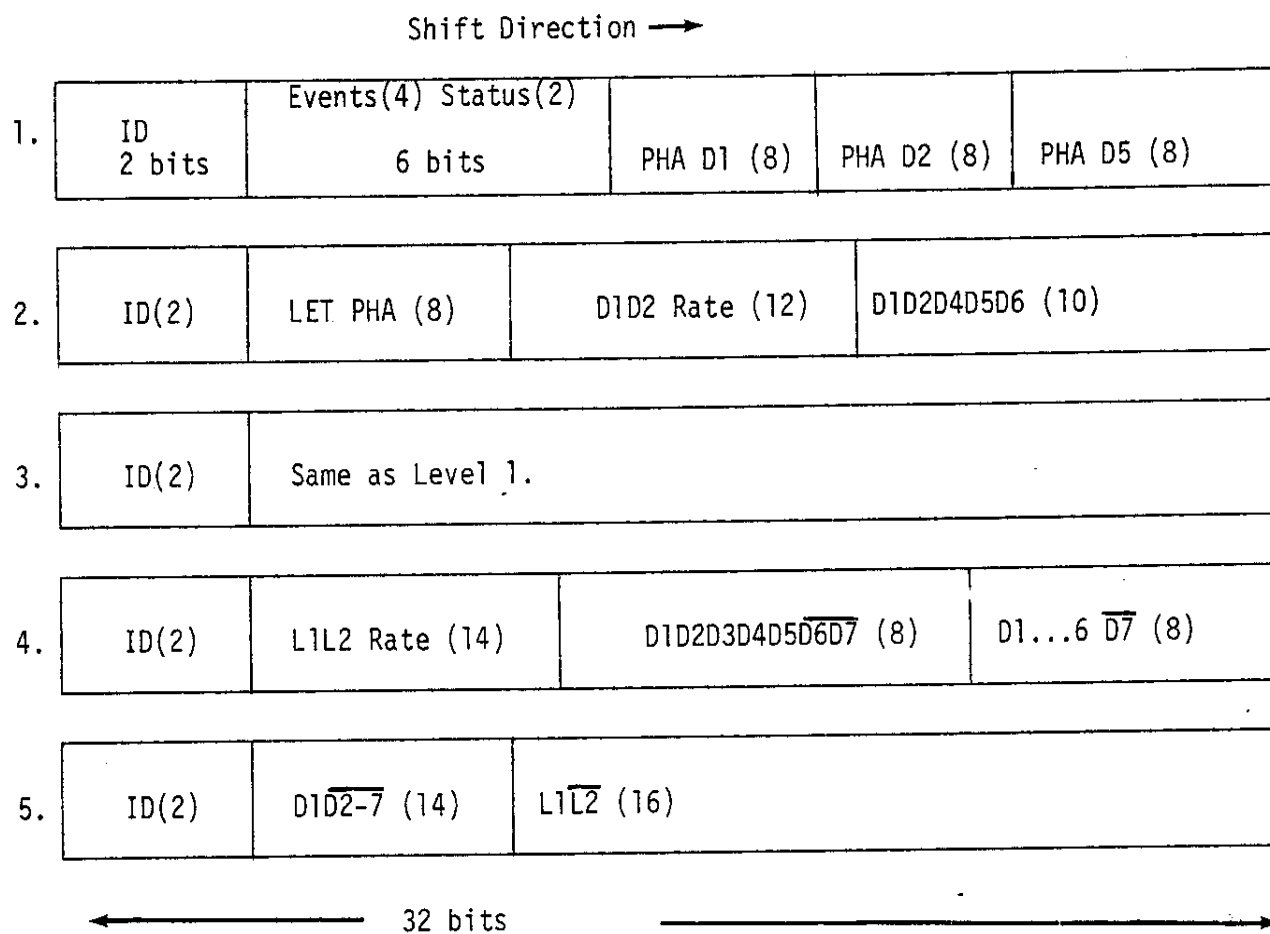
The instrument will consume 2.2 watts raw power average and 2.3 watts peak from the S/C power subsystem.

##### 6.4 Temperature Range

- a. Operating temperature shall range from  $-20^{\circ}$  to  $+50^{\circ}\text{C}$ .
- b. Non-operating temperature shall range from  $-30^{\circ}$  to  $+50^{\circ}\text{C}$ .
- c. In-flight, operating, temperature design center is  $+5^{\circ}\text{C}$  to  $+15^{\circ}\text{C}$  over the entire mission.

TABLE 1  
CPT Experiment Data Word Format

One (1) Major Frame for NIS Formats: 1 (at 2450 BPS) and 2 (at 490 BPS).



Number in parenthesis is number of bits for the assigned function.

Last bit read out in word ID bit.

A. CPT Mode Status Bit Assignments  
(Bits 25-26 of CPT data words identified by "00" in Bits 31-32)

Bit 25: 0 = Priority Mode Enabled  
1 = Priority Mode Disabled

In the Priority Mode the CPT pulse height analyzer will contain either the first low priority event that occurred while it was enabled or the last high priority event. When the Priority mode is disabled, the pulse height analyzer will contain the first event that occurred while it was enabled, regardless of its priority (see Table III B).

Bit 26: 0 = Normal Mode  
1 = Calibrate Mode

Table II (cont'd)

B. Logic Coding for Redundant Pulse Height Analysis  
 (Bits 27-30 of CPT data words identified by "00" in Bits 31-32)

Coding Bits				Event Priority	PHA Detector Coincidence Configuration	ID
27	28	29	30			
0	0	0	0	-	No Event	0
0	0	0	1	Low	D1 $\overline{D2}$ $\overline{D3}$ $\overline{D7}$ $\overline{A}$ $X1$	1
0	0	1	0	High	D1 D2 $\overline{D3}$ $\overline{D4}$ $\overline{D7}$ $\overline{A}$ $X2$	2
0	0	1	1	High	D1 D2 D3 $\overline{D4}$ $\overline{D7}$ $\overline{A}$	3
0	1	0	0	High	D1 D2 D4 $\overline{D5}$ $\overline{D6}$ $\overline{D7}$ $\overline{A}$	4
0	1	0	1	High	D1 D2 D4 D5 $\overline{D6}$ $\overline{D7}$ $\overline{A}$	5
0	1	1	0	Low	D1 D2 D4 $\overline{D5}$ D6 $\overline{D7}$ $\overline{A}$ *	6
0	1	1	1	Low	D1 D2 D4 D5 D6 $\overline{D7}$ $\overline{A}$	7
1	0	0	0	-	Unused*	8
1	0	0	1	Low	$\overline{D1}$ D2 D4 D5 $\overline{D6}$ $\overline{D7}$ $\overline{A}$ $X1$	9
1	0	1	0	Low	D1 D2 D4 D5 $\overline{D6}$ D7 $\overline{A}$ **	10
1	0	1	1	Low	D1 $\overline{D2}$ D4 D5 $\overline{D6}$ $\overline{D7}$ $\overline{A}$ $X2$ *	11
1	1	0	0	-	Unused*	12
1	1	0	1	Low	$\overline{D1}$ D2 D4 D5 D6 $\overline{D7}$ $\overline{A}$ $X1$	13
1	1	1	0	Low	D1 D2 D4 D5 D6 D7 $\overline{A}$ **	14
1	1	1	1	Low	D1 $\overline{D2}$ D4 D5 D6 $\overline{D7}$ $\overline{A}$ $X2$	15

Key:  $\overline{A}$  = No analysis (or readout or transfer in progress)

\* = Cannot occur if instrument is functioning properly

\*\* = D7 triggered (Background Event)

$X_i$  = Command to disable detector  $D_i$  (See Note)

Appendix B

In-Flight Calibration Summary of UC/CPT

This Appendix consists of a memo summarizing the in-flight calibrations of the Mariner 10 electronics during the main Mariner 10 mission from launch until Day 110, 1974. As noted in this memo, the electronics shifts of the instrument were less than  $\pm 1.0\%$  pulse height channel or less than  $\pm 1.0\%$  of the energy measurement in each pulse height analyzed detector. No electronic shift of the pulse height electronics greater than  $\sim 1.0\%$  was observed during the entire Mariner 10 mission.

## THE UNIVERSITY OF CHICAGO

DATE February 4, 1974

TO Mariner 10 Distribution

DEPARTMENT

FROM J. Eraker and G. Gabrielse

DEPARTMENT

IN RE: IFC Stability of the Mariner 10 CPT

The stability of the instrument is absolutely essential in order to accurately preserve the energy loss information. The first table shows the IFC mean channel at the last bench calibrate period. From the mean channel a value for the voltage of each IFC point, the corresponding detector energy, the slope  $\Delta$  voltage/ $\Delta$  channel plus  $\Delta$  energy/ $\Delta$  channel, and the percentage voltage change/channel ( $\Delta V/V\Delta C$ ) were calculated. Since the silicon detectors have been shown to have a linear output voltage as a function of incident energy, the percentage change of  $\Delta V/V$  also represents the uncertainty in the energy measurement. Using the 6/24/73 mean IFC channels as a zero we have plotted  $\Delta V/V$  for the mission. One can see the graphs show no consistent drift of any single IFC point or detector amplifier as a function of temperature.

The jump in  $\Delta V/V$  at launch may be attributed to drastic temperature and environment changes from the bench IFC. After the first IFC point in space on day 312 the IFC points have generally remained within  $\pm .5$  channels with a corresponding shift in  $\Delta V/V$  of  $\pm 1.0\%$ . Since the calculation of  $\Delta V/V$  with respect to  $\Delta C$  is linear the percentage shift of  $\Delta V/V$  with respect to any day can be seen by moving the zero of  $\Delta V/V$  (or  $\Delta C$ ) to that point and measuring  $\Delta V/V$  (or  $\Delta C$ ) with respect to the new axis.

The track resolution of the instrument can be estimated as a RMS error of the three apparent energy loss fluctuations.

Let  $\sigma_V$  = FWHM of Vavilov fluctuation

$\sigma_P$  = FWHM of pathlength fluctuation

$\sigma_A$  = FWHM of amplifier fluctuation

$$\sigma_{\text{TOTAL}} = (\sigma_V^2 + \sigma_P^2 + \sigma_A^2)^{1/2}$$

$$\sigma_{\text{TOTAL}} \cong (\sigma_V^2 + \sigma_P^2)^{1/2} \left( 1 + \frac{\sigma_A^2}{2(\sigma_V^2 + \sigma_P^2)} \right)$$

where  $\sigma_V^2 + \sigma_P^2 \gg \sigma_A^2$

A column in the last table shows a small compilation of  $\sigma_V^2 + \sigma_P^2$  for H and He. Typically the loss of resolution from a 1%  $\sigma_A$  is less than 2%, the only exception possibly, being the  $Z > 8$  nuclei in ID5 (where  $\sigma_V$  and  $\sigma_P$  become on the order of 1%).

June 26, 1973

Mariner 10 CPT

IFC

	$\bar{C}$	$n_i$	$\pm \sigma$	$\pm S_{\bar{X}}$
D1	46.00	1072	0.52	0.02
D1	139.35	1084	0.48	0.01
D1	173.52	1098	0.50	0.02
D1	215.58	1105	0.49	0.01
D2	51.63	1124	0.56	0.02
D2	136.32	1136	0.47	0.02
D2	171.02	1142	0.17	0.01
D2	220.43	1161	0.50	0.02
D5	41.02	1179	0.56	0.02
D5	147.07	1192	0.47	0.01
D5	187.04	1216	0.25	0.01
D5	250.00	-	-	-
LET	62.67	3108	0.57	0.01

$\bar{C}$  = mean IFC channel

$n_i$  = number of pulseheights used to determine  $\bar{C}$

$\pm \sigma$  = standard deviation of  $n_i$  distribution

$\pm S_{\bar{X}}$  = standard error of  $\bar{C}$

## Track Fluctuation for MVM 73

## Detector D1

<u>Element</u>	<u>Energy</u>	<u>Vavilov FWHM*</u>	<u>Maximum Path- Length Variation</u>	$(\sigma_V^2 + \sigma_{PL}^2)^{1/2}$ <u>Maximum Fluctuation</u>
H	10 MeV/N	5%	5.3%	7.2%
H	20	8	5.3	9.5
H	30	11	1.3	11.1
H	70	20	1.3	20.0
He <sup>4</sup>	10	3	5.3	6.1
He <sup>4</sup>	20	4	5.3	6.6
He <sup>4</sup>	30	5	1.3	5.2
He <sup>4</sup>	70	10	1.3	10.1

## Detector D2

H	30 MeV/N	8%	1.3%	8.1%
H	70	15	1.3	15.1
He <sup>4</sup>	30	3	1.3	3.2
He <sup>4</sup>	70	7	1.3	7.1

\* Calculated numerically, includes 250 keV detector noise.

## IFC DESCRIPTION

DETECTOR	CH	V (mV)	E (MeV)	$\Delta V/\Delta C$ (mV/CH)	$\Delta E/\Delta C$ (MeV/CH)	$\Delta V/(V\Delta C)$ (CH) <sup>-1</sup>
D1 (.2083 MeV/mV)	46.2	13.04	2.72	.277	.0579	.021
D1	139.25	105.35	21.94	2.69	.559	.0254
D1	173.65	213.3	44.43	10.31	2.15	.048
D1	215.8	829.0	172.7	16.13	2.98	.019
D2 (.2105 MeV/mV)	51.45	13.10	2.757	.251	.0529	.019
D2	136.25	107.95	22.72	2.21	.465	.0204
D2	171.4	214.7	45.19	9.72	2.048	.045
D2	220.65	849.2	178.8	13.6	2.86	.016
D5 (.213X19.8 MeV/mV)	40.9	12.86	54.25	.311	1.31	.024
D5	147.2	104.9	442.4	2.64	11.15	.025
D5	186.65	208.6	879.8	2.68	11.3	.0128
D5	250.0	>400.0				
LET	62.67	17.42	3.8	.275	.060	.0158

## MEAN IFC VOLTAGE

Level	Voltage (mV)
1	13.00 + .09
2	106.1 + 1.1
3	212.2 + 2.2
4	839.0

Figure 7

## SNO1 IFC CHANNELS

Date Situation	Day	T (F)	D1	D2	D5
6/24/73 Bench			46.2 139.25 173.65 215.8	51.45 136.25 171.4 220.65	40.9 147.2 186.65 250.0
				LET = 62.67	
10/19/73 Encapsulation			46.0 139.35 173.52 215.58	51.63 136.32 171.02 220.43	41.2 147.07 187.04 250.0
				LET = 62.61	
11/8/73 Space IFC	312	28.0	46.36 140.22 174.16 216.39	51.63 137.00 171.45 220.66	41.19 147.46 187.31 250.00
				LET = 62.70	
11/15/73 Space IFC	319	30.0	46.34 139.99 174.09 216.45	51.68 137.03 171.52 220.75	41.11 147.30 187.22 250.00
				LET = 62.65	
11/22/73	326	30.8	46.33 140.02 173.89 216.63	51.73 136.98 171.54 220.77	41.08 147.09 187.19 250.00
				LET = 62.60	

Figure 7a  
Mariner 10 IFC Channels

	D	T	D1	D2	D5
11/29/73 Space IFC	333	31	46.34 140.15 173.85 216.65	51.77 136.99 171.54 220.79	41.10 147.02 187.17 250.00
				LET = 62.63	
12/6/73 Space IFC	340	32.3	46.35 140.28 173.84 216.65	51.77 136.97 171.62 220.86	41.02 146.91 187.17 250.00
				LET = 62.59	
12/13/73 Space IFC	347	32.3	46.35 140.34 173.82 216.66	51.78 136.95 171.66 220.92	41.03 146.90 187.18 250.00
				LET = 62.60	
12/20/73 Space IFC	354	32.3	46.42 140.34 173.51 216.65	51.80 136.96 171.64 220.91	40.99 146.85 187.15 250.00
				LET = 62.57	
12/27/73 Space IFC	361	32.3	46.40 140.36 173.80 216.50	51.82 136.92 171.72 220.98	41.06 146.85 187.13 250.00
				LET = 62.57	

Figure 7b

		Mariner 10 IFC Channels				
	D	T	D1	D2	D5	
01/03/74 Space IFC	3	33.7	46.38	51.80	41.03	
			140.34	136.83	146.83	
			173.77	171.66	187.13	
			216.28	220.92	250.00	
			LET =	62.59		
01/10/74 Space IFC	10	33.7	46.43	51.85	41.09	
			140.33	136.81	146.82	
			173.80	171.73	187.15	
			216.22	220.97	250.00	
			LET =	62.55		
01/17/74 Space IFC	17	26.5	46.31	51.69	40.99	
			139.95	137.71	146.87	
			174.03	171.62	186.98	
			216.33	220.94	250.00	
			LET =	62.50		
01/24/74 Space IFC	24		46.36	51.65	40.99	
			140.13	137.12	147.00	
			174.21	171.54	186.96	
			216.46	220.99	250.00	
			LET =	62.50		
01/31/74 Space IFC	31	23.6	46.46	51.62	40.96	
			140.12	136.92	146.94	
			174.16	171.32	186.81	
			216.35	220.82	250.0	
			LET =	62.51		
02/04/74 Space IFC	35		46.40	51.65	40.98	
			140.19	137.10	146.97	
			174.23	171.49	186.91	
			216.49	220.95	250.00	
			LET =	62.50		

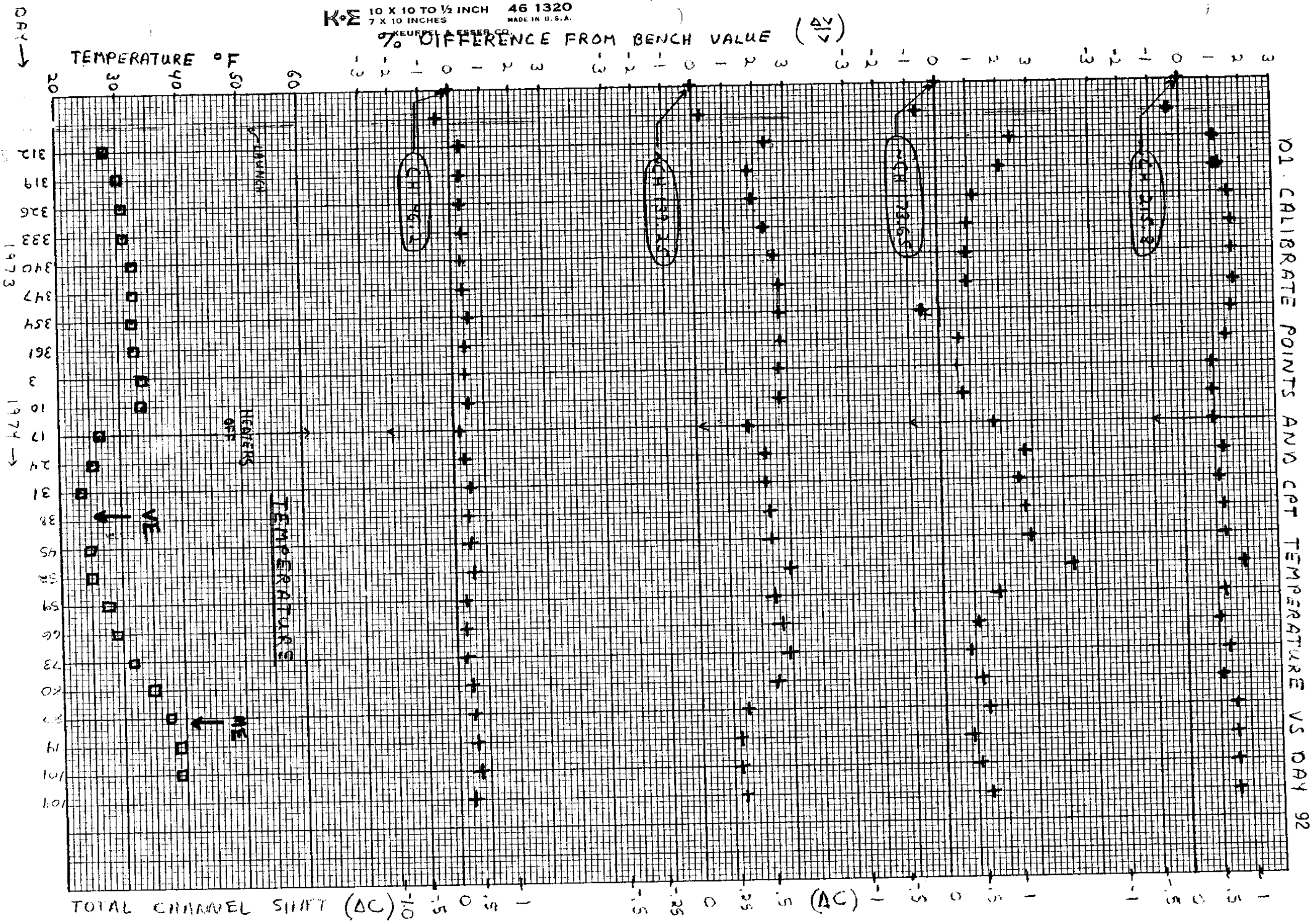
Mariner 10 IFC Channels

	D	T	D1	D2	D5
02/14/74 Space IFC	45	25.0	46.45 140.20 174.26 216.48	51.64 137.06 171.44 220.95	41.07 146.95 186.89 250.00
				LET = 62.47	
02/21/74 Space IFC	52	25.0	46.50 140.46 174.56 216.82	51.58 137.19 171.58 221.08	41.09 147.17 187.10 250.00
				LET = 62.52	
02/28/74 Space IFC	59	27.9- 29.4	46.34 140.21 174.03 216.42	51.69 137.22 171.72 221.07	40.98 146.87 187.10 250.00
				LET = 62.51	
03/07/74 Space IFC	66	29.4	46.32 140.35 173.89 216.34	51.74 137.22 171.75 221.11	41.00 146.82 187.09 250.00
				LET = 62.49	
03/14/74 Space IFC	73	32.3	46.34 140.44 173.83 216.52	51.77 137.12 171.79 221.16	40.99 146.79 187.07 250.00
				LET = 62.50	
03/21/74 Space IFC	80	35.2	46.41 140.24 173.90 216.37	51.85 136.85 171.67 221.07	41.04 146.96 187.19 250.00
				LET = 62.52	

## Mariner 10 IFC Channels

	D	T	D1	D2	D5
03/28/74 Space IFC	87	38.1	46.46 139.83 173.95 216.67	51.89 136.79 171.65 220.79	41.08 147.05 187.19 250.00
				LET = 62.53	
04/04/74 Space IFC	94	39.6	46.50 139.70 173.85 216.66	51.90 136.70 171.67 220.66	41.04 147.04 187.04 250.00
				LET = 62.49	
04/11/74 Space IFC	101	39.6	46.52 139.71 173.88 216.68	51.91 136.74 171.68 220.71	41.10 147.08 187.09 250.00
				LET = 62.53	
04/19/74 Space IFC	109		46.44 139.81 173.97 216.88	51.78 136.86 171.78 220.83	41.05 147.15 187.10 250.00
				LET = 62.49	

KEURPS KEURPS CO.  
 % DIFFERENCE FROM BENCH VALUE ( $\Delta\%$ )



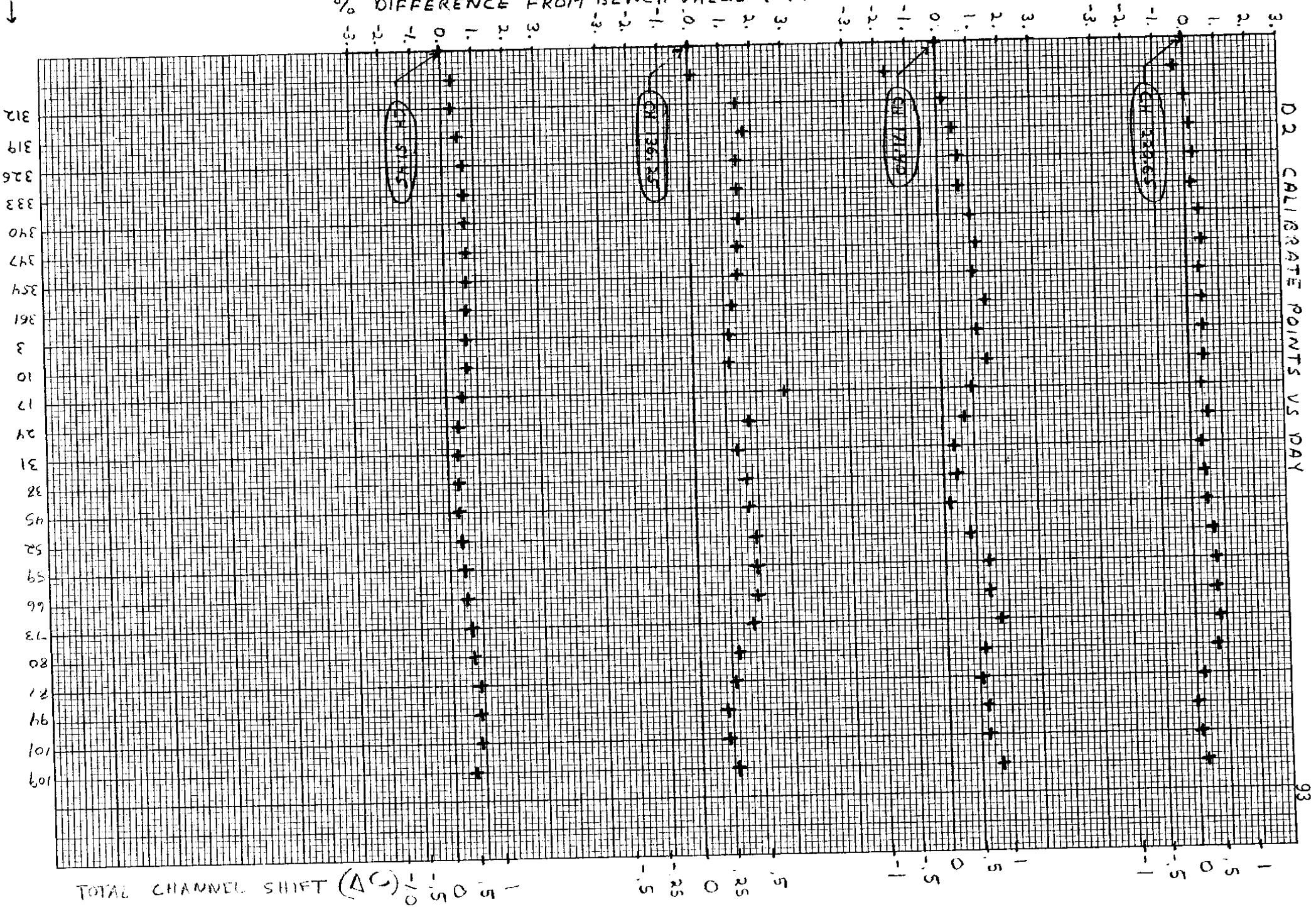
01. CALIBRATE POINTS AND CPT TEMPERATURE VS DAY 92

K&E 10 X 10 TO 1/2 INCH 46 1320  
7 X 10 INCHES MADE IN U.S.A.

7% DIFFERENCE FROM BENCH VALUE ( $\frac{\Delta V}{V}$ )

KEUFFEL & ESSER CO.

DAY →



D2 CALIBRATE POINTS VS DAY

93

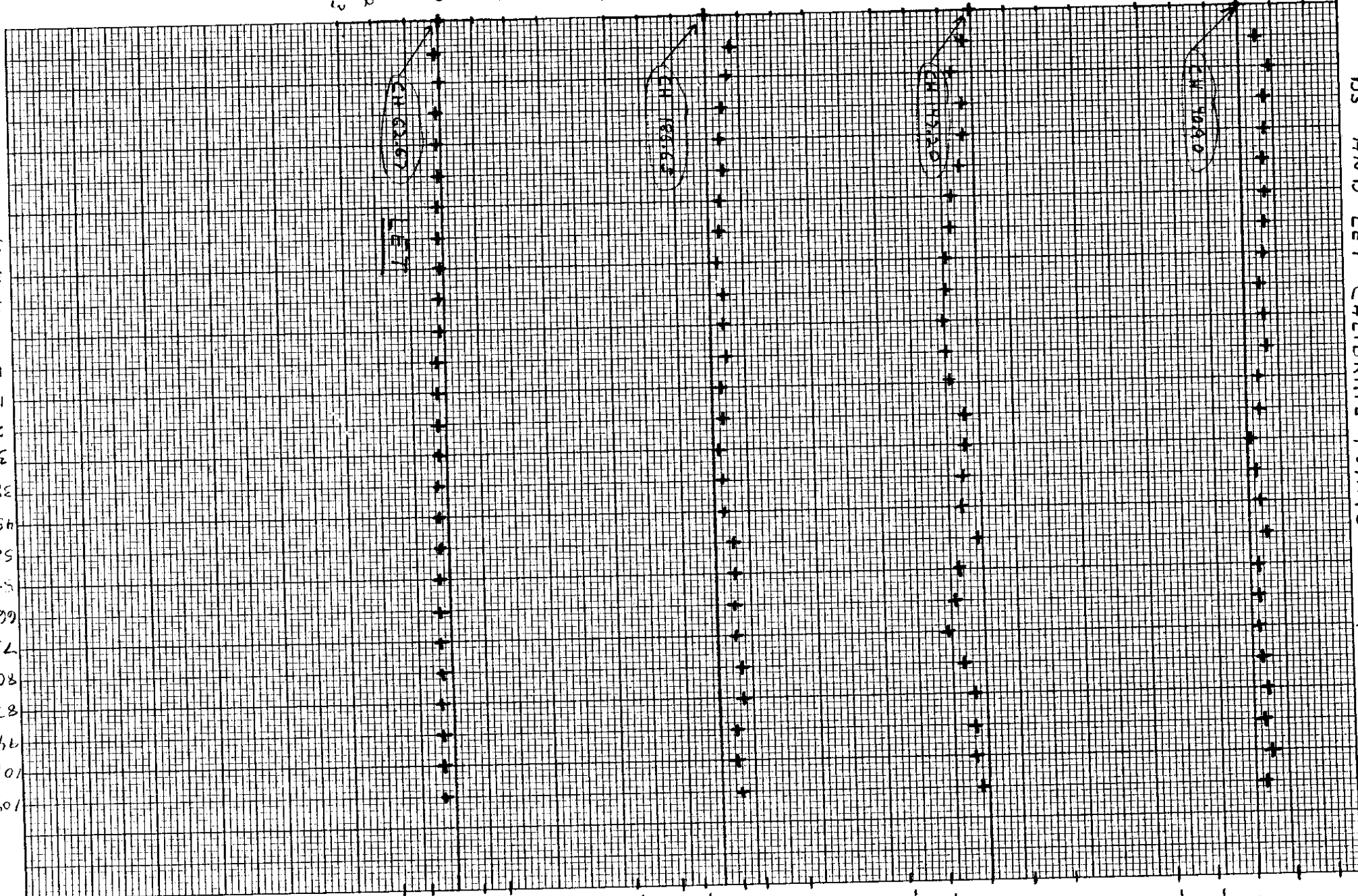
DIFFERENCE FROM BENCH VALUE ( $\frac{\Delta V}{V}$ )

DAY ↓

1973  
 312  
 319  
 326  
 333  
 340  
 347  
 354  
 361  
 3  
 10  
 17  
 24  
 31  
 38  
 45  
 52  
 59  
 66  
 73  
 80  
 87  
 94  
 101  
 109

3 2 1 0 - 1 2 3 3 2 1 0 - 1 2 3 3 2 1 0 - 1 2 3

DS AND LET CALIBRATE POINTS VS DAY



TOTAL CHANNEL SHIFT ( $\Delta C$ ) (in)

## Appendix C

### Investigation of Background in LET

This appendix consists of three memos from A. J. Tuzzolino to the Pioneer, Mariner, and IMP working groups at LASR. The information contained herein, although written specifically about the Pioneer LETs, is generally applicable to all five University of Chicago LETs. These instruments were aboard: IMP 7, IMP 8, Mariner 10, Pioneer 10 and Pioneer 11. In order to apply any of this analysis to IMP or Mariner LETs, the specific electronics and dynamic range of each instrument must be taken into consideration.

## THE UNIVERSITY OF CHICAGO

DATE

TO Distribution  
FROM Tony Tuzzolino

DEPARTMENT

DEPARTMENT

IN RE:

Section A (August 10, 1973): General "background" estimates for the IMP/Pioneer/Mariner UC/LET.

Background events in the L1N2 mode may result from two sources:

- I. nuclei which pass through the passive shield and trigger L1 only (direct energy loss background);
- II. nuclei generated in the passive shield of the LET via nuclear interactions of incident nuclei in the shield. (nuclear interaction background).

We consider Type I background first:

Type I background may result from nuclei which penetrate the shield and stop in L1 as well as from nuclei which penetrate the shield and pass through L1 where in both cases, the condition L1N2 is satisfied, as illustrated in Figure A.1.

For Type I nuclei which stop in L1, the relevant geometrical factor is  $G_1(\text{stop}) = 3.09 - 0.49 = 2.6 \text{ cm}^2 \text{ sterad}$ . Assuming that the shield is equivalent to 1.0 cm of silicon regardless of the angle of incidence of the nucleus, then the incident energy required for a proton (H) or helium (He) nucleus to penetrate the shield is  $\approx 45 \text{ MeV nucleon}^{-1}$ . The range of angles (with respect to normal to the L1 detector) for nuclei penetrating the shield and stopping in L1 is  $\Theta_{\text{Min}} = 7.5^\circ$  to  $\Theta_{\text{Max}} = 85.75^\circ$ . The path length in the L1 detector corresponding to  $\Theta_{\text{Max}}$  is  $495\mu (1\mu = 10^{-6} \text{ meters})$  which is equal to the range of an  $8.1 \text{ MeV nucleon}^{-1}$  H or He. For a "uniform" 1 cm shield, H and He incident on the shield in the range  $\sim 45 - 47 \text{ MeV nucleon}^{-1}$  will be incident on L1 with energies in the range  $\sim 0 - 8.1 \text{ MeV nucleon}^{-1}$ . If, as an upper limit

estimate, we assume that all H and He from 45 - 47 MeV nucleon<sup>-1</sup> stop in L1, then the expected LIN2 rate for these nuclei is

$$\text{LIN2}_{\text{I}}(\text{Stop}) < 2.6 \int_{45}^{47} (J_{\text{H}} + J_{\text{He}}) dE, \quad (1)$$

where  $J_{\text{H}}$  and  $J_{\text{He}}$  are the quiet time differential particle fluxes for H and He, respectively. Using 1972 quiet time differential spectra, Eq.

(1) gives

$$\text{LIN2}_{\text{I}}(\text{Stop}) < 2.6(2) [3+2] \times 10^{-5} = 2.6 \times 10^{-4} \text{ sec}^{-1} \quad (2)$$

so that the background LIN2 rate resulting from Type I H and He which stop in L1 is <1.4% of the mean quiet time LIN2 rate observed in the LETs ( $1.83 \times 10^{-2} \text{ sec}^{-1}$ ). Therefore this component of background is negligible.

For Type I nuclei which penetrate both the shield and L1, the relevant geometrical factor is  $G_{\text{I}}(\text{penetrate}) = 0.75 \text{ cm}^2 \text{ sterad}$ . The range of incident angles for these nuclei is from  $\Theta_{\text{Min.}} = 37.5^\circ$  to  $\Theta_{\text{Max.}} = 83.7^\circ$ . The path length corresponding to  $\Theta_{\text{Max}}$  is  $335 \mu$  so that both H in the energy range 45 - 120 MeV and He from 45 -  $\infty$  MeV nucleon<sup>-1</sup> incident on the shield would penetrate and trigger L1 (350 KeV discriminator level) if they were incident at  $\Theta_{\text{Max}} = 83.7^\circ$ . Because of the very large ( $\infty$ ) energy range for He, a realistic estimate of the LIN2 rate requires a rigorous calculation. The expression for the expected LIN2 rate for Type I particles which trigger and penetrate L1 is given by

$$\text{LIN2}_{\text{I}}(\text{Penetrate}) = \left\{ \int_{45}^{120} \left[ J_{\text{H}}(E) \int_{\chi(E^*)}^{335} P(\chi) d\chi \right] dE + \int_{45}^{\infty} \left[ J_{\text{He}}(E) \int_{\chi(E^*)}^{335} P(\chi) d\chi \right] dE \right\}, \quad (3)$$

where  $P(x)$  is the path length distribution for the particle, and  $X(E^*)$ , where  $X$  is in  $\mu$ , is defined by

$$\left(\frac{dE}{dX}\right)_{H,He}^{E^*} = \frac{350}{X(E^*)}$$

where  $\left(\frac{dE}{dX}\right)_{H,He}^{E^*}$  is the rate of energy loss in silicon  $\left(\frac{\text{keV}}{\mu}\right)$  at "transmitted" energy  $E^*$  corresponding to incident energy  $E$  ( $\text{MeV nucleon}^{-1}$ ) for H or He.

The normalized distribution in  $\Theta$  is shown in Figure 2A, and the corresponding normalized path length distribution  $P(x)$  is shown in Figure 2B. Numerical evaluation of Eq. (3), making use of quiet time H and He differential energy spectra and  $P(x)$  yields

$$\begin{aligned} \text{LIN2}_I(\text{Penetrate}) &= 0.75 [0.43 + 3.74] \times 10^{-3} \\ &= 3.1 \times 10^{-3} \text{ sec}^{-1} \end{aligned}$$

which is  $\sim 16\%$  of the mean quiet time rate in the LETs.

Extensive high energy runs will be required to assess the importance of Type II background. In any case, it seems that a reasonable estimate for general background (both direct energy loss and nuclear interaction) in the

LET LIN2 rate is  $\approx 20\%$ .

FIGURE A1

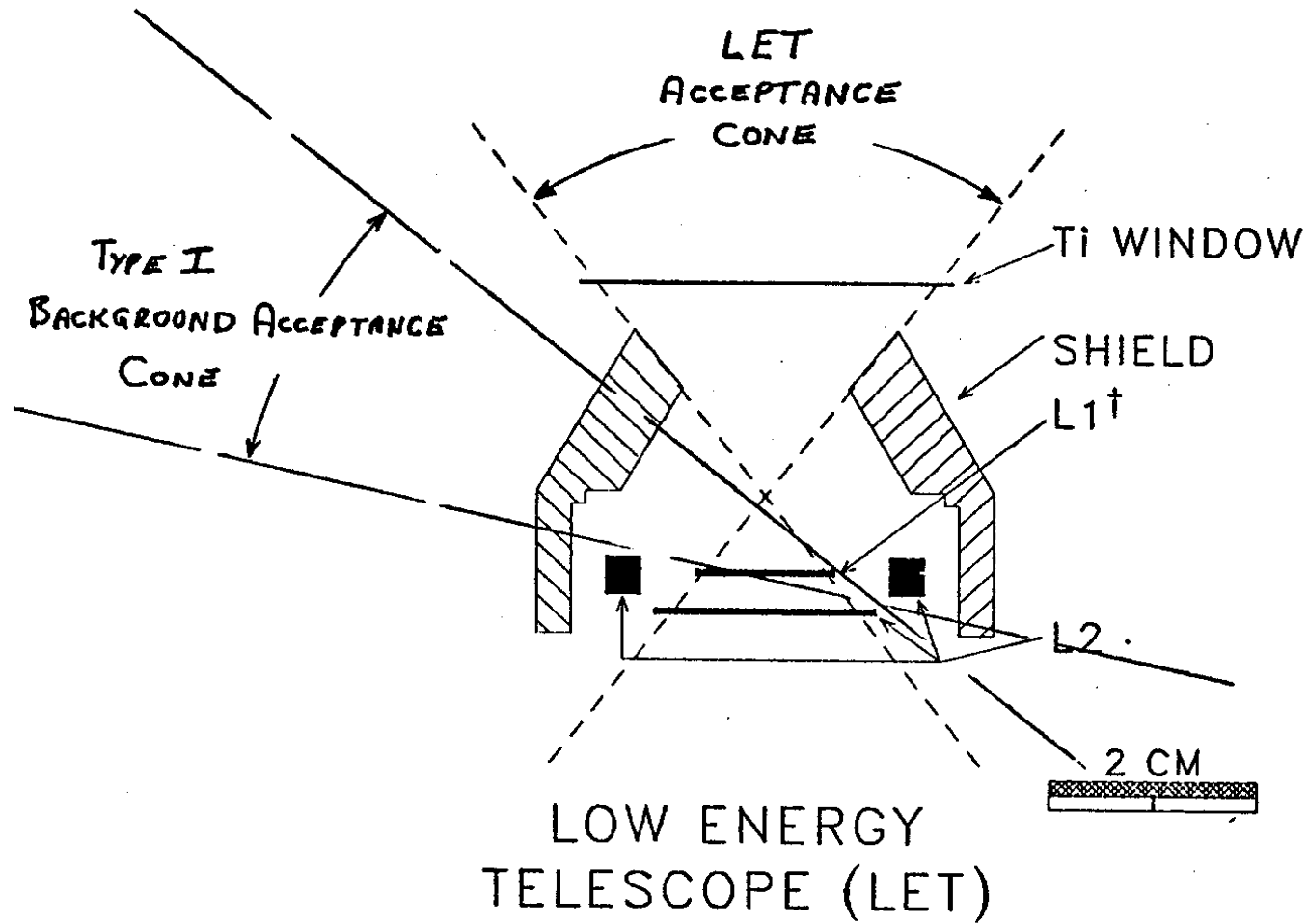


FIGURE A2

$P(\theta)$  vs  $\theta$  (A) and  $P(x)$  vs  $x$  (B) for Pioneer 10 LET

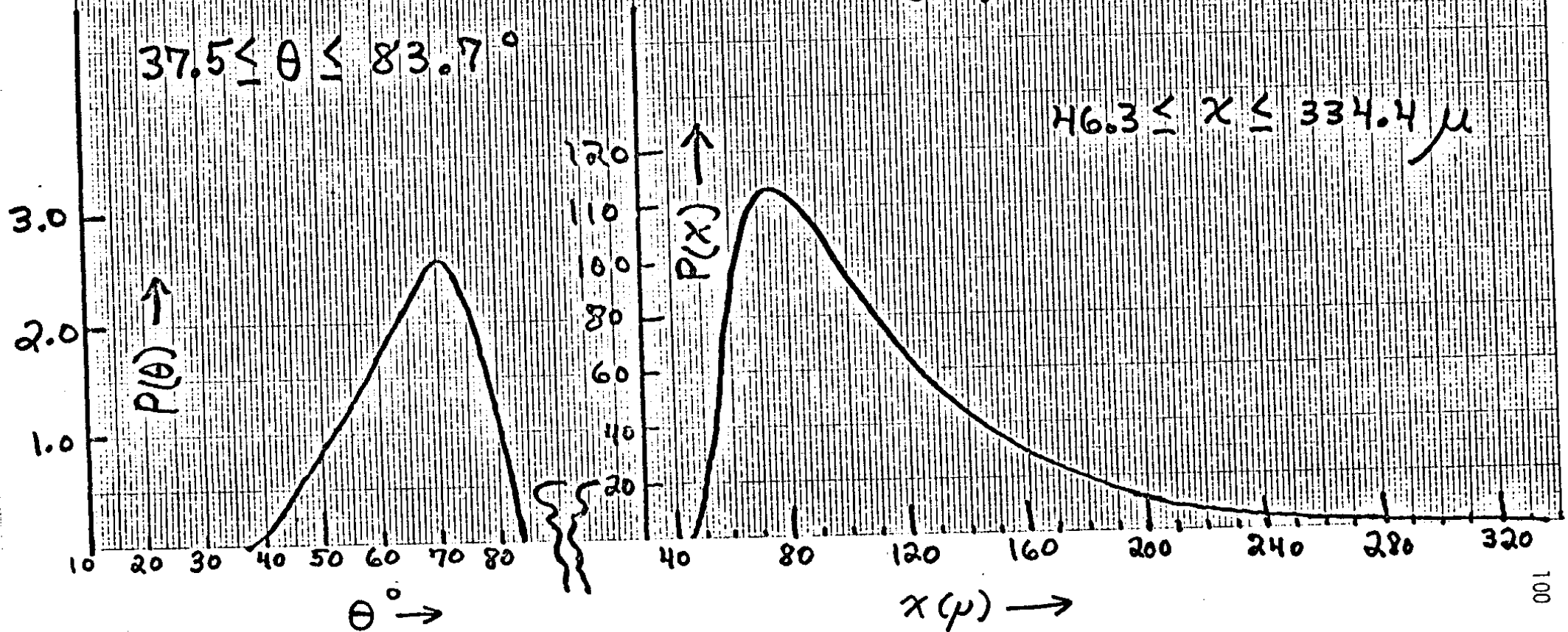
LI thick. =  $36.7 \mu$

(A)

(B)

$37.5 \leq \theta \leq 83.7^\circ$

$46.3 \leq x \leq 334.4 \mu$



## THE UNIVERSITY OF CHICAGO

DATE

TO Distribution  
 FROM Tony Tuzzolino

DEPARTMENT

DEPARTMENT

Section B (September 18, 1973): Final results of "direct-energy-loss" background calculations for the LET. (Note that energy channels referred to in this section are defined for the Pioneer spacecraft.)

The following summarizes the final results of a calculation of "direct-energy-loss" LET background in the LIN2 mode. The LIN2 background considered here results from incident nuclei which penetrate the passive shield and pass through L1, where the condition LIN2 is satisfied. A second contribution to the LIN2 background, resulting from nuclei generated in the passive shield of the LET via nuclear interactions of the incident nuclei in the shield, is not considered here.

In Section A, approximate background calculations are presented for the case of background resulting from protons and helium only. The results presented here represent refinements and extensions of those calculations.

The calculations discussed here assume the following:

- 1) the passive shield is equivalent to 1.0 cm of aluminum ( $2.7 \text{ gm/cm}^2$ ) regardless of the angle of incidence of the incident nuclei
- 2) the incident nuclei which generate the background consists of H, He, (C+N+O), and Fe;
- 3) the H and He differential energy spectra up to  $100 \text{ MeV nucleon}^{-1}$  are the 1972 "values", and for energies  $> 100 \text{ MeV nucleon}^{-1}$  are the 1965 "values";
- 4) the differential energy spectra for (C+N+O) and Fe are related to the differential energy spectra for He by  $J_{(C+N+O)} = J_{\text{He}}/15$  and  $J_{\text{Fe}} = J_{\text{He}}/625$ , for energies  $< 100 \text{ MeV nucleon}^{-1}$ ;
- 5) L1 thickness =  $36.7 \mu$ ; L1 discriminator = 350 KeV.

To calculate the background event rate distribution, the ten discriminator levels  $D_j$  ( $j = 1-10$ ) corresponding to the nine (four proton and five He) L1

channels  $C_i$  ( $i = 1-9$ ) were used to determine quantities  $X_j(E^*)$  defined by

$$\left( \frac{dE}{dX} \right)_{E^*} = \frac{D_i}{X_i(E^*)} ,$$

(background particles)

(1)

where  $\left( \frac{dE}{dX} \right)_{E^*}$  is the rate of energy  
(background particles)

loss in silicon at "transmitted" energy  $E^*$  corresponding to incident energy  $E_0$  on the shield, and the background particle is a H, He, (C+N+O) or Fe nucleus. Having determined the  $X_j$  for all incident energies and all background particles, the event rate  $R_i$  for channel  $C_i$  is calculated from

$$R_i(\text{sec}^{-1}) = G \left\{ \int_{45}^{135} \left[ J_H(E_0) \int_{X_i(E^*)}^{X_{iH}(E^*)} P(X) dX \right] dE_0 + \int_{45}^{\infty} \left[ J_{He}(E_0) \int_{X_i(E^*)}^{X_{iHe}(E^*)} P(X) dX \right] dE_0 + \int_{45}^{\infty} \left[ J_{(C+N+O)}(E_0) \int_{X_i(E^*)}^{X_{i(C+N+O)}(E^*)} P(X) dX \right] dE_0 + \int_{195}^{\infty} \left[ J_{Fe}(E_0) \int_{X_i(E^*)}^{X_{iFe}(E^*)} P(X) dX \right] dE_0 \right\} , \quad i = 1, 9$$

(2)

where  $G$  is the geometrical factor ( $0.75 \text{ cm}^2 \text{ sterad}$ ) and  $P(X)$  is the normalized path length distribution for the geometry considered here.

It is to be emphasized that the results of the calculations are to be considered as highly approximate since no account was taken of general spacecraft "material" (such as various support structures, other experiments, etc.) which would serve as additional absorbing material for some angles of incidence, so that the results are useful only in that they yield a "range" for the expected background level (factor  $\approx$ two confidence).

The results of the evaluation of Equations (1) and (2) are given in Figure B.1. The curves marked "H", "He", and "(C+N+O)", are calculated background contributions from quiet-time interplanetary H, He, and (C+N+O). In addition to the nine proton and He channels, the event rate for channels  $> 25$  [the (C+N+O) channels] is also shown. The background contribution from Fe is seen to fall in channels 25 only. The curve labeled "total background" is the summation of the proton, He, (C+N+O), and Fe background curves. The curve labeled "observed", is a quiet-time event distribution obtained from the LET on Pioneer 10. If the calculated curves in Figure B.1 are taken at face value, qualitatively, one sees that the proton channels are not dominated by background whereas the He and (C+N+O) channels are heavily contaminated by background, with the contamination in the He and (C+N+O) channels resulting primarily from background (C+N+O), which were not considered in the earlier memo referred to above. From Figure B.1, the following ratios result for the lowest L1N2 counting rates observed:

- |    |  |        |
|----|--|--------|
| a) | $\frac{\text{calculated background rate for proton channels}}{\text{observed rate for H channels}}$        | = 0.28 |
| b) | $\frac{\text{calculated background rate for He channels}}{\text{observed rate for He channels}}$           | = 0.75 |
| c) | $\frac{\text{calculated background rate for (C+N+O) channels}}{\text{observed rate for (C+N+O) channels}}$ | = 0.68 |
| d) | $\frac{\text{calculated background L1L2 rate}}{\text{observed L1L2 rate}}$                                 | = 0.32 |

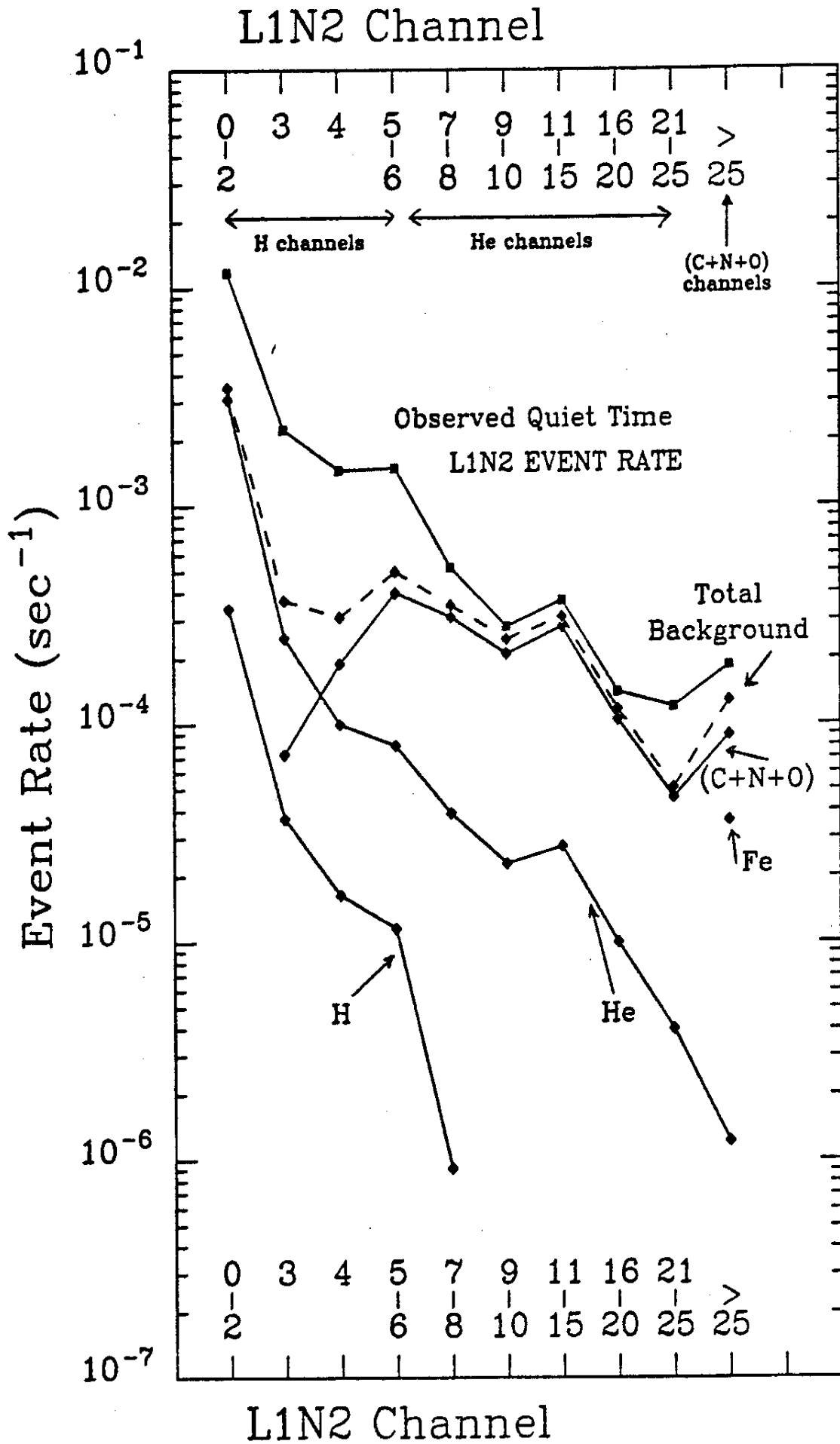
The fact that the calculated background rates for the He and (C+N+O) channels are comparable to the observed rates suggests that these channels are far more heavily contaminated background during quiet times than previously thought.

In addition to the background considered here, the importance of nuclear-interaction type background in the LET must be considered. The importance of the "nuclear interaction" background will be established during the up-coming SREL\* runs.\*\* In summary then, it appears that an overall background contamination of the Pioneer 10 quiet-time L1L2 rate of  $\approx 30\%$  is highly possibly if not probable, with the He and (C+N+O) channels being far more heavily contaminated than the proton channels.

\*Space Radiation Environment Laboratory

\*\*See Section C

FIGURE B1



## THE UNIVERSITY OF CHICAGO

DATE

TO Distribution

DEPARTMENT

FROM Tony Tuzzolino

DEPARTMENT

Section C. (November 8, 1973): Experimental Results of "direct-energy-loss" and "nuclear-interaction" background studies for the LET carried out at SREL\* during October of 1973.

The following summarizes the results obtained with the LET using protons (H) and helium (He) at the SREL during the period 10/22/73 to 10/30/73. The purpose of these studies was to obtain a reliable estimate of the background in the LET resulting from both direct-energy-loss leakage (Type I) and nuclear interactions in the passive shield (Type II). These possible background contributions have been discussed in Sections A and B.

Measurements were made using the Pioneer DVU LET (LET 1) and a "spare" LET (LET 2) as illustrated in Figure C.1. LET 1 had a detector (D1) mounted over the entrance aperture to exclude any analysis of events resulting from nuclei entering the entrance aperture, and a plastic scintillator PM tube combination which fit closely over the outer housing so that the number of protons incident on the passive shield could be determined. In the case of LET 2, it had a) no passive shield, permitting comparisons between the two LET's with regard to nuclear interaction background, and b) a "composite" L2 (flat) detector with a "variable" diameter, permitting comparisons between the two LET's with regard to direct-energy-loss leakage background. The effective sensitive diameter of the composite L2 (flat) detector could be varied by means of a switch located external to the telescope.

Measurements were made using H and He. The 10 rates and two PHA's listed in Figure I were simultaneously measured during a given run. We consider Type II background first.

Type II: Nuclear Interaction Background

Nuclear interaction effects in the LET may be studied by using protons of sufficiently high energy. For example, a single 150 MeV proton incident on L1 will not trigger the L1 discriminator (350 Kev) for angles of incidence with respect to the axis of the LET of up to 84°, so that any event which triggers L1 may be assumed to result from either nuclear interactions or proton pulse pile-up. The response of both LET 1 and LET 2 to protons of energies

\*Space Radiation Environment Laboratory

210 MeV, 350 MeV, 450 MeV, and 600 MeV was measured for angles of incidence of the protons with respect to the LET axis of  $0^\circ$ ,  $65^\circ$ ,  $85^\circ$ ,  $125^\circ$ , and  $135^\circ$ . In the case of LET 1, the results for all angles of incidence and all energies studied were found to be the same (within statistics). Therefore a "mean" response was obtained by combining the results for all angles and all energies. Defining a nuclear interaction background efficiency for LET 1 as

$$\eta(1) \equiv \frac{\text{number of nuclear-interaction LIN2 events}}{\text{number of protons incident on the passive shield}},$$

an upper limit for  $\eta(1)$  was obtained from the rates listing in Figure C.1. During each run, the D1 detector (Figure C.1) was continuously monitored so that beam "pile-up" could be "followed". A strong correlation was found between periods of strong beam pile-up and enhanced LIN2 event rate. It is estimated that at least half of the recorded LIN2 events resulted from beam pile-up. However, no correction was attempted for such cases so that the observed LIN2 events for LET 1 represent an upper limit to the LIN2 events resulting from nuclear interactions in the passive shield of the LET.

The quantity  $\eta(2)$  measured for LET 2 was found to be a factor of  $\sim$ two smaller than  $\eta(1)$ , indicating that nuclear interactions in the passive shield of LET 1 resulted in half of the recorded LIN2 events for LET 1, the remaining half of the recorded events resulting from effects unrelated to the passive shield and common to both LETs (beam pile-up, etc.). However for an upper limit value for  $\eta(1)$  it will be assumed that all recorded LIN2 events for LET 1 resulted from nuclear interactions. The mean value obtained for  $\eta(1)$  is

$$\langle \eta(1) \rangle = [1.6 + 0.2] \times 10^{-5} \quad (\text{upper limit}),$$

where the quoted error results from the statistical uncertainty in the total number of LIN2 events recorded only. From the above value for  $\langle \eta(1) \rangle$ , the quiet-time proton flux, and the geometry of the passive shield, we obtain

$$\text{LIN2} \left( \begin{array}{l} \text{nuclear interaction} \\ \text{background rate} \end{array} \right) = 5.5 \times 10^{-4} \text{ sec}^{-1} \quad (\text{upper limit}).$$

From the pulse height distribution of the recorded LIN2 events we obtain the following ratios:

- a)  $\frac{\text{Type II background rate corresponding to H channels (SREL)}}{\text{interplanetary LIN2 rate for H channels}} \leq 0.028$
- b)  $\frac{\text{Type II background rate corresponding to He channels (SREL)}}{\text{interplanetary LIN2 rate for He channels}} \leq 0.063$
- c)  $\frac{\text{Type II background LIN2 rate (SREL)}}{\text{interplanetary LIN2 rate}} \leq 0.030$

The nuclear interaction background levels indicated in the ratios a), b), and c) above are small and may essentially be neglected when compared with direct-energy-loss leakage background discussed below.

#### Type I: Direct-Energy-Loss Leakage Background

In Section B, the results of a calculation of direct-energy-loss background in the LET resulting from high energy H, He, (C+N+O), and Fe were presented. The calculated background levels were sufficiently high so as to warrant an experimental verification of any predictions based on the computational procedures used to calculate the background. Identical procedures to those used in the included memo were used to calculate the ratio  $\lambda(\theta)$ , defined as

$$\lambda(\theta) \equiv \frac{\text{LIN2}(\theta)}{\text{LIN2}(\theta) + \text{L1L2}(\theta)}$$

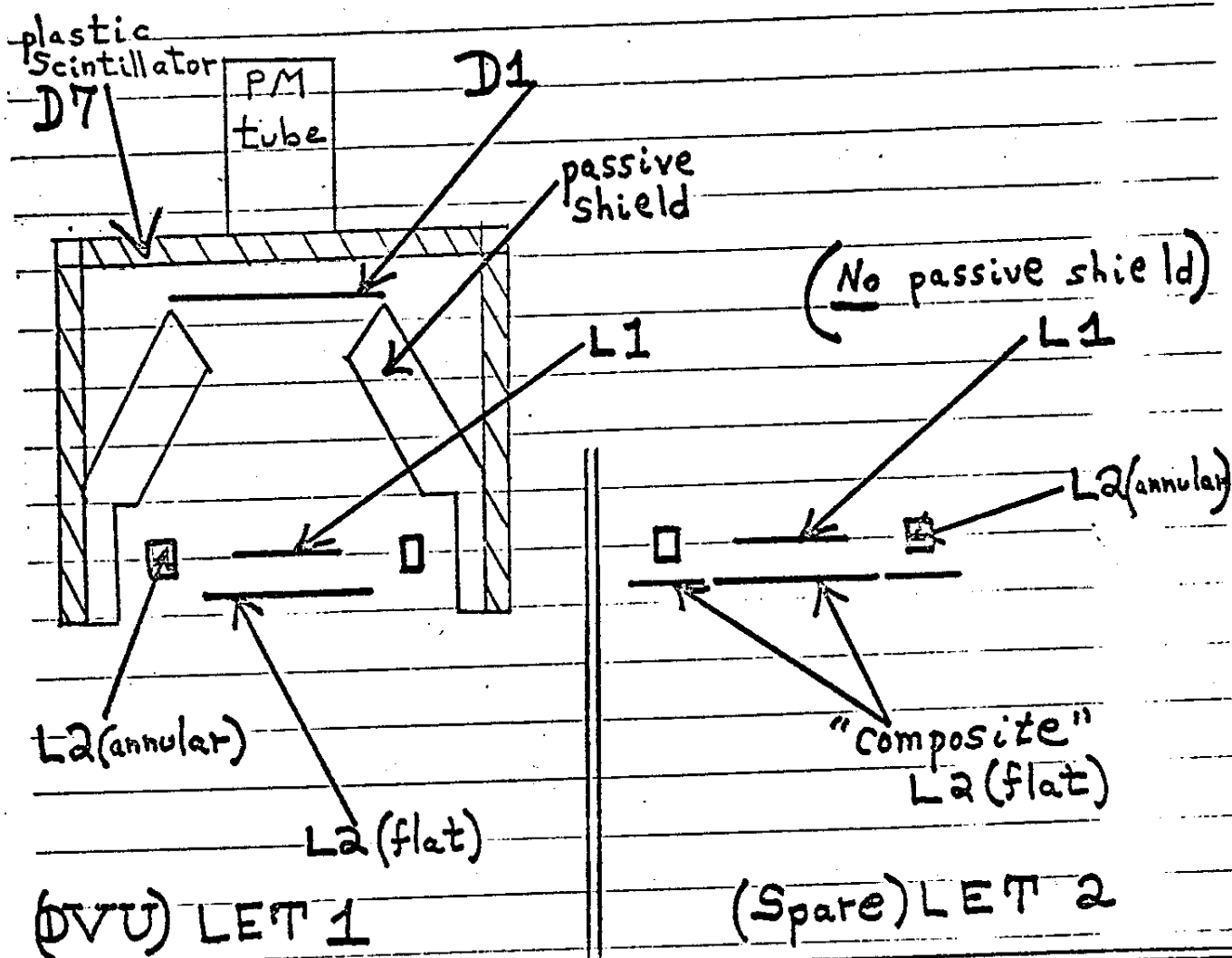
where LIN2 is the rate at which the condition LIN2 would be satisfied in a beam of He nuclei which is ideally plane-parallel, uniform in intensity and incident on the LET at angle  $\theta$  with respect to the LET axis. The calculated value for  $\lambda(\theta)$  is given by the solid curve of Figure C.2. An experimental value,  $\lambda^*(\theta)$ , was determined by making use of He of energies 131 MeV/nucleon and 178 MeV/nucleon and angles of incidence with respect to the LET axis ranging from  $0^\circ$  to  $80^\circ$  by  $5^\circ$  steps. The responses of both LET 1 and LET 2 were measured simultaneously with both LET's mounted together in a "rigid" system so as to minimize errors in angle measurement. The quantity  $\lambda(\theta)$  is a strong function of the effective diameter of the L2 (flat) detector so that the composite L2 (flat) detector in the LET 2 would permit verification of the dependence of  $\lambda(\theta)$  on effective diameter of the L2 (flat) detector. The quantity  $\lambda^*(\theta)$  was found to be identical for both the 131 MeV/nucleon and 178 MeV/nucleon He at all angles  $\theta$  for both LET's. In addition, when the effective

diameters of the L2 (flat) detectors were chosen identical, then  $\lambda^*(\theta)$  for both LET's were found to be in good agreement at most angles  $\theta$ . The experimental values obtained for  $\lambda^*(\theta)$  for LET 1 are given in Figure C.2 as obtained with the 178 NeV/nucleon He. Considering the uncertainties in alignment, angle determination, etc., the agreement between the experimentally determined  $\lambda^*(\theta)$  and the calculated  $\lambda(\theta)$  is felt to be excellent. In addition, the strong dependence of  $\lambda^*(\theta)$  on L2 (flat) diameter was verified by switching the effective L2 (flat) diameter in the LET 2 system between its two values during each run at each angle. For example, at  $\theta = 55^\circ$ , the value of  $\lambda^*(\theta)$  for LET 2 dropped from 36.4% to 22.7% by switching the composite L2 (flat) detector to its larger diameter. Similarly, at  $\theta = 75^\circ$ , a similar operation changed  $\lambda^*(\theta)$  for LET 2. The dependence of  $\lambda^*(\theta)$ , at any given angle on effective L2 (flat) diameter was verified.

The very good agreement between  $\lambda^*(\theta)$  and  $\lambda(\theta)$  strongly suggests that the computational procedures used to calculate the direct-energy-loss LET background are basically sound. Therefore the background levels presented in Section B should represent fairly reliable estimates of the background contamination in the LET proton, He, and CNO channels. Thus, the quiet time LET He channels could be contaminated up to  $\sim 75\%$ , so that any statements made about the nature of the events in the He channels will have to be highly qualified. The much lower calculated level of contamination for the proton channels ( $\approx 28\%$  total), suggests that fairly quantitative statements regarding quiet time events in these channels, i.e., our derivations of proton spectra, proton gradients, etc., may still be valid, whereas our He spectra and H/He ratios as obtained from the He channels are probably in significant error.

Again, we define "quiet time" to be those periods when the L1N2 counting rate is at its lowest observed values ( $\approx 0.02 \text{ sec}^{-1}$ ).

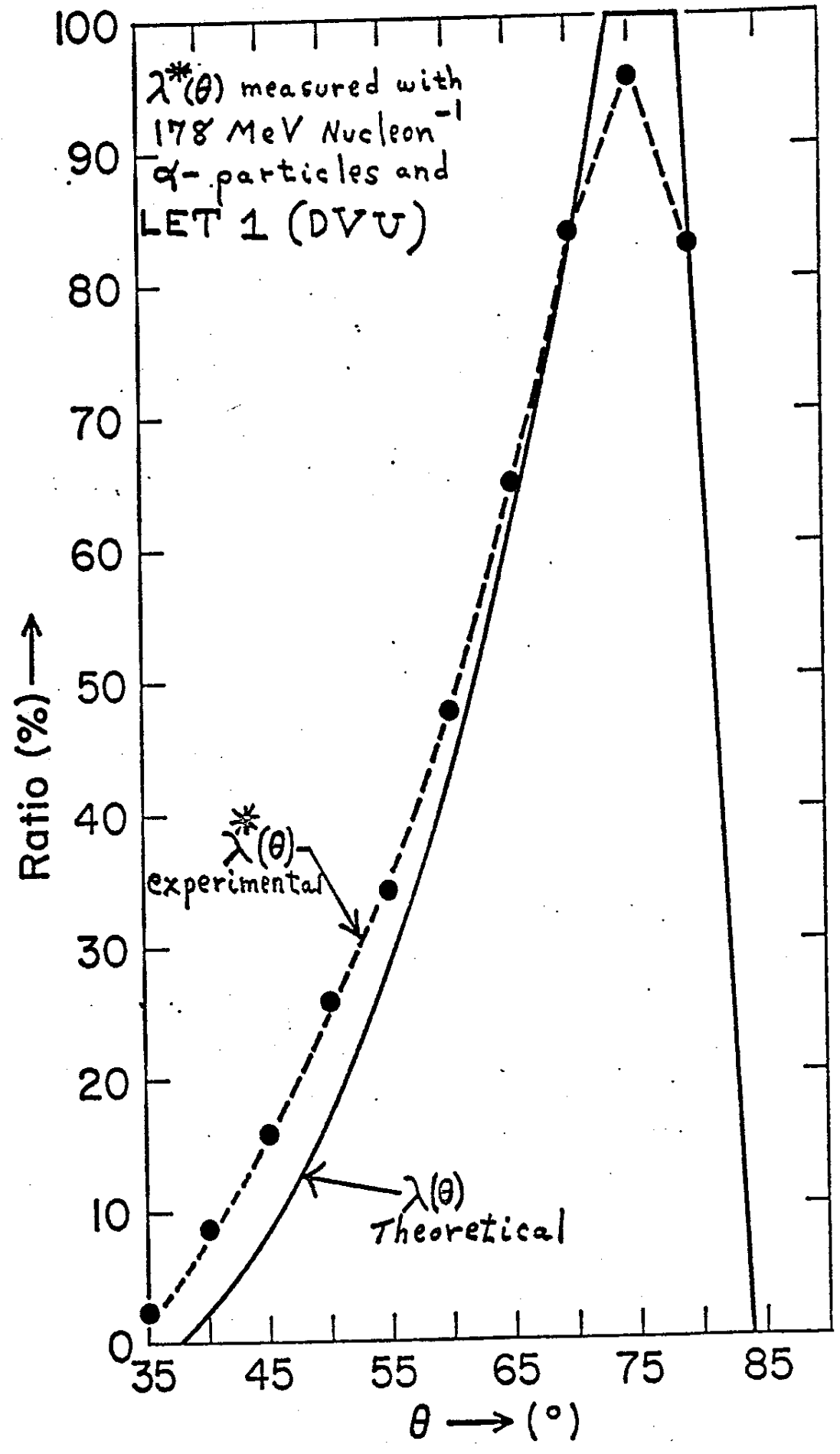
FIGURE C1



Rates and PHA'S measured simultaneously

(DVU)	(Spare)
L1 L2 D1 D7 (L1 PHA)	L1 L2 (L1 PHA)
L1 L2 D1 D7	L1 L2
L1 (singles)	L1 (singles)
L2 (singles)	L2 (singles)
D1 (singles)	
D7 (singles)	

FIGURE C2



Appendix D

Publications and Abstracts Based on  
Mariner 10 UC/CPT Data to Date

Cronological Listing of "Mariner 10" Papers and Talks  
 (\*Papers and Talks funded in part by NASA Grant HSG-7288)

- Simpson, J. A., High Energy and Nuclear Particle Studies on Mariner 10 to Venus and Mercury, Trans Am. Geophys. U. 55, 4 (1974).
- Simpson, J. A., J. H. Eraker, J. E. Lamport, P. H. Walpole, Search for Mariner 10 for Electrons and Protons Accelerated in Association with Venus, Science 183, 1218 (1974).
- Simpson, J. A., J. H. Eraker, J. E. Lamport, P. H. Walpole, Electrons and Protons Accelerated in Mercury's Magnetic Field, Science 185, 160 (1974).
- Simpson, J. A., Preliminary Report on Mercury III Observations Immediately Following Encounter, JPL Technical Memorandum 33-734, Volume 2, (1975).
- Christon, S. P., S. F. Daly, J. H. Eraker, J. E. Lamport, G. A. Lentz, J. A. Simpson, Nucleon Radial Gradients Between 0.45 and 1.0 A.U. From the Mariner 10 Mission to Mercury, 14th Int'l Cosmic Ray Conf., Munich, Conference Papers, Volume 5, 1848 (1975).
- Simpson, J. A., Reply, J.G.R. 80, 4018 (1975).
- Tuzzolino, A. J., S. P. Christon, S. F. Daly, J. H. Eraker, M. A. Perkins, J. A. Simpson, Response of Instrumentation on Mariner 10 for Low Energy High Intensity Particle Measurements in Mercury's Magnetosphere, Trans. Am. Geophys. U. 57, 315 (1976).
- \*Christon S. P. and J. A. Simpson, Relativistic Electrons in Neutral Sheet Regions at Mercury, Earth and Jupiter; invited paper, IAGA/IAMAP Joint Assembly Final Program, 115 (1977).
- \*Christon, S. P. and J. A. Simpson, Separation of Corotating Nucleon Fluxes from Solar Flare Fluxes by Radial Gradients and Nucleon Composition, Ap. J. Letters, 227, L49 (1979).
- \*Eraker, J. H., D. L. Chenette and J. A. Simpson, Jovian Electron Intensity Variations with the Period of Jupiter's Rotation Observed to Within 0.5 A.U. of the Sun, Trans Am. Geophys. U. 59 1173 (1978).
- \*Christon, S. P., S. F. Daly, J. H. Eraker, M. A. Perkins, J. A. Simpson and A. J. Tuzzolino, Electron Calibration of Instrumentation for Low-Energy High-Intensity Particle Measurement at Mercury, J. Geophys. Res., in press (1979).
- \*Eraker, J. H. and J. A. Simpson, Jovian Electron Propagation Close to the Sun (0.5 A.U.), Ap. J. Letters, 232, L131, (1979).

MARINER 10  
RATE DATA  
73-085A-07B

PSFP-00039

This data set has been restored. There were originally 6 magnetic tapes where the D tapes were 800 BPI, 7 track, and the C tapes were 1600 BPI, 9 Track. Both D and C tapes are Binary data. The tapes were condensed onto 1 DS and 1 DR, 9 track 6250 BPI, multi-filed tape.

DR	DS	DD	Files	TIME SPAN
DR02620	DS02620	DD 40360	1	11/03/73 - 12/31/73
		DD 40359	2	01/01/74 - 03/07/74
		DD 40363	3	03/07/74 - 03/28/74
		DD 40364	4	03/28/74 - 05/23/74
		DD 40361	5	06/24/74 - 09/23/74
		DD 40362	6	03/15/75 - 03/21/75

Documentation

Documentation for both data sets are in microfiche form only.  
The following microfiche numbers correspond to this data set.

B32552-00A

B32553-00A

REQ. AGENT

RSH

RAND NO.

V0218

ACQ. AGENT

WSC

MARINER 10

RATE DATA

73-0~~0~~5A-07B

This data set consists of 6 magnetic tapes which are 800 BPI, 7 track, contain BINARY data and only one file. The C# tapes are 1600 BPI, 9 track, and contain BINARY data and only one file. The D#'s, C#,s and time spans are as follows.

<u>D#</u>	<u>C#</u>	<u>TIME SPAN</u>
D-40360	C-23523	11/03/73 - 12/31/73
D-40359	C-23522	01/01/74 - 03/07/74
D-40363	C-23526	03/07/74 - 03/28/74
D-40364	C-23527	03/28/74 - 05/23/74
D-40361	C-23524	06/24/74 - 09/23/74
D-40362	C-23525	03/15/75 - 03/21/75

DOCUMENTATION

Documentation for both data sets are in microfiche form ~~only~~. The following microfiche numbers correspond to this data set.

B32552-00A

B32553-00A





